Quasi-condensation in low-dimensional Bose gases: Mean-field theories and stochastic modelling

Tim-Oliver Sauer

Thesis submitted for the degree of Master of Science

University of Potsdam
Institute of physics and astronomy
Quantum optics

August 13, 2015

Supervisors: PD. Dr. Carsten Henkel[1]
Prof. Dr. Nikolaos Proukakis[2]

[1]University of Potsdam, Institute of physics and astronomy, Potsdam, Germany
[2]University of Newcastle upon Tyne, School of Mathematics and Statistics, Newcastle upon Tyne, United Kingdom

Published online at the
Institutional Repository of the University of Potsdam:
URN urn:nbn:de:kobv:517-opus4-87247
http://nbn-resolving.de/urn:nbn:de:kobv:517-opus4-87247

Eidesstattliche Erklärung

Hiermit erkläre ich an Eides statt, dass ich die vorliegende Arbeit selbstständig und ohne unerlaubte fremde Hilfe angefertigt und keine anderen als die angegebenen Quellen und Hilfsmittel benutzt habe. Die aus fremden Quellen direkt oder indirekt übernommenen Stellen sind als solche kenntlich gemacht. Die Arbeit wurde bisher in gleicher oder ähnlicher Form keinem anderem Prüfungsamt vorgelegt und auch nicht veröffentlicht.

Potsdam, 13.08.2015 Tim-Oliver Sauer

Zusammenfassung

Gegenstand der vorgelegten Arbeit ist das ein-dimensionale Bose-Gas. Da durch Infrarot-Fluktuationen langreichweitige Ordnung zerstört wird, kann sich in einer Dimension nur ein Quasi-Kondensat ausbilden, welches sich durch unterdrückte Dichte-Fluktuationen auszeichnet, dessen Phase jedoch stark fluktuiert. Es wird gezeigt, dass entsprechend angepasste Mean-field-Theorien, ausgehend von einem symmetriebrechenden Ansatz, in der Lage sind, auch Phasenkohärenzeigenschaften eines solchen Quasi-Kondensats richtig wiederzugeben. Eine Beschreibung des Übergangs vom entarteten idealen Bose-Gas zum Quasi-Kondensat, welcher kontinuierlich ist und damit keinen Phasenübergang sondern einen Cross-over darstellt, ist jedoch nicht möglich. Grundlegende Vorraussetzungen für die Anwendung der Theorien sind in diesem Regime nicht erfüllt, sodass falsche Aussagen wie die Existenz eines kritischen Punktes getroffen werden.

Die Theorien werden anhand ihres Anregungsspektrums und ihrer Vorhersagen in Bezug auf die Zustandsgleichung, Dichte-Fluktuationen und damit in Beziehung stehenden Korrelationsfunktionen verglichen. Für die dafür notwendige numerische Auswertung der selbstkonsistenten Integralgleichungen werden Hochtemperaturentwicklungen der entsprechenden Integrale analytisch hergeleitet. Darüber hinaus wird die Stochastische Gross-Pitaevskii (SGP) Gleichung, eine nicht-lineare Langevin-Gleichung, numerisch mittels Monte-Carlo Simulationen analysiert und ihre Ergebnisse mit denen der Mean-field-Theorien verglichen. Dabei erfolgt eine intensive Auseinandersetzung mit der adäquaten Wahl der Parameter. Die Simulationen beweisen, dass die SGP Gleichung den Cross-over beschreiben kann, zeigen jedoch auch die Grenzen der oft verwendeten lokalen Dichte-Näherung auf.

Abstract

The subject of the present thesis is the one-dimensional Bose gas. Since long-rang order is destroyed by infra-red fluctuations in one dimension, only the formation of a quasi-condensate is possible, which exhibits suppressed density fluctuations, but whose phase fluctuates strongly. It is shown that modified mean-field theories based on a symmetry-breaking approach can even characterise phase coherence properties of such a quasi-condensate properly. A correct description of the transition from the degenerate ideal Bose gas to the quasi-condensate, which is a smooth cross-over rather than a phase transition, is not possible though. Basic conditions for the applicability of the theories are not fulfilled in this regime, such that the existence of a critical point is predicted.

The theories are compared on the basis of their excitation sprectum, equation of state, density fluctuations and related correlation functions. High-temperature expansions of the corresponding integrals are derived analytically for the numerical evaluation of the self-consistent integral equations. Apart from that, the Stochastic Gross-Pitaevskii equation (SGPE), a non-linear Langevin equation, is analysed numerically by means of Monte-Carlo simulations and the results are compared to those of the mean-field theories. In this context, a lot of attention is payed to the appropriate choice of the parameters. The simulations prove that the SGPE is capable of describing the cross-over properly, but highlight the limitations of the widely used local density approximation as well.

Acknowledgement

I want to give many **Thanks to:**

- Carsten Henkel, for his encouraging supervision and patiently answering all my stupid questions
- Nick Proukakis, for giving me the opportunity to come to Newcastle and pushing me further
- Vanik, for sharing the office and armenian wine with me
- Timo, for always lending a helping hand
- Hansi, Carl, Erich, Paolo, Donatello, Andre and Luca for fruitful discussions and a lot of fun beyond physics

Contents

Chapter 1

Introduction

> In his well-known papers, Einstein has already discussed a peculiar condensation phenomenon of the 'Bose-Einstein' gas; but in the course of time the degeneracy of the Bose-Einstein gas has rather got the reputation of having only a purely imaginary existence.
>
> Fritz London, 1938 [1]

Whether or not London anticipated the enormous obstacles that had to be overcome in the experimental realisation of what has come to be known as a Bose-Einstein condensate, cannot doubtlessly be clarified; it is, however, not deniable that Einstein's 1925 prediction has not found many supporters among the contemporary physics community. Above all, Uhlenbeck [2] raised questions on the validity of Einstein's argumentation. It was then London himself [1][3] who related Bose-Einstein condensation (BEC) to the at the time well known lambda-transition of liquid Helium, bringing it back to the agenda. In the same year, works of Allen and Jones [4], Kapitza [5] and Tisza [6] led to a better understanding of superfluidity, that had already been discovered in 1911 by Kamerlingh-Onnes, and other related transport phenomena like the gigantic heat conductivity beyond this transition. Although it has been found later [7] that the link between BEC and superfluidity should not be strained too far, this further established the acceptance of the two concepts.

The basis of BEC is the spin-statistics-theorem, first proven by Fierz [8] and Pauli [9]. It states that particles of integer spin behave according to Bose-Einstein statistics, which had been introduced by Bose already in 1925, origin of the denomination of such particles as bosons. He was able to naturally derive Planck's law of radiation only by dividing the phase space of the photons into boxes of size h^3, without relying on only classically justifiable assumptions that other derivations used. Einstein, who the manuscript was sent to, translated the article and submitted it for Bose [10]. In the paper cited by London [11], he extended Bose's method to massive particles, establishing the quantum theory of the ideal (Bose) gas and predicting a new state of matter, the Bose-Einstein condensate.

Due to the symmetry of the wave function of Bosons under particle exchange, they can occupy the same quantum state, making it possible that at low temperatures many particles drop to the ground state of the system. This quantum degeneracy is expected to occur when the thermal de-Broglie wavelength reaches the order of the average interparticle distance. At this point the particles actually start to "feel" each other and their quantum nature becomes apparent. If the ground state gets macroscopically occupied, a condensate is formed, which has been attributed to the establishment of long-range order [12]. This order can only by achieved by means of a phase transition, since a gas (or more generally fluid) is completely disordered and thus exhibits a fundamentally different symmetry.

In the end, it took almost 70 years from the prediction until a pure Bose-Einstein condensate could actually be produced in an experiment. The main reason for this is that at low temperatures almost all substances are in the solid state in thermodynamic equilibrium, making it impossible to observe a BEC for them. This can be achieved though by drastically reducing the density of the gas, which on one side weakens the interaction, but on the other side implies that ultra-cold temperatures below $10^{-6}\,\mathrm{K}$ are necessary. Only the development of new cooling techniques made this possible, until finally in 1995 two groups almost simultaneously succeeded in producing a condensate. Cornell *et al.* at JILA were the first using rubidium ^{87}Rb atoms [13], followed by Ketterle *et al.* at MIT with sodium ^{23}Na [14] and a bit later by Hulet *et al.* with lithium ^{7}Li [15, 16]. Most of the experiments performed today still use these alkali atoms, although BEC has been achieved for others as well over the years.

Another important step towards the realisation of BEC was the construction of appropriate trapping devices. Highly confining trap geometries can be produced nowadays, which drew the attention on lower-dimensional systems whose transverse degrees of freedom are "frozen out" by the strong trapping in this directions. Dimensionality plays in fact a crucial role for coherence properties of the gas; it has already been shown in 1966 by Mermin and Wagner [17] (applied to Bose systems by Hohenberg in 1967 [18]) that there is no long-range order and thus BEC possible in dimensions lower than $d < 3$ at finite temperatures $T \neq 0$ in the thermodynamic limit. Nevertheless, the degenerate gas behaves differently than a thermal gas. There is in fact a regime in which a so called quasi-condensate exists [19], which shows similar coherence properties with respect to density fluctuations as a true condensate. Phase coherence, however, is destroyed by enhanced long-wavelength quantum fluctuations which manifest in the theory in infra-red (IR) divergent integrals. The first experimental observation of a quasi-condensate has been made in a two-dimensional gas of spin-polarized atomic hydrogen [20]. The possibility to easily tune parameters, even the coupling strength by making use of Feshbach resonances [21], makes Bose-Einstein condensates an ideal testing playground, e.g. for non-linear dynamics [22] or even cosmology [23].

The quasi-condensate is the object under investigation in the present thesis. Particular interest is paid to its description in terms of mean-field theory, which has been quite successful in characterising true condensates. Within this perturbative method, the condensate is separated from thermal excitations and the field operator describing it is replaced by a complex function, the mean-field. Bogoliubov introduced this idea in 1947 [24], giving the first microscopic description of an interacting Bose gas. The fact that the phase coherence length is still larger than the characteristic length scales of the quasi-condensate justifies the adoption of this concept to quasi-condensates, although it implies the spontaneous breaking of the original

$\mathcal{U}(1)$-gauge symmetry. A lot of different mean-field theories based on this splitting of the field operator have been put forward. In lower dimensions, they all share the necessity of coping somehow with the mentioned IR-divergences that make a consistent description particularly difficult. Especially the cross-over from the degenerate ideal Bose gas to the quasi-condensate regime, which is not a phase transition but rather a smooth process, is a challenge for them. A technique that is actually expected to work reliably in the cross-over region is based on the so-called Stochastic Gross-Pitaevskii equation [25]. This is a non-linear Langevin equation for a complex field that describes the quasi-condensate and low-lying excitations. It has become a powerful tool for studying dynamics as well as equilibrium properties of weakly interacting Bose gases.

Outline

We start in part I with a review of the ideal Bose gas and examine the impact of dimensionality on its properties (chapter 2). A quick review of experimental techniques and the concept of second quantization is given in the beginning of chapter 3. It is continued with the introduction of correlation functions and their relation to coherence properties of the gas, followed by a revision of regimes of the one-dimensional interacting Bose gas.

Part II is dedicated entirely to the mean-field approach and starts with Bogoliubov theory (chapter 4), whose concepts have been adopted for finite temperatures in Hartree-Fock theory, Modified Popov theory [26] and theories developed by Mora and Castin [27] and Walser [28]. Their derivation is sketched in chapter 5, which is followed by a qualitative comparison of all theories in chapter 6 that is inspired by the studies of Hohenberg and Martin [29] and Griffin [30]. Finally in chapter 7, the self-consistent integral equations appearing in the theories are solved numerically and high-temperature expansions are given. The theories are compared on the basis of their equation of state (relation between chemical potential and particle density), density fluctuations and related correlation functions.

The stochastic method is treated in part III, that begins with a discussion of the zero-temperature Gross-Pitaevskii equation in chapter 8. A code designed by Cockburn [31] is used for numerical evaluation of the Stochastic Gross-Pitaevskii equation in chapter 9. Density profiles of trapped gases, the extraction of the (quasi-)condensate fraction and the local density approximation are discussed, before the results are compared to those of the mean-field theories. This part of the thesis arose from a visit to the University of Newcastle upon Tyne in February and March 2015 under the kind supervision of Nikolaos Proukakis.

Part I

Background and basic principles

Chapter 2

The ideal Bose gas

To get started, it is convenient to review the ideal Bose gas. Although there are of course some aspects that get lost by neglecting interactions, it is a good way to illustrate what Bose-Einstein condensation is all about. For matters of simplicity, we consider first the three-dimensional case which is treated in introductory text books like [32][33], making it easy to point out the important differences of the lower-dimensional cases later on.

Throughout this thesis, we adopt a description using the grand canonical ensemble. One key element of the statistical calculus is the grand canonical partition function given by ($\beta = 1/(k_B T)$)

$$\mathcal{Z} = \sum_{(l)} \exp\left(-\beta\left(E_l - \mu N_l\right)\right), \tag{2.0.1}$$

where the sum runs over all possible micro-states l which are characterized by the set of occupation numbers $\{N_\lambda\}$ of the single particle states λ, μ is the chemical potential and $N_l = \sum_\lambda N_\lambda$, $E_l = \sum_\lambda \epsilon_\lambda N_\lambda$. Thus the summand of (2.0.1) factorizes and taking into account the nature of bosons, the resulting sum is a geometric series giving

$$\mathcal{Z} = \prod_{(\lambda)} \sum_{N_\lambda=0}^{\infty} \left\{\exp\left(-\beta\left(\epsilon_\lambda - \mu\right)\right)\right\}^{N_\lambda} = \prod_{(\lambda)} \frac{1}{1 - \exp\left(-\beta\left(\epsilon_\lambda - \mu\right)\right)}. \tag{2.0.2}$$

Fixing the chemical potential μ, the average total particle number $\langle N\rangle \equiv N$ can be calculated using the relation

$$N = \frac{1}{\beta}\frac{\partial}{\partial\mu} \ln \mathcal{Z} = \sum_{(\lambda)} \frac{1}{\exp\left(\beta\left(\epsilon_\lambda - \mu\right)\right) - 1} = \sum_{(\lambda)} N_{BE}(\epsilon_\lambda - \mu) \tag{2.0.3}$$

The energy is now used to characterize the single particle states and N_{BE} is the Bose-Einstein distribution. Since it gives an averaged occupation number, $N_{BE} \geq 0$ and thus restricts the

chemical potential to values $\mu \leq \epsilon_0$. Choosing the energy of the lowest one particle state to be $\epsilon_0 = 0$, we see that for the ideal Bose gas the chemical potential cannot reach positive values.

For practical uses it is likely that the particle number is given instead. In this case the relation (2.0.3) represents the normalization condition for the chemical potential and has to be used to compute its value, which is necessary for the calculation of other thermodynamic quantities.

The sum in (2.0.3) can be converted into an integral using the density of states $D(\epsilon)$, given that it varies slowly on the scale of consecutive energy levels such that the discrete spectrum can be approximated by a continuous function. Hence for the level spacing $\Delta\epsilon$ the condition

$$k_B T \ll \Delta\epsilon \tag{2.0.4}$$

must be satisfied[1], which is true for a macroscopic system with $N \gg 1$. Nonetheless, if the ground state gets highly populated, this conversion is not valid anymore which gets clear by examining the occupation number of the ground state, written in terms of the fugacity $z = e^{\beta\mu}$, $N_0 = (z^{-1} - 1)^{-1}$. For small $z \ll 1$, this term can be neglected, whereas it gets dominant with increasing fugacity and diverges at its maximum value $z = 1$. In the integral, this contribution is not accounted for since with $D(0) = 0$ (in three dimensions, see (2.2.1)) its statistical weight is zero. Consequently, only the higher lying states are taken into the integral while treating the macroscopically occupied ground state separately:

$$N = \int_0^\infty \frac{D(\epsilon)\,\mathrm{d}\epsilon}{e^{\beta(\epsilon-\mu)} - 1} + \underbrace{\frac{1}{e^{-\beta\mu} - 1}}_{\equiv N_0}. \tag{2.0.5}$$

2.1 Free ideal Bose gas in three dimensions

As we are considering an ideal gas, there is no interaction and thus the free particle dispersion relation

$$\epsilon(k) = \frac{\hbar^2 k^2}{2m} \tag{2.1.1}$$

is being applied. In three dimensions, the density of states is

$$D(\epsilon) = \frac{L^3}{2\pi^2}\frac{g_s m^{3/2}}{\hbar^3}\sqrt{2}\,\epsilon^{1/2} \qquad d = 3 \tag{2.1.2}$$

[1] This is only required if we want the density of states to be continuous, otherwise the summation could be written as an integral over a sum of delta distributions.

and thus a converging integral is obtained from (2.0.5) ($g_s = 2s+1$ is here the spin-degeneracy and L the length of the system which is generally considered to be a cubic box). Substituting $x = \beta\epsilon$, we get the following expression

$$N - N_0 = g_s V \frac{(mk_BT)^{3/2}}{\sqrt{2}\pi^2\hbar^3} \int_0^\infty \frac{x^{1/2}\,\mathrm{d}x}{z^{-1}e^x - 1} = \frac{2g_sV}{\sqrt{\pi}} \frac{1}{\lambda_{dB}^3} \int_0^\infty \frac{x^{1/2}\,\mathrm{d}x}{z^{-1}e^x - 1}, \tag{2.1.3}$$

where the thermal de-Broglie wavelength has been introduced:

$$\lambda_{dB} = \sqrt{\frac{2\pi\hbar^2}{mk_BT}}. \tag{2.1.4}$$

We will encounter many times integrals of the type (2.1.3) in this thesis. Its general form is called Bose-Einstein integral, which is defined by

$$g_n(z) = \frac{1}{\Gamma(n)} \int_0^\infty \frac{x^{n-1}\,\mathrm{d}x}{z^{-1}e^x - 1}. \tag{2.1.5}$$

Since $\Gamma(3/2) = \sqrt{\pi}/2$, we have consequently

$$N - N_0 = \frac{g_sV}{\lambda_{dB}^3} g_{3/2}(z). \tag{2.1.6}$$

The evaluation of the integral is not easy in general, but it is possible to simplify the problem by analysing the behaviour of the fugacity. As mentioned before, the chemical potential for the ideal Bose gas cannot be greater than zero. At this critical point, the fugacity reaches its maximum $z = 1$, leading to a maximum of the Bose-Einstein integral as well which is a monotonically increasing function of z (see figure 2.1.1). Hence its value is limited from above by $g_{3/2}(1)$, which can be calculated easily and turns out to be the analytically continued Riemann Zeta function (see appendix A.1):

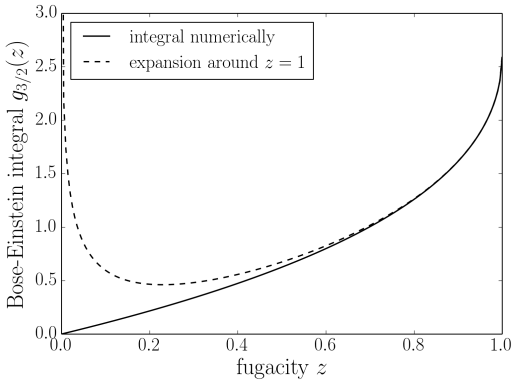

Figure 2.1.1: Numerically evaluated Bose-Einstein integral compared to its small $\alpha = -\ln(z)$ expansion (see appendices A.1 and C.3 for details)

$$N - N_0 \leq \frac{g_sV}{\lambda_{dB}^3} g_{3/2}(1) = \frac{g_sV}{\lambda_{dB}^3}\zeta(3/2) \approx \frac{g_sV}{\lambda_{dB}^3} 2.612. \tag{2.1.7}$$

From that we can deduce that the number of particles not being in the ground state $N' = N - N_0$, i.e. the number of excited particles, is limited. If the total number of particles is

bigger than this quantity, $N > \frac{g_s V}{\lambda_{dB}^3}\zeta(3/2)$, the system has to macroscopically occupy the ground state. This translates into a condition for the temperature or equivalently for the particle density $n = N/V$:

$$T < T_c = \frac{2\pi\hbar^2}{mk_B}\left(\frac{n}{g_s\zeta(3/2)}\right)^{2/3} \Leftrightarrow n > n_c = g_s\zeta(3/2)\left(\frac{mk_BT}{2\pi\hbar^2}\right)^{3/2} = \frac{g_s\zeta(3/2)}{\lambda_{dB}^3}. \tag{2.1.8}$$

Below the critical temperature (or above the critical density), the ground state occupation is non-zero and grows with shrinking temperature (rising density), it can therefore be seen as the onset of condensation. For a typical experiment with a dilute gas of ^{87}Rb atoms (spin $s = 3/2$) at a particle density of $n = 10^{13}\text{cm}^3$, equation (2.1.8) gives a critical temperature of about 34 nK (see section 2.2 for a comparison). At this point, the thermal de-Broglie wavelength, which is a measure of the quantum mechanical uncertainty of the particle's location and can be viewed as its "expansion", becomes of the same order as the average particle distance in the gas, the latter being defined by the particle density via $\langle d\rangle = n^{-1/3}$. This provides an intuitive picture of the condition for BEC: the particles or rather their wave functions start to overlap and their quantum nature becomes apparent.

From (2.1.8) the following relation can be obtained, which will be useful hereafter:

$$\frac{g_s V}{N\lambda_{dB}^3} = \frac{1}{\zeta(3/2)}\left(\frac{T}{T_c}\right)^{3/2} \tag{2.1.9}$$

In the regime defined by (2.1.8), the system consists of two different phases: one containing the condensed and one the excited particles. The relative amount of particles in the condensed phase, the condensate fraction, is characteristic for the ordering of the system. It is given by (using (2.1.9))

$$\frac{N_0}{N} = 1 - \frac{N'}{N} = \begin{cases} 1 - (T/T_c)^{3/2} & T \le T_c \\ 0 & T > T_c \end{cases} \tag{2.1.10}$$

and illustrated in figure 2.1.2. This splitting into two parts will also be an essential point of the concepts in the following chapters on Bogoliubov theory (section 4).

Other thermodynamic quantities can be calculated in a similar way, as has been done for the particle density. The mean energy is a sum over energies of the single particle states weighted by their occupation number. Again the sum is converted into an integral which is identified with another Bose-Einstein integral:

$$E = \sum_\epsilon \frac{\epsilon}{\exp\left(\beta\left(\epsilon - \mu\right)\right) - 1} = \frac{2g_s V}{\sqrt{\pi}}\frac{k_BT}{\lambda_{dB}^3}\int_0^\infty \frac{x^{3/2}\,\mathrm{d}x}{z^{-1}e^x - 1} = \frac{3}{2}g_s V\frac{k_BT}{\lambda_{dB}^3}g_{5/2}(z). \tag{2.1.11}$$

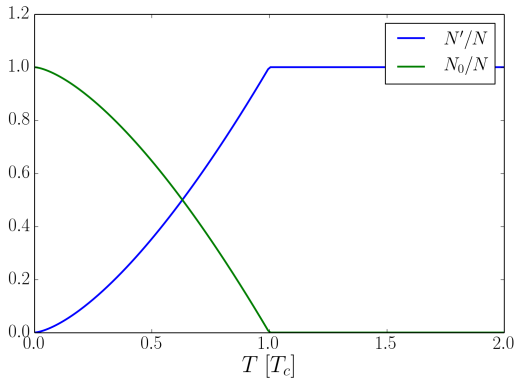

Figure 2.1.2: Condensate and excited particle fraction in dependence of the temperature for the ideal Bose gas

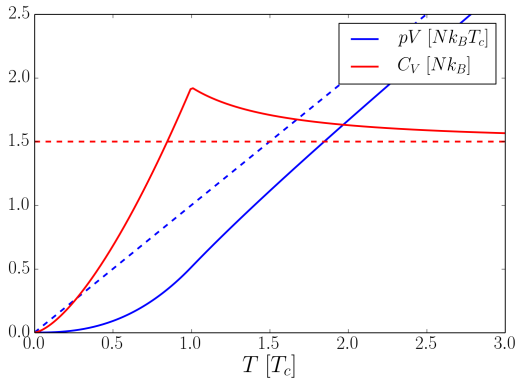

Figure 2.1.3: Pressure and specific heat of the ideal Bose gas (solid) in comparison to the classical ideal gas (dashed)

Since the ground state does not have any energy, this term can in fact be neglected here. Below the critical temperature, the Bose-Einstein integral can be replaced by the Zeta function, $g_{5/2}(0) = \zeta(5/2)$, and the result may be simplified using (2.1.9). For $T > T_c$, the expression in (2.1.11) is the one given in many textbooks, but is it not easy to evaluate. In principle, the fugacity can be obtained from (2.1.6), although this requires values for both temperature and particle density. Wang [34] showed a way of getting an expression with an explicit temperature dependence similar to that for $T < T_c$. He uses an expansion of the Bose-Einstein integral in powers of $\alpha = -\ln z$, according to the results from Robinson [35], just as we have done for different mean-field theories for the weakly interacting Bose gas in order to get high temperature approximations (see section 7.3). The details of the calculation are presented in appendices A.1 and A.2. The final result is:

$$E = \begin{cases} \dfrac{3}{2} N k_B T \dfrac{\zeta(5/2)}{\zeta(3/2)} \left(\dfrac{T}{T_c}\right)^{3/2} & T \leq T_c \\ \dfrac{3}{2} N k_B T \left\{ a_1 + a_2 \left(\dfrac{T_c}{T}\right)^{3/2} + a_3 \left(\dfrac{T_c}{T}\right)^3 \right\} & T > T_c, \end{cases} \tag{2.1.12}$$

with the coefficients $a_1 \approx 0.997$, $a_2 \approx -0.454$ and $a_3 \approx -0.030$.

The pressure can be obtained from $p = \frac{2E}{3V} = g_s \frac{k_B T}{\lambda_{dB}^3} g_{5/2}(z)$, it is thus independent of the volume for $T < T_c$ which corresponds to an infinite compressibility. This unphysical feature stems of course from the fact that there are no interactions between the particles in the ideal Bose gas. Further calculation yields (details in appendix A.2):

$$p = \begin{cases} \dfrac{N k_B T}{V} \dfrac{\zeta(5/2)}{\zeta(3/2)} \left(\dfrac{T}{T_c}\right)^{3/2} & T \leq T_c \\ \dfrac{N k_B T}{V} \left\{ a_1 + a_2 \left(\dfrac{T_c}{T}\right)^{3/2} + a_3 \left(\dfrac{T_c}{T}\right)^3 \right\} & T > T_c. \end{cases} \tag{2.1.13}$$

In figure 2.1.3, the pressure of the ideal Bose gas is compared to that of the classical ideal gas. Remarkably, the pressure at the critical point is about one half of that of the latter and approaches the same values for high temperatures. Finally we have a look at the heat capacity, given by the derivative $C_V = \frac{\partial E}{\partial T}\big|_V$:

$$C_V = \begin{cases} Nk_B \dfrac{15}{4}\dfrac{\zeta(5/2)}{\zeta(3/2)}\left(\dfrac{T}{T_c}\right)^{3/2} & T \leq T_c \\ Nk_B \left\{ \dfrac{3}{2}a_1 - \dfrac{3}{4}a_2 \left(\dfrac{T_c}{T}\right)^{3/2} - 3\,a_3 \left(\dfrac{T_c}{T}\right)^{3} \right\} & T > T_c. \end{cases} \tag{2.1.14}$$

We observe that for all three calculated quantities, the value below the critical temperature is proportional to the number of excited particles $N(T/T_c)^{3/2}$ only. The condensed particles do not have any influence on the thermodynamic behaviour of the gas in this regime. It is therefore not surprising that the heat capacity is lower than that of the classical ideal gas close to $T = 0$, as can be seen in figure 2.1.3. It increases with higher temperature, exceeding the classical value, having a maximum at the critical point and than falls off approaching the classical value for high temperatures.

The characteristic cusp that it shows at the critical point suggests that there is a phase transition and has been associated to the lambda transition of liquid helium ^4He from the normal to the superfluid phase (first by London in [3][1]) because it resembles the typical lambda-shaped curve (see figure on the right or [37]). This seems natural since ^{4}He is a bosonic system in contrast to ^{3}He which is fermionic and does not show a lambda transition[2]. Moreover, the prediction of the critical temperature for liquid helium at atmospheric pressure $T_c \approx 3.14K$ ((2.1.8) with $n = 2.18 \cdot 10^{22}\text{cm}^{-3}$) is in good agreement with the transition temperature of the lambda transition $T_\lambda \approx 2.18K$ [39].

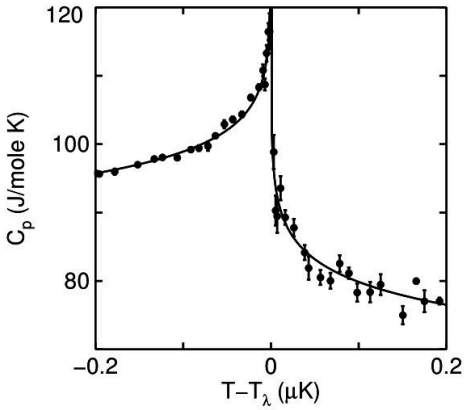

Figure 2.1.4: heat capacity of ^{4}He at the lambda point measured in microgravity on the space shuttle (figure taken from [36])

The cusps of the heat capacity of these two phenomena are resembling as well, but for the ideal Bose gas it is continuous at the critical point, since from (2.1.14) we get $C_V(T_c^+) - C_V(T_c^-) = 0$ (Wang gives mistakenly a finite value in [34]). A (finite) jump of the heat capacity is obtained for the ideal Bose gas when put into a trap [40], but the divergence observed in measurements of liquid helium cannot be described with that model. Furthermore, it has been shown [7] that in the superfluid phase only about 8% of the helium atoms are actually Bose-condensed. This shows that there is no direct relation between superfluidity and Bose-Einstein condensation, but still there exist many features that they have in common.

[2] ^{3}He does have a superfluid phase at much lower temperatures though, which is associated to the pairing of two fermions forming a boson [38], similar to the pairing of electrons in superconductivity.

2.2 Trapped and low-dimensional systems

As we have seen, the ideal gas description in three dimensions can provide a qualitative understanding of Bose-Einstein condensation. Under certain conditions on the other hand, the physics of the system in consideration may effectively be two- or even one-dimensional. This happens if the system is in some sense limited in at least one direction of space, which is normally related to a confinement of the gas by an external potential or some surface interaction forces. In section 3.1, we will sketch how such situations may be realized experimentally.

The physics in lower dimensions can be very different from the three dimensional case. Since in this thesis we want to focus on one-dimensional systems, we examine some aspects of the ideal Bose gas if suspended in a trap and in lower dimensions. For this purpose, we go back to the evaluation of the integral in (2.0.5). We need the density of states, which is given for different dimensions d by

$$D(\epsilon) = \begin{cases} \dfrac{L^3}{2\pi^2}\dfrac{g_s m^{3/2}}{\hbar^3}\sqrt{2}\,\epsilon^{1/2} & d = 3 \\ \dfrac{L^2}{2\pi}\dfrac{g_s m}{\hbar^2} & d = 2 \\ \dfrac{L}{2\pi}\dfrac{g_s m^{1/2}}{\hbar}\dfrac{1}{\sqrt{2}}\,\epsilon^{-1/2} & d = 1. \end{cases} \tag{2.2.1}$$

Thus we see that $D(\epsilon) \propto \epsilon^{d/2-1}$ if the gas is free (or trapped in a box). If it is trapped by a harmonic potential, the excitation energies are those of the quantum harmonic oscillator,

$$\epsilon(n_i) = \sum_{i=1}^{d}\left(n_i + \frac{1}{2}\right)\hbar\omega_i, \qquad n_i \in \mathbb{N}_0 \tag{2.2.2}$$

and it can be shown [40] that the density of states is in this case (if the zero-point motion can be neglected)

$$D(\epsilon) = \frac{\epsilon^{d-1}}{(d-1)!\prod_{i=1}^{d}\hbar\omega_i}. \tag{2.2.3}$$

In order to simplify matters, the calculations that have been carried out for the three dimensional case can be repeated for a general density of states $D(\epsilon) = C_\alpha \epsilon^{\alpha-1}$. As before, the condensate fraction and the critical temperature can be obtained [41]:

$$\frac{N_0}{N} = 1 - \left(\frac{T}{T_c}\right)^{\alpha}, \qquad T < T_c = \frac{N^{1/\alpha}}{k_B\left[C_\alpha \Gamma(\alpha)\zeta(\alpha)\right]^{1/\alpha}}. \tag{2.2.4}$$

In the case of a three dimensional harmonically trapped gas, $\alpha = 3$ and we have thus

$$\frac{N_0}{N} = 1 - \left(\frac{T}{T_c}\right)^3, \qquad T < T_c = \frac{\hbar\,\overline{\omega}}{k_B}\left(\frac{N}{\zeta(3)}\right)^{1/3}, \tag{2.2.5}$$

where $\overline{\omega} = (\omega_x\omega_y\omega_z)^{1/3}$ is the harmonic mean of the oscillator frequencies. These results show a surprisingly good agreement with typical experimental data; for example, with parameters taken from the first experiment with evidence of BEC by Cornell and Wiemann [13], (2.2.5) gives a critical temperature of $T_c \simeq 230$ nK which is very close to the actual measured value of 170 nK. In another pioneering experiment [42], equation (2.2.5) for the condensate fraction has been proven to describe the experimental findings reasonably well. Other early theoretical works [43] [44] showed as well that an interacting system can exhibit a transition similar to the one of the ideal gas. Therefore it can be concluded that the interaction between the particles affects the behaviour of the gas only slightly due to the diluteness of the gas. This already indicates that the assumption of weak interaction, which will be a key element of the theories analysed in this thesis, can be justified under certain conditions.

Thermodynamic quantities can be obtained as well as before, but we will not focus on them here and get now to the influence of lower dimensionality. The calculation of the sum for the number of particles in equation (2.0.3) is not straightforward anymore if the dimension is lower than three. If we proceed as before, converting the sum into an integral, we end up with infra-red divergences in the integrals. It will be necessary to examine the relevance of the system size in more detail in order to understand this part properly.

Until now, we have been describing a system of infinite size since we have argued that the lowest energy eigenvalue ϵ_0 is assumed to be zero (and that the spectrum can be approximated by a continuous function). Any physical system is finite though, implying constraints on the possible energy values as we have seen already for the harmonically confined gas (2.2.2). A simple model for a system of finite size is a free gas that is trapped in a box with impenetrable walls or subject to periodic boundary conditions. This restricts the possible values of the wave vectors to be

$$k_n = \frac{2\pi}{L}n \qquad , n \in \mathbb{N} \tag{2.2.6}$$

for every dimension of space. For a macroscopic system the condition for the smoothness of the density of states is therefore fulfilled and in the limit of $L \to \infty$, the lowest energy value $\epsilon(k) = \hbar^2k^2/2m$ is indeed zero. In this case we get into trouble when converting the sum into an integral, which gets most obvious if we examine the low-energy behaviour (the Bose-Einstein distribution cuts the high energy contribution independently of dimensionality).

Expanding the Bose-Einstein distribution for small arguments, the expression for the maximum number of excited particles ($N'(\mu = 0)$, see (2.1.7)) is

$$N'_{max} \propto \int_0^\infty \mathrm{d}\epsilon\, \epsilon^{d/2-2} = \begin{cases} 2\epsilon^{1/2}\Big|_0^\infty & d=3 \\ \ln\epsilon\Big|_0^\infty & d=2 \\ -2\epsilon^{-1/2}\Big|_0^\infty & d=1. \end{cases} \tag{2.2.7}$$

For three dimensions, we already know that we get a convergent integral even in the thermodynamic limit ($N, L \to \infty$ with $N/L^d = const$) and thus a finite number of excited particles if the degeneracy is high enough $n\lambda_{dB}^3 \gg 1$. In two dimensions, the integral diverges logarithmically and in one dimension even faster. This means that the number of excited particles is not limited any more, hence the ground state is not getting macroscopically occupied and no BEC can occur in the thermodynamic limit. But this does not hold for a finite system size, which can be taken into account by introducing a finite infrared cut-off of the order of the energy of the ground state which for the free gas is $\epsilon_{min} = \frac{2(\pi d\hbar)^2}{mL^2}$ (taking $k_{min} = 2\pi/L$ from (2.2.6)).

For the evaluation of the integral with cut-off in one or two dimensions, it will be sufficient to consider the low-energy contribution and to proceed as we have done in equation (2.2.7). The contribution of high-energy modes to the integrals is not favoured by the density of states in lower dimensions and therefore it can be neglected in a first approximation. Thus we can use the low-energy approximation of the Bose-Einstein distribution, but then in 2d we have to be careful with the upper bound that creates another divergence ($\lim_{\epsilon\to\infty} \ln\epsilon$). This stems from the approximation and has to be neglected since the original Bose-Einstein distribution falls off exponentially for large arguments. Consequently, we get for two dimensions:

$$N'_{max} \simeq \frac{L^2 m k_B T}{2\pi\hbar^2} \int_{\epsilon_{min}/k_BT} \mathrm{d}\epsilon\, \epsilon^{-1} = \frac{L^2}{\lambda_{dB}^2} \ln k_B T \epsilon_{min}^{-1} = \frac{L^2}{\lambda_{dB}^2} \ln\left(\frac{mL^2 k_B T}{8\pi^2\hbar^2}\right) \qquad d=2 \tag{2.2.8}$$

This yields

$$\frac{N}{N'_{max}} = \frac{n\lambda_{dB}^2}{\ln \frac{L^2}{4\pi\lambda_{dB}^2}}, \qquad d=2 \tag{2.2.9}$$

and similarly we obtain for one dimension

$$N'_{max} \simeq \frac{L m^{1/2} k_B T}{2^{3/2}\pi\hbar} \int_{\epsilon_{min}} \mathrm{d}\epsilon\, \epsilon^{-3/2} = \frac{L^2}{\pi\lambda_{dB}^2}, \qquad d=1. \tag{2.2.10}$$

A similar result can be obtained alternatively by evaluating the original sum [45], $N'_{max} \simeq \sum_{n\neq 0} \frac{k_B T}{\hbar^2 k_n^2/2m} = \frac{4mk_BT}{\hbar^2}(\frac{2\pi}{L})^2 \sum_{n=1}^\infty \frac{1}{n^2} = \frac{\pi L^2}{3\lambda_{dB}^2}$.

It follows with (2.2.10)

$$\frac{N}{N'_{max}} = \pi \frac{n\lambda_{dB}^2}{L}, \qquad d = 1. \tag{2.2.11}$$

The two equations (2.2.9) and (2.2.11) confirm again that in the thermodynamic limit, no matter how high the degeneracy may be, there is no BEC possible, with one exception: in 2d, we see that, since the dependence on the system size is only logarithmic, in the limit $T \to 0$ we get $N/N'_{max} \to \infty$ even in the thermodynamic limit $L \to \infty$ with $n = const.$ Quantum degeneracy can still be achieved in lower dimensions even in the thermodynamic limit. This means that low-momentum states up to certain cut-off are highly occupied, but there is no macroscopically occupied state as in three dimensions. The temperature associated to that can be defined in one dimension by setting $n\lambda_{dB} = 1$ as

$$T_d = 2\pi \frac{\hbar^2 n^2}{m k_B}. \tag{2.2.12}$$

2.3 Ideal degenerate Bose gas in one dimension

We will take a closer look on the one-dimensional case, as the main focus of this thesis lies on these systems. For that we notice that all the above integrals can be rewritten in momentum space using the free particle dispersion relation. In one dimension, we have $D(\epsilon)\mathrm{d}\epsilon = \frac{L}{2\pi}\mathrm{d}k$, such that the expression for the non-condensed particles (2.1.3) is just an integration of the Bose-Einstein distribution over momentum space. In the degenerate regime (see equation (2.2.12)), we have a high occupancy of the low-momentum modes and therefore the Bose-Einstein distribution can be expanded as $N_{BE}(\epsilon(k) - \mu) \simeq (\beta(\epsilon(k) - \mu))^{-1}$ in a first approximation. We have therefore

$$N = L \int_{-\infty}^{\infty} \frac{\mathrm{d}k}{2\pi} \frac{k_B T}{\hbar^2 k^2/2m - \mu} = \frac{L}{\pi} \frac{k_B T}{\hbar} \sqrt{\frac{m}{-2\mu}} \int_{-\infty}^{\infty} \frac{\mathrm{d}x}{x^2 + 1}, \tag{2.3.1}$$

which yields the so-called equation of state for the one-dimensional ideal degenerate Bose gas

$$n'(\mu) \equiv n(\mu) = \frac{1}{\hbar\beta} \sqrt{\frac{m}{-2\mu}}. \tag{2.3.2}$$

Just as we have seen before, it diverges for $\mu \to 0$ and is only defined for negative chemical potential. We want to consider now a more general case, namely the Fourier transform of the momentum distribution, whose significance is going to be pointed out later (section 3.3). In the degenerate regime, the resulting integral is similar to that in (2.3.1) and thus its integrand is holomorphic except for two complex poles. It can therefore be solved by integration over the complex plane

$$g_1(z) = \frac{1}{\pi\hbar\beta}\sqrt{\frac{m}{-2\mu}}\oint_\gamma \frac{\mathrm{d}q\, e^{iqz'}}{(q+i)(q-i)}, \tag{2.3.3}$$

where $z' = \frac{\sqrt{-2m\mu}}{\hbar}z$. Since the numerator goes to zero for $\mathrm{Im}\, q \to \pm\infty$ if $z' \gtrless 0$, we have to close the contour in the upper/lower half plane enclosing the pole $q_\pm = \pm i$ for $z' \gtrless 0$, respectively. The residue theorem yields therefore for the integral

$$I = \pm 2\pi i \lim_{q\to q_\pm} \frac{e^{iqz'}}{q \pm i} = \pi e^{\mp z'}, \qquad z' \gtrless 0. \tag{2.3.4}$$

Hence we get

$$g_1(z) = \frac{1}{\hbar\beta}\sqrt{\frac{m}{-2\mu}}e^{-\frac{\sqrt{-2m\mu}}{\hbar}|z|} = ne^{-|z|/l_\vartheta}, \tag{2.3.5}$$

where

$$l_\vartheta = \sqrt{\frac{\hbar^2}{-2m\mu}} = \frac{\hbar^2 n}{mk_BT} = 2\pi\lambda_{dB}^2 n \tag{2.3.6}$$

is the phase coherence length of the ideal Bose gas. For $z = 0$ we recover the particle density n, but $g_1(z)$ contains information on coherence properties of the gas as well. In section 3.3 we will have a more detailed look on this.

Chapter 3

The interacting Bose gas

3.1 Interaction, trapping and cooling

In order to produce a Bose-Einstein condensate, the mentioned necessity of low densities implies that the gas has to be cooled to ultra-cold temperatures. This was only possible due to the development of new cooling techniques like laser cooling [46]. In the most common version of this method, the atoms are cooled by a red-detuned laser beam. Due to the Doppler effect, the absorption is enhanced for atoms moving towards the laser, such that their mean velocity decreases. In this way temperatures of some hundred μK can be reached. The last step in the cooling process is generally evaporative cooling [47]. The most energetic atoms of the cloud are removed by inducing spin flips at the boundaries of the trap applying radio frequency radiation. The remaining gas thermalises due to two-body interaction at a lower temperature.

The cooling is normally combined with a trapping mechanism of the atomic cloud in magneto-optical traps [48], which have to be used for neutral atoms since Penning- and Paul-traps are suited for charged particles only. In a magneto-optical trap, the splitting of the energy levels due to the Zeeman effect is used in an inhomogeneous magnetic field which in combination with the laser light creates a force directed to the minimum of the field.

Another consequence of the diluteness of the gas is the almost complete absence of three-body interactions[1]. This is quite convenient, since the remaining two-body interaction is much easier to model. This can be done by solving the Schrödinger equation in the centre of mass frame. For neutral atoms the interaction is generally modelled by the Lennard-Jones potential. Since this is of quite short range and the energy of cooled atoms is comparably low, the s-wave scattering dominates. Thus the whole process can be characterised by the s-wave scattering length a_s. The actual interaction potential is then replaced by a pseudo potential that has the same scattering properties in the low-energy limit in order to be able to apply the Born approximation [49]. The simplest pseudo potential is the contact potential described by a delta function,

[1] In fact these interactions would be responsible for the forming of a solid [33], which has to be avoided.

$$V(\mathbf{r}, \mathbf{r}') = g\,\delta^{(d)}(\mathbf{r} - \mathbf{r}'), \tag{3.1.1}$$

whose strength is determined such that its scattering amplitude is the same as that of the original potential, which in three dimensions gives:

$$g_{3d} = \frac{4\pi\hbar^2 a_s}{m}. \tag{3.1.2}$$

The scattering lengths can be determined in experiments; for alkali atoms they are typically of the order of a hundred Bohr radius, for example for ^{87}Rb, $a_s \approx 93\,a_0$ [50].

The traps used in experiments are normally highly elongated (cigar shaped) and can be assumed to be harmonic. If the transverse trapping frequency $\omega_\perp$ is large enough, it can be achieved that the physics of the system is effectively one-dimensional, or quasi-one-dimensional, where the transverse degrees of freedom are "frozen out". For that, the energy associated to the transverse trap $\hbar\omega_\perp$ must be much larger than the thermal energy $k_B T$ and the interaction energy characterised by μ. This leads to an effective one-dimensional coupling strength that involves the trapping frequency as well (assuming $a_s \ll l_\perp$, [51]):

$$g_{1d} = \frac{g_{3d}}{2\pi l_\perp^2} = 2\hbar a_s \omega_\perp, \tag{3.1.3}$$

where $l_\perp = \sqrt{\hbar/m\omega_\perp}$ is the harmonic oscillator length. In recent years, atom chips have become a convenient tool for producing low-dimensional Bose gases [52]. These micro-fabricated structures are able to produce highly confining and easily controllable potentials close to their surface. The first BEC on an atom chip has been realised in 2001 by two groups simultaneously [53][54]. Still it has to be emphasized that in some experimental realisations the gas is not well approximated by the quasi-one-dimensional approach, such that transverse excitations have to be taken into account as well.

In a typical experiment on an atom chip [55], we find trapping frequencies of about $\omega_z \approx 50\,\mathrm{Hz} \ll \omega_\perp \approx 20\,\mathrm{kHz}$, temperatures of about $T \sim 400\,\mathrm{nK}$ and a particle number of some 10^4 atoms. This yields an approximate effective (quasi-) one-dimensional coupling constant of $g_{1d} \sim 10^{-37}\,\mathrm{Nm}^2 (g_{1d}/k_B \sim 10\,\mathrm{nK}\,\mu\mathrm{m})$ for ^{87}Rb.

3.2 Second quantization

The general framework of quantum many-body physics which takes the indistinguishability of the particles into account is the formalism of second quantization [56], that makes use of creation and annihilation operators. Any many-particle state is represented in terms of occupation number states. Each of these states corresponds to a fixed particle number and together they form a basis of the many-particle Hilbert space, called Fock space [57]. Applying the creation operator $a_l^\dagger$ to the many-body wave function adds a particle in the single-particle

state $|l\rangle$, whereas the annihilation operators a_l destroys one. As we are considering bosons, these operators obey the following commutation relations,

$$\left[a_l^\dagger, a_m^\dagger\right] = [a_l, a_m] = 0 \tag{3.2.1}$$

$$\left[a_l, a_m^\dagger\right] = \delta_{lm}. \tag{3.2.2}$$

The total particle number is then given by the sum of all occupation numbers:

$$N = \sum_l \langle a_l^\dagger a_l \rangle. \tag{3.2.3}$$

With the single-particle wave functions φ_l forming a complete set of orthonormal functions of Hilbert space $\mathcal{H}$, that is

$$\sum_l |\varphi_l\rangle\langle\varphi_l| = \mathbb{1}, \tag{3.2.4}$$

we can define quantum field operator, which create and annihilate a particle at position $\mathbf{r}$, respectively:

$$\Psi(\mathbf{r}) = \sum_l \varphi_l(\mathbf{r})\, a_l \tag{3.2.5}$$

$$\Psi^\dagger(\mathbf{r}) = \sum_l \varphi_l^*(\mathbf{r})\, a_l^\dagger. \tag{3.2.6}$$

The field operators are linked to the density operator, whose expectation value is the particle density

$$n(\mathbf{r}) = \langle \Psi^\dagger(\mathbf{r})\Psi(\mathbf{r}) \rangle. \tag{3.2.7}$$

They also obey bosonic commutation relations:

$$\left[\Psi^\dagger(\mathbf{r}), \Psi^\dagger(\mathbf{r}')\right] = \left[\Psi(\mathbf{r}), \Psi(\mathbf{r}')\right] = 0 \tag{3.2.8}$$

$$\left[\Psi(\mathbf{r}), \Psi^\dagger(\mathbf{r}')\right] = \delta(\mathbf{r} - \mathbf{r}'). \tag{3.2.9}$$

A general Hamiltonian with two-body interaction $V(\mathbf{r})$ and external trapping potential $U(\mathbf{r})$ can be written in terms of these operators as

$$H = \int_V \mathrm{d}\mathbf{r}\ \Psi^\dagger(\mathbf{r},t)\left(-\frac{\hbar^2\nabla^2}{2m} + U(\mathbf{r}) - \mu\right)\Psi(\mathbf{r},t) + \frac{1}{2}\int_V \mathrm{d}\mathbf{r}\mathrm{d}\mathbf{r}'\ \Psi^\dagger(\mathbf{r}',t)\Psi^\dagger(\mathbf{r},t)V(\mathbf{r}-\mathbf{r}')\Psi(\mathbf{r},t)\Psi(\mathbf{r}',t). \tag{3.2.10}$$

In the following we are going to use the Hamiltonian with contact potential (3.1.1):

$$H = \int_V \mathrm{d}\mathbf{r}\ \Psi^\dagger(\mathbf{r},t)\left(-\frac{\hbar^2\nabla^2}{2m} + U(\mathbf{r}) - \mu\right)\Psi(\mathbf{r},t) + \frac{g}{2}\int_V \mathrm{d}\mathbf{r}\ \Psi^\dagger(\mathbf{r},t)\Psi^\dagger(\mathbf{r},t)\Psi(\mathbf{r},t)\Psi(\mathbf{r},t). \tag{3.2.11}$$

3.3 Correlation functions and long-range order

A lot of insight into the physics of many-particle systems can be gained from studying correlations, quantified by correlation functions. The field operators provide a simple definition, for example for the first order spatial correlation function

$$g_1(\mathbf{r},\mathbf{r}') = \langle\Psi^\dagger(\mathbf{r})\Psi(\mathbf{r}')\rangle. \tag{3.3.1}$$

$g_1(\mathbf{r},\mathbf{r}')$ is related to phase fluctuations, which becomes apparent by writing the field operator as $\Psi(\mathbf{r}) = |\Psi(\mathbf{r})|e^{i\vartheta(\mathbf{r})}$. We get

$$g_1(\mathbf{r},\mathbf{r}') = \langle\sqrt{n(\mathbf{r})n(\mathbf{r}')}e^{i(\vartheta(\mathbf{r}')-\vartheta(\mathbf{r}))}\rangle \simeq n(\mathbf{r})\langle e^{i(\vartheta(\mathbf{r}')-\vartheta(\mathbf{r}))}\rangle, \tag{3.3.2}$$

where the latter only holds if we assume small density fluctuations (see section 3.4). The exponential can now be expanded in a Taylor series in powers of $\vartheta(\mathbf{r}') - \vartheta(\mathbf{r})$. If we assume Gaussian statistics for the phase operator, we can apply Wick's theorem, which states on the one hand that the expectation value of all odd numbers of operators vanish. Hence

$$g_1(\mathbf{r},\mathbf{r}') = n(\mathbf{r})\left\{1 + \sum_{n=1}^{\infty}\frac{i^n}{n!}\langle\left[\vartheta(\mathbf{r}') - \vartheta(\mathbf{r})\right]^n\rangle\right\} = n(\mathbf{r})\left\{1 + \sum_{n=1}^{\infty}\frac{(-1)^n}{(2n)!}\langle\left[\vartheta(\mathbf{r}') - \vartheta(\mathbf{r})\right]^{2n}\rangle\right\}. \tag{3.3.3}$$

On the other hand, even powers of operators can be written as the sum over all possible contractions. There are $(2n-1)!!$ possible ways of pairing $2n$ operators and therefore

$$\langle\left[\vartheta(\mathbf{r}') - \vartheta(\mathbf{r})\right]^{2n}\rangle = (2n-1)!!\,\langle\left[\vartheta(\mathbf{r}') - \vartheta(\mathbf{r})\right]^2\rangle^n \tag{3.3.4}$$

Using $\frac{(2n-1)!!}{(2n)!} = \frac{1}{2^n n!}$ we have consequently

$$g_1(\mathbf{r},\mathbf{r}') = n(\mathbf{r})\left\{1+\sum_{n=1}^{\infty}\frac{1}{n!}\left\langle -\frac{[\vartheta(\mathbf{r}')-\vartheta(\mathbf{r})]^2}{2}\right\rangle^n\right\} = n(\mathbf{r})e^{-\langle[\vartheta(\mathbf{r}')-\vartheta(\mathbf{r})]^2\rangle/2}. \tag{3.3.5}$$

Higher order correlation functions can be defined in a similar way; particularly interesting is the second-order correlation function[2]

$$g_2(\mathbf{r},\mathbf{r}') = \langle\Psi^\dagger(\mathbf{r})\Psi(\mathbf{r})\Psi^\dagger(\mathbf{r}')\Psi(\mathbf{r}')\rangle = \langle n(\mathbf{r})n(\mathbf{r}')\rangle. \tag{3.3.6}$$

It is related to density fluctuations via

$$\delta n^2(\mathbf{r}) = g_2(\mathbf{r},\mathbf{r}) - n^2(\mathbf{r}). \tag{3.3.7}$$

Long-range order, or coherence, that is correlation of different parts of the system over long distances which is typical for solids but also Bose-Einstein condensates (both in three dimensions!), is therefore provided if the corresponding correlation function is non-zero at infinitely separated points in space. Equivalently, a system displays disorder if the correlation function falls off exponentially and drops to zero[3], like for normal liquids and gases. This leads to a criterion for Bose-Einstein condensation that goes back to Landau [60][61]:

$$\begin{aligned}&\lim_{\mathbf{r}\to\infty} g_1(\mathbf{r}) \neq 0 \Leftrightarrow \text{BEC}\\ &\lim_{\mathbf{r}\to\infty} g_1(\mathbf{r}) = 0 \Leftrightarrow \text{no BEC}.\end{aligned} \tag{3.3.8}$$

It follows from equation (2.3.5) that there is no BEC for the one-dimensional ideal Bose gas according to the Landau criterion. This reproduces the conclusion of the famous Mermin-Wagner theorem [17][18]: there is no long-range order in one or two dimensions (in the thermodynamic limit) at finite temperatures, if the ordering corresponds to the spontaneous breaking of a continuous symmetry[4]. The reason for this is that in lower dimensions a diverging number of low-momentum excitations associated to quantum fluctuations which destroy the long-range order are produced. The typical IR-divergent integrals that appear in the description of low-dimensional systems, as those of the ideal Bose gas that we have already seen, are a manifestation of that.

$g_1(\mathbf{r},\mathbf{r}')$ is also called the one-particle density matrix, and the particle densities at different points $\mathbf{r}$ are the diagonal elements of that matrix. With criterion (3.3.8), the existence of BEC

[2] sometimes the correlation functions are defined with a normalisation factor and/or normal ordered

[3] There are systems that display quasi-long-range order, an intermediate case for which the correlation goes to zero at infinity like for disordered systems, but the decay is much slower following typically a power law. In [58][59] such a behaviour has been found for the one-dimensional Bose gas at $T = 0$.

[4] BEC is in fact associated to the spontaneous breaking of the internal $\mathcal{U}(1)$ gauge symmetry (see section 6.3).

is therefore related to a one-particle density matrix with non-vanishing off-diagonal elements. That is why one often speaks of off-diagonal long-range order (ODLRO) [12].

The condition (3.3.8) is only applicable to homogeneous systems. Combining different analogies between interacting and ideal gas [62], Penrose and Onsager [7] gave another criterion which equally holds for inhomogeneous systems. Instead of demanding the ground state to be macroscopically occupied, they identify Bose-Einstein condensation with the largest eigenvalue λ_1 of the single-particle density matrix being of the order of N, or as they put it[5],

$$\begin{aligned} \lambda_1/N = e^{\mathcal{O}(1)} &\Leftrightarrow \text{BEC} \\ \lambda_1/N = o(1) &\Leftrightarrow \text{no BEC.} \end{aligned} \tag{3.3.9}$$

In section 9 we will make use of this in order to determine the condensate fraction of a numerically obtained single-particle density matrix.

It turns out that although there is no true condensate in one dimension in the thermodynamic limit, there is a regime in which the one-dimensional interacting Bose gas still shows a different behaviour than a thermal gas and exhibits properties of a condensate. The fluctuations that destroy long-range order are associated with the internal phase of the quantum field - otherwise the $\mathcal{U}(1)$-gauge symmetry of the Hamiltonian would be spontaneously broken. Thus there is no coherence with respect to g_1, but density fluctuations are suppressed and therefore there is coherence with respect to g_2. This regime has been named quasi-condensate [63].

3.4 Regimes of the one-dimensional Bose gas

The quasi-condensate is just one of the regimes of the one-dimensional homogeneous degenerate Bose gas, which have been identified by Petrov *et al.* [64] and Kheruntsyan *et. al.* [65]. Their results are based on the numerical evaluation of the Lieb Liniger - Yang Yang integral equations.

Lieb and Liniger found in 1963 [66, 67] the exact solution of the Schrödinger equation associated with the (canonical) Hamiltonian of a gas of bosons interacting via a contact potential of the form (3.1.1) in first quantized form:

$$H = -\sum_{i=1}^{N} \frac{\hbar^2}{2m} \frac{\partial^2}{\partial z_i^2} + 2g \sum_{i<j}^{N} \delta(z_i - z_j). \tag{3.4.1}$$

Periodic boundary conditions are used to determine the coefficients of the solution which is found by using the Bethe-Ansatz [68] to solve the equation on the strip defined by $0 \leq x_1 \leq \cdots \leq x_N \leq L$. The latter assumption is justified because a bosonic wave function has to be symmetric under particle exchange. In this way they find explicit eigenfunctions and energies

[5] A quite long-winded definition of this notion is given in the article. $A = e^{\mathcal{O}(1)}$ means that there exist upper and lower bounds for A, $A = o(1)$ means that $A \ll 1$.

for the ground state and excitations. The only free parameter of the equations is in fact the so called Lieb-Liniger parameter of the reduced coupling strength

$$\gamma = \frac{mg}{\hbar^2 n} = \frac{1}{2(n\xi)^2}. \tag{3.4.2}$$

$\xi = \frac{\hbar}{\sqrt{2mgn_0}}$ is a characteristic length scale of the quasi-condensate, called the healing length (details in section 8.1). Equation (3.4.2) shows an interesting property of the one-dimensional Bose gas: it actually becomes more strongly interacting if the density decreases. Lieb and Liniger found that for small γ, Bogoliubov theory gives correct results for the energy of the ground state, but fails for $\gamma \gtrsim 2$. If the interactions become dominant, the system approaches the Tonks-Girardeau gas regime [69, 70]. For this model of impenetrable bosons it can be shown that the spectrum and the configurational probability distributions are the same as for a gas of free fermions. The bosons act in some sense as if they were fermions, but do have a different momentum distribution (due to the Pauli exclusion principle for the fermions).

C.N. Yang and C.P. Yang [71] generalised the Lieb-Liniger model in order to determine thermodynamic properties for finite temperatures. They actually demonstrated the analyticity of the thermodynamic functions at all temperatures and therefore the absence of phase transitions. Their equations have been evaluated numerically in the mentioned paper [65] and the second order correlation function is calculated. On the basis of their results, Kheruntsyan *et al.* identify three limiting regimes (see figure 3.4.1) of the homogeneous one-dimensional interacting Bose gas in the parameter space of the Lieb-Liniger parameter γ and the reduced temperature (T_d is the quantum degeneracy temperature (2.2.12))

$$\tau = \frac{T}{T_d} = \frac{1}{2\pi n l_\vartheta}. \tag{3.4.3}$$

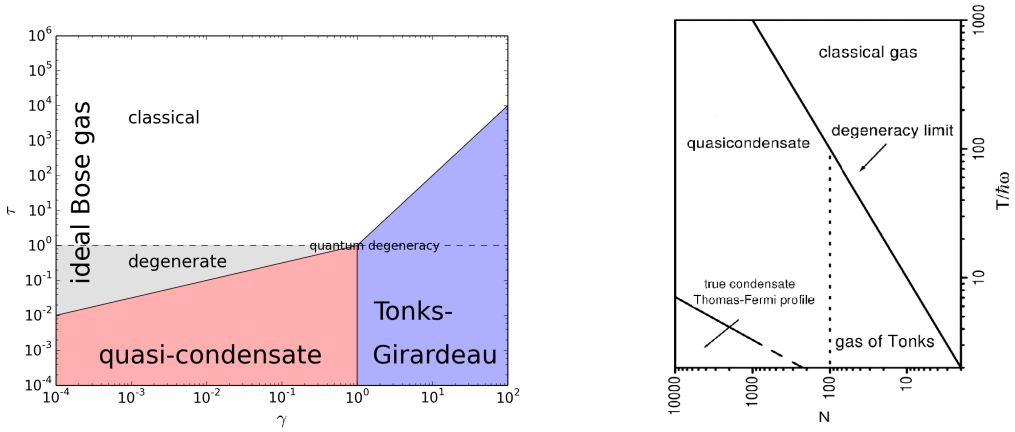

Figure 3.4.1: Regimes of the homogeneous (left) and the harmonically trapped (right) one-dimensional Bose gas (figures inspired by [72] and adapted from[64], respectively)

The strongly interacting (or Tonks-Girardeau) regime of fermionisation mentioned before exists for strong coupling $\gamma \gtrsim \max(1, \sqrt{\tau})$ (see left of figure 3.4.1), for which $g_2(0)/n^2 \simeq 0$

since the repulsion is that strong that the particles cannot approach each other. Then there is the (nearly) ideal Bose gas or decoherent regime at high temperature $\gamma \lesssim \min(\tau^2, \sqrt{\tau})$, where we have the typical bosonic bunching $g_2(0)/n^2 \simeq 2$. It is subdivided into the degenerate and classical regime at the quantum degeneracy temperature corresponding to $\tau \simeq 1$. The quasi-condensate is an intermediate regime with the coherent result $g_2(0)/n^2 \simeq 1$ for $\tau^2 \lesssim \gamma \lesssim 1$. The phase coherence length of the gas is in this regime larger than the typical length scale of the quasi-condensate, the healing length ξ (see also section 7.1). There is thus some kind of local phase coherence [65] which justifies the separation of the field operator into a contribution from a macroscopic component, that is represented by a c-number, and a contribution from excitations (see chapter 4 for details).

It has to be emphasised that these regimes are not separated by sharp boundaries. There are no phase transitions passing from one to the other, but rather smooth cross-overs in accordance with the Mermin-Wagner theorem and Yang and Yang's results [71]. The cross-over from the degenerate ideal Bose gas to the quasi-condensate regime is the main concern of this thesis.

However, a completely different situations arises if the gas is trapped by a potential. We have already seen in chapter 2.2 on the ideal Bose gas that finite-size effects can change the properties of the system drastically. We review the regimes of such systems because they are closer to the experimental reality than a homogeneous gas. In part III of this thesis concerned with the stochastic modelling of a Bose gas, we study some of their properties as well.

The density of states for a one-dimensional harmonically trapped Bose gas has in fact the same structure of a free two-dimensional Bose gas (see (2.2.3)). At $T = 0$, we know that the latter develops a true condensate [17][18], it is therefore expected to happen for the former as well. Ketterle and van Druten proved this in [73] and demonstrated the importance of the discrete energy levels of the potential for this phenomenon. They showed that below a critical temperature

$$T_c = \frac{N}{\ln 2N} \frac{\hbar\omega_z}{k_B}, \tag{3.4.4}$$

the ground state population of the gas grows very quickly, such that there is sharp transition to the BEC regime. Petrov *et al.* showed that very weak interaction is actually needed for that [64]. This is achieved if the parameter $\alpha = mgl_z/\hbar^2$ (l_z is the harmonic oscillator length) introduced by them is very small (compared to one). In the same paper, they identify different regimes of the trapped gas and create a state diagram for large α (see right of figure 3.4.1). There is still the strongly-interacting Tonks-Girardeau regime, which is reached for $N \ll N^* = \alpha^2$ corresponding to $\gamma \gg 1$. For larger $N > N^*$, we have a quasi-condensate with suppressed density fluctuations, which is reached as for the homogeneous case in smooth cross-over from the ideal gas lowering the temperature under T_c. The ideal gas itself is degenerate below the quantum degeneracy temperature associated to the trap:

$$T_d = \frac{N\hbar\omega_z}{k_B} = T_c \ln 2N. \tag{3.4.5}$$

Finally, for really small temperatures below

$$T_\vartheta = \frac{T_d \hbar\omega_z}{\mu} = \frac{N(\hbar\omega_z)^2}{\mu k_B} \tag{3.4.6}$$

we have a true condensate, for which the long-wavelength phase fluctuations are suppressed due to the finite size of the system. With the same parameters from section 3.1, we have $T_d \approx 20\,\mu\mathrm{K} > T_c \approx 2\,\mu\mathrm{K} > T_\vartheta \approx 60\,\mathrm{nK}$ (with $\mu \sim \hbar\omega_\perp$).

Part II

Mean-field theories of the weakly interacting Bose gas

Chapter 4

Bogoliubov theory

The ideal Bose gas description has proven to capture some important aspects of BEC, but it exhibits unphysical features like the infinite compressibility below the critical temperature (see equation (2.1.13)) and is only suited for $\mu < 0$. One step further would be to include weak interactions as a perturbation to the ideal gas, but this is not possible in an ordinary way because the ground state energy of the ideal Bose gas is zero. A different technique that copes with these difficulties was developed by Bogoliubov in 1947 [24], which has become a standard tool for the analysis of Bose-Einstein condensates and has been applied to many other topics as well, for example in the context of BCS theory of superconductivity [74].

One key element of the theory is the splitting of the field operator into a contribution from the condensate $\hat{\phi}(\mathbf{r}, t)$ and one from the non-condensed particles $\delta\hat{\psi}(\mathbf{r}, t)$:

$$\hat{\Psi}(\mathbf{r}, t) = \hat{\phi}(\mathbf{r}, t) + \delta\hat{\psi}(\mathbf{r}, t). \tag{4.0.1}$$

The latter part is considered small in comparison to the first. It is thus a perturbation of the pure condensate and describes quantum fluctuations and particles excited to higher states due to the interaction at zero temperature.

The splitting (4.0.1) is equivalent to the separation of the zero-momentum mode $\hat{a}_0$ from those with higher momentum. Since the ground state is macroscopically occupied in a true condensate, $\hat{a}_0^\dagger \hat{a}_0$ can be replaced by its expectation value N_0 or, equivalently, $\hat{a}_0^\dagger$ and $\hat{a}_0$ by the square root of the number of condensed particles $\sqrt{N_0}$. Therefore $\hat{\phi} = \hat{a}_0 \varphi_0 \equiv \sqrt{N_0/V}$ is not an operator any more (the zero-momentum single particle wave function is $\varphi_0 = V^{-1/2}$) and can be replaced by a (more generally complex) classical field $\phi(\mathbf{r}, t) = |\phi| e^{i\vartheta}$. Its modulus gives the particle density of the condensate $n_0 = |\phi(\mathbf{r}, t)|^2$. From now on we will drop the hat of the operators, bearing in mind that $\delta\psi$ is still an operator obeying the commutation relations (3.2.9).

The replacement of the field operator by a complex number amounts to the breaking of the original $\mathcal{U}(1)$-gauge symmetry since a concrete phase is attributed to the field. For a true condensate, this is a natural thing to do since there is long-range order with respect to the

phase as well, which does not hold for a quasi-condensate. Still this separation can be justified, as we have argued already in section 3.4. Viewed on the scale of the healing length, there is actually some kind of local phase coherence, making it possible to apply the symmetry breaking approach as well to quasi-condensates. Differently from a true condensate, the order parameter ϕ does not contain only the zero-momentum mode now, but small finite momentum excitations (there is no macroscopically occupied ground state). It is not expected though, that this description works on larger length scales. Phase fluctuations of the (quasi-)condensate are actually eliminated in this approach, which is justified in three dimensions. In lower dimensions, phase fluctuations play an enhanced role and therefore the symmetry breaking approach will presumably fail in describing phase coherence properties of a quasi-condensate.

In the following derivations (chapters 4, 5 and 6), the term condensate is used without paying much attention on the difference to the quasi-condensate, since formally they are treated in the same way (with some exceptions). In the chapters after that, we try to rigorously distinguish between both terms or use *(quasi-)condensate*, if this distinction is not crucial; *condensate* refers to a quasi-condensate in the context of low-dimensional homogeneous systems, even though it may not be denoted in this way in some cases.

4.1 Diagonalisation of the Hamiltonian

In the following, the Hamiltonian (3.2.10) with contact potential is expanded in powers of the operator $\delta\psi$, retaining terms up to second order:

$$H_0 = \int_V \mathrm{d}\mathbf{r} \left\{ \left(h_0 - \mu + \frac{g}{2} |\phi|^2 \right) |\phi|^2 \right\} \tag{4.1.1}$$

$$H_1 = \int_V \mathrm{d}\mathbf{r} \left\{ \delta\psi^\dagger \left(h_0 - \mu + g |\phi|^2 \right) \phi + h.c. \right\} \tag{4.1.2}$$

$$H_2 = \int_V \mathrm{d}\mathbf{r} \left\{ \delta\psi^\dagger \left(h_0 - \mu + 2g |\phi|^2 \right) \delta\psi + \frac{g}{2} \left(\phi^2 \delta\psi^{\dagger 2} + \phi^{*2} \delta\psi^2 \right) \right\}, \tag{4.1.3}$$

where $h_0 = -\frac{\hbar^2 \nabla^2}{2m} + U(\mathbf{r})$. Minimizing the ground state energy with respect to the condensate density yields

$$\left(h_0 - \mu + g|\phi|^2 \right) \phi = 0. \tag{4.1.4}$$

This is the stationary Gross-Pitaevskii equation, which describes the condensate in terms of a classical field at zero temperature. It appears very often in the context of BEC and we are going to analyse it in more detail in section 8. For now we content ourselves with noticing that minimising the ground state energy cancels all linear contributions of $\delta\psi$, that is $H_1 = 0$.

For a homogeneous system, $U(\mathbf{r}) = 0$, $\phi(\mathbf{r}, t) \equiv \phi(t)$ and therefore $h_0\phi = 0$. Equation (4.1.4) simplifies consequently to

$$\mu = g|\phi|^2. \tag{4.1.5}$$

This is the equation of state of a pure homogeneous condensate for which the chemical potential is thus always positive for repulsive interaction ($g > 0$). The zero-th order Hamiltonian H_0 yields the ground state energy in a first approximation,

$$E_0 = -\frac{g}{2} n_0^2 V. \tag{4.1.6}$$

The pressure can be calculated from the grand potential Ω via

$$p = -\frac{\partial \Omega}{\partial V} = -\frac{\partial}{\partial V}(E_0 + \mu N_0) = \frac{g N_0^2}{2V^2}, \tag{4.1.7}$$

that now is dependent on the volume, which is physically reasonable. Consequently, the compressibility is not infinite any more but attains the value $\kappa = -\frac{1}{V}\frac{\partial V}{\partial p} = \frac{1}{g n_0^2}$, fixing the ideal Bose gas' deficiency.

We are left with the Hamiltonian $H = E_0 + H_2$, which is going to be diagonalised in the following. For that we use the Fourier representation of the field operator

$$\delta\psi(\mathbf{r}) = V^{1/2} \int \frac{\mathrm{d}\mathbf{k}}{(2\pi)^d} \delta\psi_{\mathbf{k}} e^{i\mathbf{k}\cdot\mathbf{r}}, \tag{4.1.8}$$

which is equivalent to the expansion (3.2.6) with plane waves as the single particle wave functions $\varphi_l = e^{i\mathbf{k}_l \cdot \mathbf{r}}/\sqrt{V}$ for the homogeneous system and converting the sum into an integral with the momentum density $V/(2\pi)^d$. The plane wave approach is even valid for inhomogeneous systems if the local density approximation is justified (see 9.4). Equation (3.2.9) yields the commutation relation of the Fourier components:

$$\left[\psi_k, \psi_q^\dagger\right] = \frac{1}{V} \int_V \mathrm{d}\mathbf{r}\mathrm{d}\mathbf{r}' \left[\psi(\mathbf{r}), \psi^\dagger(\mathbf{r}')\right] e^{-i(\mathbf{k}\cdot\mathbf{r} - \mathbf{q}\cdot\mathbf{r}')} = \frac{1}{V} \int_V \mathrm{d}\mathbf{r}\, e^{-i(\mathbf{k}-\mathbf{q})\cdot\mathbf{r}} = \frac{(2\pi)^d}{V} \delta^{(d)}(\mathbf{k} - \mathbf{q}). \tag{4.1.9}$$

Using (4.1.5), the Hamiltonian takes the following form for one-dimensional homogeneous systems:

$$\frac{H_2}{L} = \int_{-\infty}^{\infty} \frac{\mathrm{d}k}{2\pi} \left\{ \left(\epsilon(k) + g\,|\phi|^2\right) \delta\psi_k^\dagger \delta\psi_k + \frac{g}{2}\left(\phi^2 \delta\psi_k^\dagger \delta\psi_{-k}^\dagger + \phi^{*2} \delta\psi_k \delta\psi_{-k}\right) \right\}, \tag{4.1.10}$$

where $\epsilon(k) = \frac{\hbar^2 k^2}{2m}$. We perform a canonical transformation, known as Bogoliubov transformation:

$$\delta\psi_k = u_k b_k + v_{-k}^* b_{-k}^\dagger, \qquad \delta\psi_k^\dagger = u_k^* b_k^\dagger + v_{-k} b_{-k}. \tag{4.1.11}$$

The new operators b,$b^\dagger$ are required to obey the same commutation relations as the original operators (4.1.9), which leads to the following condition for the coefficients:

$$|u_k|^2 - |v_{-k}|^2 = 1. \tag{4.1.12}$$

They can therefore be parametrised as follows:

$$u_k = e^{i\varphi_k}\cosh(\theta_k/2), \qquad v_{-k} = -e^{-i\varphi_{-k}}\sinh(\theta_k/2). \tag{4.1.13}$$

In order to make the Hamiltonian diagonal in the new operators, the parameters have to be chosen such that all terms mixed in k and $-k$ vanish. This leads to the condition:

$$-\left(\epsilon(k) + g\,|\phi|^2\right)\cosh(\theta_k/2)\sinh(\theta_k/2) + \frac{g}{2}\phi^{*2}e^{2i\varphi_k}\sinh^2(\theta_k/2) + \frac{g}{2}\phi^2 e^{-2i\varphi_{-k}}\cosh^2(\theta_k/2) = 0 \tag{4.1.14}$$

This fixes the phases of the Bogoliubov coefficients

$$\varphi_{\pm k} - \vartheta = \frac{\pi}{2}n, \qquad n \in \mathbb{N}_0, \tag{4.1.15}$$

where the condensate phase $\phi \sim e^{i\vartheta}$ has been introduced. We choose $n = 0$ for both $\varphi_k = \varphi_{-k} = \vartheta$, yielding

$$\phi^{*2}e^{2i\varphi_{\pm k}} = \phi^2 e^{-2i\varphi_{\pm k}} = |\phi|^2, \tag{4.1.16}$$

to finally obtain

$$-\left(\epsilon(k) + g\,|\phi|^2\right)\cosh(\theta_k/2)\sinh(\theta_k/2) + \frac{g}{2}|\phi|^2\left(\sinh^2(\theta_k/2) + \cosh^2(\theta_k/2)\right) = 0. \tag{4.1.17}$$

This can be re-written in the compact form

$$\tanh(\theta_k) = \frac{g|\phi|^2}{\epsilon(k) + g|\phi|^2}, \tag{4.1.18}$$

where $\epsilon(k)$ is the free particle dispersion relation. The Bogoliubov coefficients obey the eigenvalue equation

$$\begin{pmatrix} \frac{\hbar^2 k^2}{2m} + gn_0 & gn_0 \\ -gn_0 & -\left(\frac{\hbar^2 k^2}{2m} + gn_0\right) \end{pmatrix} \begin{pmatrix} u_k \\ v_{\text{-}k} \end{pmatrix} = E(k) \begin{pmatrix} u_k \\ v_{\text{-}k} \end{pmatrix}, \tag{4.1.19}$$

leading to the Bogoliubov dispersion relation

$$E(k) = \left(\frac{\hbar^2 k^2}{2m} \left(\frac{\hbar^2 k^2}{2m} + 2gn_0 \right) \right)^{1/2} = \hbar ck \sqrt{1 + \frac{k^2 \xi^2}{2}}, \tag{4.1.20}$$

where we have introduced the speed of sound

$$c = \frac{1}{\hbar} \frac{\partial E}{\partial k} = \sqrt{\frac{gn_0}{m}}. \tag{4.1.21}$$

Using (4.1.18) in (4.1.13) we obtain eventually

$$u_k, v_{\text{-}k} = \pm e^{\pm i\vartheta} \left(\frac{\epsilon(k) + g|\phi|^2}{2E(k)} \pm \frac{1}{2} \right)^{1/2}, \tag{4.1.22}$$

which yields $u_k v_{\text{-}k} = -\frac{g|\phi|^2}{2E(k)}$ as well. We need this in order to obtain the coefficients of the diagonal terms in the Hamiltonian (4.1.10):

$$\left\{ \left(\epsilon(k) + g\left|\phi\right|^2 \right) \left|u_k\right|^2 + \frac{g}{2} \left(\phi^{*2} u_k v_k^* + c.c. \right) \right\} b_k^\dagger b_k = \frac{1}{2} \left(E(k) + \epsilon(k) + g\left|\phi\right|^2 \right) b_k^\dagger b_k \tag{4.1.23}$$

$$\left\{ \left(\epsilon(k) + g\left|\phi\right|^2 \right) \left|v_{\text{-}k}\right|^2 + \frac{g}{2} \left(\phi^{*2} u_{\text{-}k} v_{\text{-}k}^* + c.c. \right) \right\} b_{\text{-}k} b_{\text{-}k}^\dagger = \frac{1}{2} \left(E(k) - \epsilon(k) - g\left|\phi\right|^2 \right) b_{\text{-}k} b_{\text{-}k}^\dagger. \tag{4.1.24}$$

Since all terms are quadratic in k and we integrate from $-\infty$ to ∞, we can substitute $-k \to k$ and get the Hamiltonian which is finally diagonalised:

$$\frac{H_2}{L} = \int_{-\infty}^{\infty} \frac{\mathrm{d}k}{2\pi} \left\{ E(k) b_k^\dagger b_k + \frac{1}{2} \left(E(k) - \epsilon(k) - g\left|\phi\right|^2 \right) \left[b_k, b_k^\dagger \right] \right\}. \tag{4.1.25}$$

We have commuted the operators in expression (4.1.24), yielding the zero-point energy (second term in the Hamiltonian). The commutator appearing there may be evaluated by converting the integral back into a sum where $\left[b_k, b_k^\dagger \right] \to \delta_{kk} \equiv 1$.

4.2 Ground state energy and elementary excitations

The complete diagonalised Hamiltonian is composed of the ground state energy and a contribution corresponding to excitations:

$$H = E_0 + \int_{-\infty}^{\infty} \frac{\mathrm{d}k}{2\pi} E(k) b_k^\dagger b_k. \tag{4.2.1}$$

The ground state energy is the one from (4.1.6) with a small correction from the zero-point energy of excitations. In three dimensions, this integral is actually UV-divergent and one has to go further than the zero momentum approximation of the effective coupling strength to get a convergent integral. It has been calculated for the first time in [75]. In one dimension, the integral is convergent and can be calculated right away, as we have done in appendix B.1. The ground state energy density can be written as:

$$\frac{E_0}{L} = -\frac{g}{2} n_0^2 - \frac{2\sqrt{m}}{3\pi\hbar} (g n_0)^{3/2} = -\frac{g}{2} n_0^2 - \frac{\sqrt{2}}{3\pi} \frac{g n_0}{\xi}. \tag{4.2.2}$$

Having diagonalised the Hamiltonian in the form of (4.2.1) shows that the behaviour of the interacting particles can effectively be described by the superposition of non-interacting quasi-particles, also called collective excitations, having a dispersion relation (4.1.20). For high momenta, they behave like "real" free particles since in this limit, (4.1.20) approaches the free particle dispersion relation. Likewise, we observe from (4.1.22) that $u_k \simeq 1$ and $v_{-k} \simeq 0$ and therefore $\delta\psi_k \sim b_k$, which corresponds to a single particle of momentum $\hbar k$.

In the low-momentum limit, we have approximately $E(k) \simeq \hbar k c$. The dispersion relation is therefore linear in this case like for phonons. Again we see from (4.1.22) that $u_k \simeq v_{-k} \gg 1$, thus $\delta\psi_k \sim u_k(b_k - b_{-k}^\dagger)$. Therefore for low momentum, the excitations are phonon-like.

4.3 Condensate depletion and thermodynamics

Now that we know the spectrum of the excitations, we want to examine their contribution to total particle density,

$$n = n_0 + n' = |\phi|^2 + \langle \delta\psi^\dagger(z)\delta\psi(z)\rangle, \tag{4.3.1}$$

called the depletion of the condensate n'. These excitations stem from quantum fluctuations[1]. Their density can be obtained using the relations (4.1.8) and (4.1.11), which yields:

$$n' = \left\langle L \int_{-\infty}^{\infty} \frac{\mathrm{d}k\mathrm{d}q}{4\pi^2} \psi_k^\dagger \psi_q e^{i(k-q)z} \right\rangle = L \int_{-\infty}^{\infty} \frac{\mathrm{d}k\mathrm{d}q}{4\pi^2} \left\{ u_k^* u_q \langle b_k^\dagger b_q\rangle + v_{\text{-}k}^* v_{\text{-}q} \langle b_{\text{-}k} b_{\text{-}q}^\dagger\rangle \right\} e^{i(k-q)z} \tag{4.3.2}$$

In thermodynamic equilibrium, we expect the occupation of the excited modes to obey the Bose-Einstein distribution and the expectation value to be consequently

$$\langle b_k^\dagger b_q\rangle = \frac{2\pi}{L} \frac{\delta(k-q)}{e^{\beta E(k)} - 1}, \tag{4.3.3}$$

such that an excitation is weighted by its energy according to the Bogoliubov dispersion relation (4.1.20). Changing the order in the second term in (4.3.2) using the commutator, this leads to:

$$n' = \int_{-\infty}^{\infty} \frac{\mathrm{d}k}{2\pi} \left\{ \frac{|u_k|^2 + |v_{\text{-}k}|^2}{e^{\beta E(k)} - 1} + |v_{\text{-}k}|^2 \right\} = \int_{-\infty}^{\infty} \frac{\mathrm{d}k}{2\pi} \left\{ \frac{\epsilon(k) + gn_0}{E(k)} \left(\frac{1}{e^{\beta E(k)} - 1} + \frac{1}{2} \right) - \frac{1}{2} \right\}. \tag{4.3.4}$$

It is easy to see from the low-k asymptote of the integrand $\frac{m}{\beta\hbar^2}\frac{1}{k^2} + \frac{\sqrt{gn_0 m}}{2\hbar}\frac{1}{k} + const.$ (see appendix C.1) that this integral is again IR-divergent even for zero temperature, which reaffirms that there is no real Bose-Einstein condensation possible in one dimension. For a finite system size, the integral can of course be calculated with an IR energy cut-off as we have done for ideal Bose gas.

Another related quantity, which will be important in the course of this thesis, is the so-called anomalous average. It is defined by $m' = \langle \delta\psi(z)\delta\psi(z)\rangle$ and non-zero (that is why it is called anomalous) because $\delta\psi(z)$ contains both creation and annihilation operators. Proceeding in a similar way as for the depletion, one obtains

[1] We apply the term condensate depletion only in the original Bogoliubov theory; for the finite temperature mean-field theories, n' is called thermal density.

$$
\begin{aligned}
m' &= L \int_{-\infty}^{\infty} \frac{\mathrm{d}k\mathrm{d}q}{4\pi^2} \left\{ u_k v_{-q}^* \langle b_k b_{-q}^\dagger \rangle + v_{-k}^* u_q \langle b_{-k}^\dagger b_q \rangle \right\} e^{i(k+q)z} \\
&= \int_{-\infty}^{\infty} \frac{\mathrm{d}k}{2\pi} \left\{ u_k v_k^* \left(N_{BE}(E(k)) + 1 \right) + v_k^* u_k N_{BE}(E(k)) \right\} \\
&= -\int_{-\infty}^{\infty} \frac{\mathrm{d}k}{2\pi} \left\{ \frac{gn_0}{E(k)} \left(\frac{1}{e^{\beta E(k)} - 1} + \frac{1}{2} \right) \right\} e^{2i\vartheta},
\end{aligned} \tag{4.3.5}
$$

which is as well IR-divergent (the integrand has the same low-k asymptote as n' without the constant).

Since for Bogoliubov theory excitations are effectively free and don't interact with each other, the system can in principle be dealt with as if it was an ideal Bose gas with the Bogoliubov dispersion relation (4.1.20). Thus it is possible to calculate all thermodynamic quantities in the same way we have done for the ideal gas in section 2, for example the total energy contribution of the excitations. Interestingly, even in one dimension we get a convergent integral, since the additional factor ϵ eliminates the divergence, making the integral structurally equal to that of the particle density in three dimensions. In the low-temperature limit it is easy to get an approximation of the integral. This is the natural scope of the theory anyway, since for higher temperatures interactions between the excitations become important and cannot be neglected any more. Details of the calculation are presented in appendix (B.2), yielding:

$$
\frac{E - E_0}{L} = \frac{(k_B T)^2}{\pi \hbar} \sqrt{\frac{m}{gn_0}} = 2^{3/2} \frac{k_B T}{\lambda_{dB}^2 / \xi}. \tag{4.3.6}
$$

The heat capacity per volume is therefore

$$
\frac{C_V}{L} = 2^{5/2} \frac{k_B}{\lambda_{dB}^2 / \xi}. \tag{4.3.7}
$$

Chapter 5

Finite temperature mean-field theories

As mentioned before, within Bogoliubov theory excitations are effectively free and don't interact with each other. This a good approximation for temperatures very close to zero, but gets more and more inaccurate for higher temperatures. There exist a couple of theories for that regime which are all based on a mean-field description. Just as in the Gross-Pitaevskii equation, interactions are described by an effective mean-field that is produced self-consistently by all particles. The mean-field concept is widely used throughout physics and can help to give an understanding of the collective behaviour of large quantities of interacting particles, as we have seen for Bogoliubov theory. The analysis always involves an expansion of the Hamiltonian in fluctuations around the mean-field, which are considered small compared to it.

The theories examined in this thesis differ in the way higher moments of the quantum field are taken into account, which will become clear when we compare them in section 6. Here we will give a short sketch of their derivation, the most simple and popular being Hartree-Fock theory.

5.1 Hartree-Fock theory

Hartree-Fock theory is known from atomic physics where it plays an important role in the approximate calculation of molecular orbitals. There, the minimisation of the energy functional with respect to the single particle wave functions, whose antisymmetric product is taken as an ansatz for the wave function, gives rise to two terms in the energy, the Hartree and the Fock-term. The first corresponds to the average Coulomb interaction of the electrons, the second is due to the (anit-)symmetrisation of the wave function and therefore a quantum effect. Qualitatively the same arises if the theory is applied to bosonic gases, which has been done for the first time in [76].

For a system of interacting bosons, the interaction Hamiltonian (second part of (3.2.10)) is decomposed in eigenfunctions φ_i of the free Hamiltonian (3.2.6):

$$U = \frac{1}{2}\sum_{ijkl}\int_V \mathrm{d}\mathbf{r}\mathrm{d}\mathbf{r}' \left\{\varphi_i^*(\mathbf{r})\varphi_j^*(\mathbf{r})V(\mathbf{r}-\mathbf{r}')\varphi_k(\mathbf{r})\varphi_l(\mathbf{r})\right\} a_i^\dagger a_j^\dagger a_k a_l = \frac{1}{2}\sum_{ijkl}\langle ij|V(\mathbf{r}-\mathbf{r}')|kl\rangle\, a_i^\dagger a_j^\dagger a_k a_l \tag{5.1.1}$$

Following the reasoning of [40], we evaluate the expectation value of this expression. Since the φ_i's are orthogonal, the only terms that survive the summation are those for which either

- $i = k \wedge j = l$, then: $\langle a_i^\dagger a_j^\dagger a_k a_l\rangle = N_i(N_j - \delta_{ij})$

  or

- $i = l \wedge j = k$, then: $\langle a_i^\dagger a_j^\dagger a_k a_l\rangle = N_i N_j \quad , i \neq j$ ($i = j$ already included above).

We have thus:

$$U = \frac{1}{2}\sum_i \langle ii|V(\mathbf{r}-\mathbf{r}')|ii\rangle N_i(N_i-1) + \frac{1}{2}\sum_{i\neq j}\left(\langle ij|V(\mathbf{r}-\mathbf{r}')|ij\rangle + \langle ij|V(\mathbf{r}-\mathbf{r}')|ji\rangle\right) N_i N_j. \tag{5.1.2}$$

For a contact potential $V(\mathbf{r}-\mathbf{r}') = g\,\delta(\mathbf{r}-\mathbf{r}')$, we see that the two terms in the second sum of (5.1.2) equally give:

$$\langle ij|V(\mathbf{r}-\mathbf{r}')|ij\rangle = \langle ij|V(\mathbf{r}-\mathbf{r}')|ji\rangle = g\int_V \mathrm{d}\mathbf{r}\ |\varphi_i(\mathbf{r})|^2|\varphi_j(\mathbf{r})|^2. \tag{5.1.3}$$

Again we consider (normalized) plane waves as single particle wave functions for the homogeneous system, yielding:

$$\langle ij|V(\mathbf{r}-\mathbf{r}')|ij\rangle = \frac{g}{V}. \tag{5.1.4}$$

The total energy including the kinetic term is therefore:

$$E = \sum_k \epsilon_k N_k + \frac{g}{2V}\sum_{k,k'} N_k(N_{k'} - \delta_{kk'}) + \frac{g}{2V}\sum_{k\neq k'} N_k N_{k'}. \tag{5.1.5}$$

The sums may be written as

$$\begin{aligned}\sum_{k,k'} N_k(N_{k'} - \delta_{kk'}) =& \sum_k N_k^2 - \sum_k N_k + \sum_{k\neq k'} N_k N_{k'} \\ =& \left(\sum_k N_k\right)^2 - \sum_{k\neq k'} N_k N_{k'} - \sum_k N_k + \sum_{k\neq k'} N_k N_{k'} \\ =& N^2 - N \end{aligned} \tag{5.1.6}$$

and

$$\sum_{k\neq k'} N_k N_{k'} = \sum_{k,k'} N_k N_{k'} - \sum_k N_k^2 = N^2 - \sum_k N_k^2. \tag{5.1.7}$$

Since we have a macroscopic system, we can neglect N against $N^2 \gg N$ in these expressions. Hence (5.1.5) simplifies to

$$E = \sum_k \epsilon_k N_k + \frac{g}{V}\left(N^2 - \frac{1}{2}\sum_k N_k^2\right). \tag{5.1.8}$$

The energy that is needed to add a particle to the system $E(k)$ may now be obtained by calculating the difference

$$E(k) = E(N_k + 1) - E(N_k) = \epsilon_k + \frac{gN}{V} + \frac{g(N - N_k)}{V} = \begin{cases} g(2n - n_0) & , k = 0 \\ \epsilon_k + g(2n - n_k) & , k \neq 0. \end{cases} \tag{5.1.9}$$

We observe the two different contributions to the energy: the Hartree or direct term which describes the interaction of a particle with all other particles, and the Fock or exchange term due to the indistinguishability of the particles and therefore to their quantum nature. The corresponding term is consequently proportional to the number of particles in states different from that of the particle in consideration.

If the ground state is macroscopically occupied (and the others are not), the chemical potential has to be of the order of the energy of adding a particle to the ground state, thus

$$\mu = g(2n - n_0). \tag{5.1.10}$$

On the other hand, we can than neglect n_k against $n \gg n_k$ in the expression of the energy of an excited particle ((5.1.9) for $k \neq 0$), such that the dispersion relation is

$$E(k) = \epsilon(k) + 2gn - \mu. \tag{5.1.11}$$

Assuming that the excitations are free (quasi)-particles with energy (5.1.11), this leads finally to the following non-condensate or thermal density

$$n' = \int_{-\infty}^{\infty} \frac{\mathrm{d}\mathbf{k}}{(2\pi)^d} \frac{1}{e^{\beta(\epsilon(k)+2gn-\mu)} - 1} = \int_{-\infty}^{\infty} \frac{\mathrm{d}\mathbf{k}}{(2\pi)^d} \frac{1}{e^{\beta(\epsilon(k)+gn_0)} - 1}. \tag{5.1.12}$$

We observe that the excitations are actually free particles whose interaction with each other is described by an effective mean-field potential $\overline{V} \simeq 2ng$ that is produced self-consistently by themselves. The resulting integral is convergent because the excitation spectrum (5.1.11) attains a finite value as $k \to 0$. This property of the spectrum is referred to as conserving (we will analyse this in more detail in section 6.2) and brings about a convergent integral, which has to be evaluated self-consistently. In [76] similar expressions are used to calculate density profiles for a trapped gas.

From (5.1.10) we can see that the chemical potential is always positive in Hartree-Fock theory, just as for the Bogoliubov theory. We will refer to this regime as the dense side of the cross-over. Hartree-Fock theory can be adapted in order to describe the opposite, the dilute side as well. There, no condensate is expected to be present and we therefore neglect it in the above expressions. This leads to an integral which still has to be solved self-consistently but includes the chemical potential now as a free parameter which can be chosen negative as well:

$$n' = \int_{-\infty}^{\infty} \frac{\mathrm{d}\mathbf{k}}{(2\pi)^d} \frac{1}{e^{\beta(\epsilon(k)+2gn'-\mu)} - 1} \qquad \text{(dilute side)}. \tag{5.1.13}$$

As we shall see, the integral is solvable for positive values of the chemical potential as well, but physically this is of course not justified.

This result can be motivated as well if we assume that the particles produce a self-consistent interaction potential $\overline{V} = g|\delta\psi|^4$ (from the functional derivative of an energy functional of the type (8.0.2)), with the field $\delta\psi$ obeying Gaussian statistics. On this condition we can apply Wick's theorem [77],

$$\langle|\delta\psi|^4\rangle = 2\langle|\delta\psi|^2\rangle^2 + |\langle\delta\psi^2\rangle|^2. \tag{5.1.14}$$

The second term (which is actually m'^2 of the type of (4.3.5)) is neglected in this context and hence we have an effective interaction potential

$$\overline{V} = 2gn'. \tag{5.1.15}$$

5.2 Modified Popov theory

Modified Popov theory is based on the Popov theory, which has originally been derived in [63] using path integral methods. Unfortunately, the latter yields IR-divergent integrals for lower dimensions; this problem is fixed within Modified Popov theory.

As we shall see later on, the results of Popov theory for a homogeneous system can easily be derived within a general framework. In contrast to Hartree-Fock theory, it allows for the mixing of particle- and hole-like excitations, and excitations are not "free" any more but phonon-like. Still, we want to sketch the derivation that is used for Modified Popov theory, which is similar to the original approach from Popov. It has been developed by Andersen *et al.* in [78], whose steps we follow.

The partition function is calculated within the imaginary time formalism of the path integral approach to statistical physics:

$$\mathcal{Z} = \int\limits_{\Psi(\mathbf{r},\tau+\hbar\beta)=\Psi(\mathbf{r},\tau)} [\mathrm{d}\Psi^*]\,[\mathrm{d}\Psi]\, e^{-S[\Psi^*,\Psi]/\hbar}, \tag{5.2.1}$$

where $[\mathrm{d}\Psi]$ denotes the functional integration over the c-number field $\Psi(\mathbf{r},\tau)$ and the Euclidian action can be written as

$$S[\Psi^*,\Psi] = \int\limits_0^{\hbar\beta} \mathrm{d}\tau \left\{ \hbar \int\limits_V \mathrm{d}\mathbf{r}\, \Psi^*(\mathbf{r},\tau) \frac{\partial}{\partial\tau} \Psi(\mathbf{r},\tau) + H(\Psi^*,\Psi) \right\}, \tag{5.2.2}$$

with the Hamiltonian H from (3.2.10) (but Ψ, Ψ^* are no operators here). For a homogeneous system, the fields can be expanded in planes waves using bosonic Matsubara frequencies $\omega_n = \frac{2\pi n}{\hbar\beta}$:

$$\Psi(\mathbf{r},\tau) = \frac{1}{\sqrt{\hbar\beta V}} \sum_{\mathbf{k},n} a_{\mathbf{k},n} e^{i(\mathbf{k}\cdot\mathbf{r}-\omega_n\tau)}. \tag{5.2.3}$$

This leads to

$$S[a^*,a] = \sum_{\mathbf{k},n} (-i\hbar\omega_n + \epsilon_k - \mu) a^*_{\mathbf{k},n} a_{\mathbf{k},n} + \frac{g}{2\hbar\beta\omega_n} \sum_{\substack{\mathbf{k},\mathbf{k}',\mathbf{q} \\ n,n',m}} a^*_{\mathbf{k}+\mathbf{q},n+m} a^*_{\mathbf{k}'-\mathbf{q},n'-m} a_{\mathbf{k}',n'} a_{\mathbf{k},n}. \tag{5.2.4}$$

If only the first part of the action is taken into account, the partition function can easily be evaluated using standard techniques for calculating Gaussian functional integrals. This leads directly to the partition function of the ideal Bose gas (2.0.2). Including the interaction term

complicates the calculus a bit; consistent with the mean-field approach and the separation of the field operator into a macroscopic component and fluctuations, the sum is split into sums over low and high momenta $k \lessgtr k_0$[1]. In the following, the action is diagonalised by a Bogoliubov transformation. Then the functional integration can be carried out and the free energy is obtained via $F = -\frac{1}{\beta} \ln \mathcal{Z} + \mu N$. Minimizing F with respect to the chemical potential or the condensate density yields implicit expressions for the density and chemical potential, respectively. Approximating those recursively gives rise to

$$n' = \int_{-\infty}^{\infty} \frac{\mathrm{d}\mathbf{k}}{(2\pi)^d} \left\{ \frac{\epsilon(k) + gn_0}{E(k)} \left(\frac{1}{e^{\beta E(k)} - 1} + \frac{1}{2} \right) - \frac{1}{2} \right\} \tag{5.2.5}$$

$$\frac{\mu}{g} = \int_{-\infty}^{\infty} \frac{\mathrm{d}\mathbf{k}}{(2\pi)^d} \left\{ \frac{2\epsilon(k) + gn_0}{E(k)} \left(\frac{1}{e^{\beta E(k)} - 1} + \frac{1}{2} \right) - 1 \right\} + n_0. \tag{5.2.6}$$

$E(k)$ is the Bogoliubov dispersion relation, making (5.2.5) exactly equal to the standard Bogoliubov result, including its divergences. This brings about the idea of Modified Popov theory to solve this problem making use of certain subtractions and a renormalisation of the coupling constant. In appendix C.1 it is shown in detail that it is actually the term involving the coupling constant g which is responsible for IR-divergences in both expressions in lower dimensions $d \leq 2$ (except for $T = 0$ in 2d). In [78], this term is related to the quadratic contribution of phase fluctuations, i.e.

$$\int_{-\infty}^{\infty} \frac{\mathrm{d}\mathbf{k}}{(2\pi)^d} \frac{gn_0}{E(k)} \left(\frac{1}{e^{\beta E(k)} - 1} + \frac{1}{2} \right) \equiv n_0 \langle \vartheta(\mathbf{r}) \vartheta(\mathbf{r}) \rangle. \tag{5.2.7}$$

Since higher-order terms of the quantum field Ψ are neglected in the Hamiltonian, higher orders of the phase fluctuations are not taken into account either. All these terms summed up would give no contribution at all to the density because

$$g_1(\mathbf{r}, \mathbf{r}) \sim n_0 \langle e^{-i\vartheta(\mathbf{r})} e^{i\vartheta(\mathbf{r})} \rangle = n_0 (1 + \langle \vartheta(\mathbf{r}) \vartheta(\mathbf{r}) \rangle + ...) \equiv n_0 \tag{5.2.8}$$

Hence the term from (5.2.7) has to be removed in (5.2.5) and (5.2.6). As a matter of fact, the resulting integrals,

[1] As usual, $k_0 \to 0$ in three dimensions since there is a macroscopically occupied ground state. In lower dimensions there is no condensate and thus the sum diverges for $k_0 \to 0$.

$$n' = \int_{-\infty}^{\infty} \frac{\mathrm{d}\mathbf{k}}{(2\pi)^d} \left\{ \frac{\epsilon(k)}{E(k)} \left(\frac{1}{e^{\beta E(k)} - 1} + \frac{1}{2} \right) - \frac{1}{2} \right\} \tag{5.2.9}$$

$$\frac{\mu}{g} = \int_{-\infty}^{\infty} \frac{\mathrm{d}\mathbf{k}}{(2\pi)^d} \left\{ \frac{2\epsilon(k)}{E(k)} \left(\frac{1}{e^{\beta E(k)} - 1} + \frac{1}{2} \right) - 1 \right\} + n_0, \tag{5.2.10}$$

are now UV-divergent in three dimensions (see appendix C.1). This can be solved by renormalising the coupling constant g, which consists effectively in replacing it by the two-body T-matrix $T(-2\mu)$ evaluated at the energy -2μ and adding a term to the integral (see [79]), leading to:

$$n' = \int_{-\infty}^{\infty} \frac{\mathrm{d}\mathbf{k}}{(2\pi)^d} \left\{ \frac{\epsilon(k)}{E(k)} \left(\frac{1}{e^{\beta E(k)} - 1} + \frac{1}{2} \right) + \frac{T(-2\mu)\, n_0}{2\epsilon(k) + 2\mu} - \frac{1}{2} \right\} \tag{5.2.11}$$

$$\mu = (2n' + n_0)\, T(-2\mu). \tag{5.2.12}$$

Apart from using the T-matrix, this renormalisation amounts to replacing the IR-divergent term (5.2.7) by its large-k limit in n' and using the zero-temperature expression of the chemical potential $\mu = gn_0$ in it. The resulting integral is convergent in all dimensions and has to be evaluated self-consistently using (5.2.10). As a matter of fact, in lower dimensions the integrals (5.2.9) and (5.2.10) are not UV-divergent and it is known that in one dimension the coupling constant does not have to be renormalised (see [45] as well). For that reason we continue using the bare coupling constant g in one dimension, but still consider the expressions (5.2.11) and (5.2.12) that are valid in all dimensions. The term that has been added,

$$\int_{-\infty}^{\infty} \frac{\mathrm{d}k}{2\pi} \frac{gn_0}{2\epsilon(k) + 2\mu}, \tag{5.2.13}$$

is quite small in one dimension anyhow as we shall see later (see equation (C.6.2) and table 7.1 (green term)).

5.3 Mora-Castin theory

Mora and Castin present another theory for the quasi-condensate regime in [27] (a review can be found in [45]). It is based on the assumption that density fluctuations are suppressed in this regime. The Hamiltonian is therefore expanded in powers of a small parameter which is related to the density fluctuations, rather than the density of excited particles as in standard Bogoliubov theory. For that, the field operator is used in the density-phase representation,

$$\hat{\Psi}(\mathbf{r}) = e^{i\hat{\theta}(\mathbf{r})}\sqrt{\hat{n}(\mathbf{r})}, \tag{5.3.1}$$

with the density $\hat{n}(\mathbf{r}) = \hat{\Psi}^\dagger(\mathbf{r})\hat{\Psi}(\mathbf{r})$ and the phase operator $\hat{\theta}(\mathbf{r})$, which are canonically conjugate variables

$$\left[\hat{n}(\mathbf{r}), \hat{\theta}(\mathbf{r}')\right] = i\delta^{(d)}(\mathbf{r} - \mathbf{r}'). \tag{5.3.2}$$

The separation of the (quasi-)condensate and the remaining particles is only done for the density, i.e.

$$\hat{n}(\mathbf{r}) = n_0(\mathbf{r}) + \delta\hat{n}(\mathbf{r}). \tag{5.3.3}$$

However, this formalism involves some difficulties. There is no Hermitian phase operator that strictly obeys the commutation relation (5.3.2) and the contact potential of the interaction leads to UV-divergences in higher dimensions (details see [27]). The solution to these problems for the authors is the discretisation of space into cells of length l, leading to the Modified expressions for the interaction potential and the commutation relations:

$$V(\mathbf{r}, \mathbf{r}') = \frac{g}{l^d}\delta_{\mathbf{r}\mathbf{r}'}, \qquad \left[\hat{\Psi}(\mathbf{r}), \hat{\Psi}^\dagger(\mathbf{r}')\right] = \frac{\delta_{\mathbf{r}\mathbf{r}'}}{l^d}. \tag{5.3.4}$$

A similar expression is obtained for the commutator (5.3.2), which now is approximately satisfied under the assumption that the probability of finding no particle in a box of size l is negligible[2]. The choice of the grid spacing has to be made by considering the energy cut-off which is linked to it, $\epsilon_{max} \simeq \hbar^2/(ml^2)$. In order to leave the physics of the problem unchanged, it is required that this cut-off must be big enough to still include all characteristic energy scales, that is

$$\mu, k_B T \ll \epsilon_{max}. \tag{5.3.5}$$

The Hamiltonian looks as follows in this representation

$$H = \sum_{\mathbf{r}} l^d \left\{ \hat{n}\left(U(\mathbf{r}) - \mu + \frac{g}{2}\left(\hat{n} - \frac{1}{l^d}\right)\right) - \frac{\hbar^2}{2ml^2}\sum_{j=1}^{d}\left(\hat{n}^{1/2}e^{i(\hat{\theta}_{+j}-\hat{\theta})}\hat{n}_{+j}^{1/2} + h.c. - 2\hat{n}\right)\right\}, \tag{5.3.6}$$

[2]In one dimension, the regime of weak interactions corresponds to high densities (see section 3.4.), which together with the assumption of small density fluctuations assures that this condition is fulfilled.

where the notation $f_{\pm j} \equiv f(\mathbf{r} \pm l\mathbf{e}_j)$ is applied. The expansion of the Hamiltonian is done in powers of the small parameters: one which is linked to density fluctuations as mentioned before, and another which is related to the introduction of the grid,

$$\epsilon_1 = \frac{|\delta n|}{n_0}, \qquad \epsilon_2 = |l\,\nabla\theta| \ll 1. \tag{5.3.7}$$

As in Bogoliubov theory, the ground state energy is minimised leading to a vanishing first-order Hamiltonian. In the following, the second-order Hamiltonian (including contributions from ϵ_1 of order s and ϵ_2 of order t with $s+t=2$) is used to get Heisenberg equations of motion for the phase operator $\hat{\theta}$ and the density fluctuation operator $\delta\hat{n}$. The transformation

$$\hat{B} = \frac{\delta\hat{n}}{2n_0^{1/2}} + in_0\hat{\theta} \tag{5.3.8}$$

maps those onto equations of the form of the Gross-Pitaevskii equation for the new operators $\hat{B}$ and $\hat{B}^\dagger$, for which a standard Bogoliubov transformation diagonalises the Hamiltonian [80]. Unfortunately, there is no correction to the zero-order result of the density for the quadratic Hamiltonian, therefore the contribution from the cubic Hamiltonian has to be taken into account. A rather tedious calculation including a whole series of transformations leads to the final expression, which takes the following form for a homogeneous gas:

$$\begin{aligned}\frac{\mu}{g} &= n_0 + \int_{-\infty}^{\infty} \frac{\mathrm{d}\mathbf{k}}{(2\pi)^d} \left\{ \left(|u_k|^2 + |v_k|^2 \right) N_{BE}(E(k)) + v_k \left(v_k + u_k \right) \right\} \\ &= n_0 + \int_{-\infty}^{\infty} \frac{\mathrm{d}\mathbf{k}}{(2\pi)^d} \left\{ \frac{\epsilon(k)}{E(k)} \left(\frac{1}{e^{\beta E(k)} - 1} + \frac{1}{2} \right) - \frac{1}{2} \right\}, \end{aligned} \tag{5.3.9}$$

where the excitation spectrum and the Bogoliubov coefficients involve the chemical potential

$$u_k, v_{-k} = \frac{\epsilon^{1/2}(k) \pm (\epsilon(k) + 2\mu)^{1/2}}{2E^{1/2}(k)} = \frac{\epsilon(k) \pm E(k)}{2\left(\epsilon(k)E(k)\right)^{1/2}} \tag{5.3.10}$$

$$E(k) = \sqrt{\frac{\hbar^2 k^2}{2m} \left(\frac{\hbar^2 k^2}{2m} + 2\mu \right)}. \tag{5.3.11}$$

The integral in (5.3.9) is convergent in one dimension and UV-divergent in higher dimensions, making it necessary to renormalise the coupling constant in dimensions $d \geq 2$ as in Modified Popov theory. In fact without the renormalisation, the integral of the latter would be structurally identical to that of Mora-Castin theory.

5.4 Walser theory

Finally, the most complex of the mean-field theories we are considering was proposed by Walser [28, 81]; it is in fact formally identical to [82]. We are going to mention only some key points of the original derivation involving Green's functions, since its results can be obtained in an easier way if we are only interested in equilibrium properties of a homogeneous gas. As we shall see in chapter 6.1, it is the most general form of an approach that emphasizes the similarities and the differences of all the mentioned theories.

In Walser's theory, the occupation numbers of the excitations (it is actually distinguished between two types of excitations; we will get back to this in 6.2) are obtained from the eigenvalues of the Hartree-Fock Bogoliubov self-energy

$$\Sigma = \begin{pmatrix} \Sigma_{\mathcal{N}} & \Sigma_{\mathcal{A}} \\ -\Sigma_{\mathcal{A}}^* & \Sigma_{\mathcal{N}}^* \end{pmatrix}, \tag{5.4.1}$$

where $\Sigma_{\mathcal{N}} = h_0 - \mu + 2g(|\phi|^2 + n')$ and $\Sigma_{\mathcal{A}} = g(\phi^2 + m')$ for the homogeneous case. An eigenvalue equation can be established for this matrix, $\Sigma W_i = E_i W_i$, whose eigenvectors W_i are planes waves with some Bogoliubov-like amplitudes u_k,v_k, leading to

$$\Sigma \begin{pmatrix} u_k \\ v_k \end{pmatrix} = E_k \begin{pmatrix} u_k \\ v_k \end{pmatrix}, \tag{5.4.2}$$

which directly yields the Bogoliubov-de Gennes equations that we derive and analyse more in detail in 6.1. A generalised Gross-Pitaevskii equation provides an expression for the chemical potential and the hydrodynamic fields n', m' (the anomalous average is called pairing field in the articles mentioned above), which appear in elements of the correlation matrix G, are calculated from the decomposition

$$G = W_+ P_+ W_+^\dagger + W_-(1 + P_+)W_-^\dagger \tag{5.4.3}$$

where $W_- = \sigma_1 W_+^*$ (with Pauli matrix σ_1) is eigenvector to eigenvalue $E_- = -E_+$ and P_+ is the Bose-Einstein distribution with an excitation spectrum obtained from the Bogoliubov-de Gennes equations. For a homogeneous gas in thermodynamic equilibrium, this procedure is equivalent to that of the next section as mentioned before; expressions for the hydrodynamic fields may therefore be taken from there (equations (6.1.14) and (6.1.15)).

Chapter 6

Qualitative comparison of the theories

The resemblance of the resulting expressions already suggests that all the mentioned theories, although derived in slightly different contexts with different formalisms, are actually quite similar to each other. Key elements of all theories are the mean-field approach with small fluctuations and a Bogoliubov transformation, making it possible to capture all theories within a general framework. Adopting the approach of Griffin [30] will allow us to highlight similarities and to show that the difference consists in the way higher moments of the quantum field (that is the hydrodynamic fields n',m') are taken into account, which leads directly to a classification of all theories. Furthermore, we will analyse the theories according to their excitation spectra and categorize them in two groups, both fulfilling one kind of fundamental laws.

6.1 General derivation within Hartree-Fock Bogoliubov theory

Hartree-Fock Bogoliubov theory (HFB) is based on Bogoliubov theory, but incorporates the interaction between excitations by taking higher orders of the quantum field into account. In the course of the derivation which follows the steps of [30], one way of proceeding is the diagonalisation of the Hamiltonian, just as we have done for the standard Bogoliubov theory, only that now third and fourth-order terms of the quantum field $\delta\psi$ are not neglected anymore (see appendix C.2).

Equivalently to that, the Hamiltonian (3.2.10) can be used to obtain the Heisenberg equation of motion for the quantum field operator $\Psi(\mathbf{r},t)$:

$$i\hbar\frac{\partial}{\partial t}\Psi(\mathbf{r},t) = [\Psi(\mathbf{r},t),H] = \left(-\frac{\hbar^2\nabla^2}{2m} + U(\mathbf{r}) - \mu + g\,\Psi^\dagger(\mathbf{r},t)\Psi(\mathbf{r},t)\right)\Psi(\mathbf{r},t). \tag{6.1.1}$$

If we consider the zero-temperature case, the quantum field operator $\Psi(\mathbf{r},t)$ may be substituted by a classical field $\phi(\mathbf{r},t)$ which describes the condensate only. (6.1.1) is then converted into the famous Gross-Pitaevskii equation, which has been successful in characterising both equilibrium properties and dynamics of the ground state (see chapter 8).

For the finite-temperature case, $\Psi(\mathbf{r},t)$ is split as before into a condensate part, the classical field $\phi(\mathbf{r})$ (now stationary since we are interested in equilibrium properties), and a part originating from the excitations, the operator $\delta\psi(\mathbf{r},t)$. As the latter describes fluctuations around the mean-field, its average or expectation value is considered to vanish, $\langle\delta\psi\rangle = 0$. Inserting this in (6.1.1) gives a term that is cubic in $\delta\psi(\mathbf{r},t)$. Consistent with a mean-field approach, the "self-consistent quadratic approximation", as it is called in [30], is applied:

$$\delta\psi^\dagger\delta\psi\delta\psi \approx 2\langle\delta\psi^\dagger\delta\psi\rangle\delta\psi + \langle\delta\psi\delta\psi\rangle\delta\psi^\dagger. \tag{6.1.2}$$

This is actually quite similar to assuming Gaussian statistics for $\delta\psi$ and applying Wick's theorem (in (C.2.4) this is even more evident). A pair of operators is approximated by its mean value and then all possible combinations of the operators are summed up. We therefore obtain for the interaction term of (6.1.1)

$$\Psi^\dagger\Psi\Psi \simeq |\phi|^2\phi + 2\left(|\phi|^2 + \langle\delta\psi^\dagger\delta\psi\rangle\right)\delta\psi + 2\left(\phi^2 + \langle\delta\psi\delta\psi\rangle\right)\delta\psi^\dagger + 2\phi\delta\psi^\dagger\delta\psi + \phi^*\delta\psi\delta\psi, \tag{6.1.3}$$

which after averaging becomes:

$$\langle\Psi^\dagger\Psi\Psi\rangle \simeq |\phi|^2\phi + 2\phi\langle\delta\psi^\dagger\delta\psi\rangle + \phi^*\langle\delta\psi\delta\psi\rangle. \tag{6.1.4}$$

The average of (6.1.1) yields therefore an equation for the condensate field, which with the identification $n' = \langle\delta\psi^\dagger\delta\psi\rangle$ and $m' = \langle\delta\psi\delta\psi\rangle$ reads:

$$\left(-\frac{\hbar^2\nabla^2}{2m} + U(\mathbf{r}) - \mu\right)\phi(\mathbf{r}) + g\left(|\phi|^2 + 2\langle\delta\psi^\dagger\delta\psi\rangle\right)\phi(\mathbf{r}) + g\langle\delta\psi\delta\psi\rangle\phi^*(\mathbf{r}) = 0. \tag{6.1.5}$$

Neglecting fluctuations leads again to the (now stationary) Gross-Pitaevskii equation.

We assume the condensate to have the phase $\phi \sim e^{i\vartheta}$ as before; in order to get consistent phases in equation (6.1.5), the anomalous average has to obey $m' \sim e^{2i\vartheta}$. Kinetic energy of the condensate and the external potential are zero for a homogeneous system. Hence, we obtain:

$$\mu = g(n + n' + m'e^{-2i\vartheta}). \tag{6.1.6}$$

Taking equation (6.1.1) and subtracting its average yields for the excitations:

$$i\hbar\frac{\partial}{\partial t}\delta\psi = \left(-\frac{\hbar^2\nabla^2}{2m} - \mu\right)\delta\psi + 2g(\underbrace{n_0 + n'}_{n})\delta\psi + g(\underbrace{\phi^2 + m'}_{\tilde{m}})\delta\psi^\dagger, \tag{6.1.7}$$

where we introduce the notation $\tilde{m} = \phi^2 + m'$. As before, we expand the field in plane waves (see (4.1.8)) and carry out a Bogoliubov transformation (4.1.11), leading to:

$$i\hbar\frac{\partial}{\partial t}(u_k b_k + v_{-k}^* b_{-k}^\dagger) = (\epsilon(k) - \mu + 2gn)\,(u_k b_k + v_{-k}^* b_{-k}^\dagger) + g\tilde{m}(u_k^* b_k^\dagger + v_{-k} b_{-k}). \tag{6.1.8}$$

If we assume an implicit time dependence of the Bogoliubov coefficients $u_k, v_{-k} \sim e^{iE_k t/\hbar}$, equation (6.1.8) and its hermitian conjugate yield the Bogoliubov-de Gennes equations:

$$\begin{pmatrix} \epsilon(k) - \mu + 2gn & g\tilde{m} \\ -g\tilde{m}^* & -(\epsilon(k) - \mu + 2gn) \end{pmatrix} \begin{pmatrix} u_k \\ v_{-k} \end{pmatrix} = E_k \begin{pmatrix} u_k \\ v_{-k} \end{pmatrix}. \tag{6.1.9}$$

This equation, compared to (4.1.19), exposes the connection to standard Bogoliubov theory. The excitation spectrum may be deduced from it as well:

$$E^2(k) = (\epsilon(k) - \mu + 2gn)^2 - g^2|\tilde{m}|^2. \tag{6.1.10}$$

Now we still need to determine the hydrodynamic fields; for that, we multiply the two Bogoliubov-de Gennes equations (6.1.9) and obtain with $\mathcal{L}_{HF} = \epsilon(k) - \mu + 2gn$:

$$\left(E_k^2 - \mathcal{L}_{HF}^2 + g^2|\tilde{m}|^2\right) u_k v_{-k} = 2\mathcal{L}_{HF}^2 u_k v_{-k} = -g\mathcal{L}_{HF}\left(\tilde{m}^* u_k^2 + \tilde{m} v_{-k}^2\right). \tag{6.1.11}$$

Parametrizing the Bogoliubov coefficients according to (4.1.13), we see that their phases are as well fixed by the condensate, $\varphi_k = \varphi_{-k} \equiv \vartheta$, and applying the same relations for the hyperbolic functions, we get

$$\tanh(\theta_k) = \frac{g(n_0 + m' e^{-2i\vartheta})}{\epsilon(k) - \mu + 2gn}, \tag{6.1.12}$$

which yields for the Bogoliubov coefficients:

$$u_k, v_{-k} = \pm e^{\pm i\vartheta}\left(\frac{\epsilon(k) - \mu + 2gn}{2E(k)} \pm \frac{1}{2}\right)^{1/2}. \tag{6.1.13}$$

We set the condensate phase to $\vartheta = 0$, and proceeding as we have done before (equations (4.3.2) - (4.3.5)), we obtain the final results:

$$n' = \int_{-\infty}^{\infty} \frac{dk}{2\pi} \left\{ \frac{\epsilon(k) + g(n_0 - m')}{E(k)} \left(N_{BE}(E(k)) + \frac{1}{2} \right) - \frac{1}{2} \right\} \tag{6.1.14}$$

$$m' = -\int_{-\infty}^{\infty} \frac{dk}{2\pi} \frac{g(n_0 + m')}{E(k)} \left(N_{BE}(E(k)) + \frac{1}{2} \right) \tag{6.1.15}$$

$$\mu = g(n + n' + m') \tag{6.1.16}$$

$$E(k) = \sqrt{(\epsilon(k) - \mu + 2gn)^2 - g^2\tilde{m}^2} \tag{6.1.17}$$

As mentioned before, these results can be obtained as well by diagonalising the Hamiltonian. Applying the self-consistent quadratic approximation to the higher-order terms, one realizes that the resulting cubic Hamiltonian cancels the linear Hamiltonian. One is left with a Hamiltonian that can be diagonalised in the same way as was done in Bogoliubov theory. In appendix C.2 details of the calculation are presented, which recovers all results obtained in this section yet and additionally yields the ground state energy (stemming from H_0):

$$\frac{E_0}{L} = -gn_0 \left(\frac{n_0}{2} + 2n' + m' \right). \tag{6.1.18}$$

It is now determined as well by the terms related to fluctuations and reduces to the Bogoliubov result when those are set to zero.

6.2 Classification within the general approach

We will now take a closer look at equations (6.1.14) - (6.1.17) and compare them to the corresponding expressions of the mean-field theories of chapter 5. All of them fit somehow into the scheme of the last section 6.1, although for some it is much more obvious and clear than for others. The main difference between them is the way higher moments of the quantum field are taken into account:

1. Ideal Bose gas: $g = 0$ in (6.1.14) - (6.1.17)
   Even the ideal Bose gas can be captured within this scheme, although here the classification is of course not made on the basis of how the higher moments are treated, but simply by setting the coupling constant to zero in all equations.

2. Bogoliubov theory: $m' = 0$ in (6.1.14) - (6.1.17), $n' = 0$ in (6.1.16) and (6.1.17)
   Excitations are present in Bogoliubov theory, but they do not effect each other (since temperatures close to zero are considered) which manifests through the exclusion of the condensate depletion in the chemical potential. The integral for n' is therefore not implicit and does not have to be solved self-consistently.

3. Hartree-Fock theory (dense, HF^+): $m' = 0$ in (6.1.14), (6.1.15) and (6.1.16); $\tilde{m} = 0$ in (6.1.17)
   In the most simple of the finite temperature mean-field theories, the anomalous average is neglected in the expressions for the chemical potential and the thermal density. In the excitation spectrum, the entire $\tilde{m} = m' + n_0$ is neglected. The interactions are accounted for via the Hartree (or direct) term and the Fock (or exchange) term.

4. Hartree-Fock theory (dilute, HF^-): like HF^+, but additionally $n_0 = 0$
   If we want to describe interactions in the absence of a condensate, we take the results of Hartree-Fock theory and set additionally n_0 to zero. This corresponds to a thermal, interacting gas.

5. Popov theory: $m' = 0$ in (6.1.14) - (6.1.17)
   The difference of the Popov theory to Hartree-Fock theory is that in the former mixing of particle- and hole-like excitation is allowed (off-diagonal elements of (6.1.9)) and thus only m' is neglected in (6.1.17), which leads to an IR-divergent integral. Applying some modifications (see chapter 5.2), the integral is made convergent, establishing Modified Popov theory.

6. Mora-Castin theory: $m' = 0$ (6.1.14) - (6.1.17)
   Mora and Castin's theory cannot be fit into this scheme that easily, but effectively it can be described by setting m' to zero everywhere, only that (6.1.15) is incorporated into the thermal density (6.1.14). If (6.1.14) and (6.1.15) are summed up setting $m' = 0$ in the integrand, they combine to give a convergent integral. If we have a look at the original expression (5.3.9) and compare it to (4.3.4) and (4.3.5), we see that (condensate phase $\vartheta = 0$)

$$\begin{aligned} n' + m'|_{\mathrm{HFB}} &= \int_{-\infty}^{\infty} \frac{\mathrm{d}k}{2\pi} \left\{ \left(u_k^2 + v_k^2\right) N_{BE}(E(k)) + v_k^2 + u_k v_k \left(2N_{BE}(E(k)) + 1\right) \right\} \\ &= \int_{-\infty}^{\infty} \frac{\mathrm{d}k}{2\pi} \left\{ \left(u_k + v_k\right)^2 N_{BE}(E(k)) + v_k \left(u_k + v_k\right) \right\} = n'|_{\text{Mora-Castin}}. \end{aligned} \tag{6.2.1}$$

   One can thus adopt the following picture: the anomalous average gives a contribution to the density through the incorporation in the thermal density, $n = n_0 + n' + m' \to n_0 + n'$. This yields a convergent integral (it is actually similar to the Popov expression after removing the IR-divergent term (5.2.7)) and makes the chemical potential equivalent to that of Popov theory. The excitation spectrum is obtained by setting $m' = 0$ in (6.1.17) and replacing gn_0 by its zero-temperature value μ.

7. Walser theory: $n_0, n', m' \neq 0$ everywhere
   Taking the anomalous average, condensate and thermal density into account in all the expressions yields the results of the theory proposed by Walser.

All results are summarized in table 6.1. Other structurally similar gapless theories have been proposed by Proukakis *et al.* [83] and Yukalov and Kleinert [84] (see section 6.3).

Theory	thermal density n'	anomalous average m'	chemical potential μ	spectrum $E^2(k)$	gapless
ideal Bose gas	$\int_{-\infty}^{\infty} \frac{\mathrm{d}k}{2\pi} N_{BE}(\epsilon(k))$	–	–	$\left(\frac{\hbar^2k^2}{2m} - \mu\right)^2$	(✓)
Bogoliubov	$\int_{-\infty}^{\infty} \frac{\mathrm{d}k}{2\pi} \left\{ \frac{\epsilon(k)+gn_0}{E(k)} \left(N_{BE}(E(k)) + \frac{1}{2} \right) - \frac{1}{2} \right\}$	–	gn_0	$\frac{\hbar^2k^2}{2m} \left(\frac{\hbar^2k^2}{2m} + 2gn_0 \right)$	✓
Hartree-Fock (dense)	$\int_{-\infty}^{\infty} \frac{\mathrm{d}k}{2\pi} N_{BE}(\epsilon(k) + gn_0)$	–	$g(n_0 + 2n')$	$\left(\frac{\hbar^2k^2}{2m} + gn_0 \right)^2$	✗
Hartree-Fock (dilute)	$\int_{-\infty}^{\infty} \frac{\mathrm{d}k}{2\pi} N_{BE}(\epsilon(k) - \mu + 2gn')$	–	–	$\left(\frac{\hbar^2k^2}{2m} - \mu + 2gn' \right)^2$	✗
Popov	$\int_{-\infty}^{\infty} \frac{\mathrm{d}k}{2\pi} \left\{ \frac{\epsilon(k)+gn_0}{E(k)} \left(N_{BE}(E(k)) + \frac{1}{2} \right) - \frac{1}{2} \right\}$	–	$g(n_0 + 2n')$	$\frac{\hbar^2k^2}{2m} \left(\frac{\hbar^2k^2}{2m} + 2gn_0 \right)$	✓
Modified Popov	$\int_{-\infty}^{\infty} \frac{\mathrm{d}k}{2\pi} \left\{ \frac{\epsilon(k)}{E(k)} \left(N_{BE}(E(k)) + \frac{1}{2} \right) - \frac{1}{2} + \frac{gn_0}{2\epsilon(k)+2\mu} \right\}$	–	$g(n_0 + 2n')$	$\frac{\hbar^2k^2}{2m} \left(\frac{\hbar^2k^2}{2m} + 2gn_0 \right)$	✓
Mora-Castin	$\int_{-\infty}^{\infty} \frac{\mathrm{d}k}{2\pi} \left\{ \frac{\epsilon(k)}{E(k)} \left(N_{BE}(E(k)) + \frac{1}{2} \right) - \frac{1}{2} \right\}$	–	$g(n_0 + 2n')$	$\frac{\hbar^2k^2}{2m} \left(\frac{\hbar^2k^2}{2m} + 2\mu \right)$	✓
Walser	$\int_{-\infty}^{\infty} \frac{\mathrm{d}k}{2\pi} \left\{ \frac{\epsilon(k)+g(n_0-m')}{E(k)} \left(N_{BE}(E(k)) + \frac{1}{2} \right) - \frac{1}{2} \right\}$	(6.1.15)	$g(n_0 + 2n' + m')$	$\left(\frac{\hbar^2k^2}{2m} + 2gn_0 \right) \left(\frac{\hbar^2k^2}{2m} - 2gm' \right)$	✗
Yukalov Kleinert	$\int_{-\infty}^{\infty} \frac{\mathrm{d}k}{2\pi} \left\{ \frac{\epsilon(k)+g(n_0+m')}{E(k)} \left(N_{BE}(E(k)) + \frac{1}{2} \right) - \frac{1}{2} \right\}$	(6.1.15)	$g(n_0 + 2n' - m')$	$\frac{\hbar^2k^2}{2m} \left(\frac{\hbar^2k^2}{2m} + 2(n_0 + m') \right)$	✓

Table 6.1: Comparison of different mean-field theories

6.3 Gapless vs. conserving approximations

We have seen that all theories are related to each other in some sense, and we observe that they may be divided in two groups according to their excitation spectra. For some theories, the spectrum is gapless, meaning that excitations with zero momentum have a vanishing energy, i.e. $E(k = 0) = 0$. The opposite is called a conserving spectrum. In order to understand this and get an idea of its importance, we will first introduce some well established concepts and theorems related to this topic:

Spontaneous symmetry breaking

Spontaneous symmetry breaking is a fundamental concept that is widely applied in theoretical physics, its most popular example in recent times appearing probably in the Higgs mechanism [85, 86] in the standard model of elementary particle physics[1]. It occurs if a solution of a theory does not exhibit the same symmetries as the original theory. The system as a whole and the Langrangian (or equivalently equations of motion) that describes it, show certain internal symmetries, but the system will never be found in a state with the same symmetries, but rather in a specific asymmetric state. The probability of all these specific solutions is equal, reflecting the underlying symmetry of the system; therefore one also speaks of a hidden symmetry.

One popular example of a system showing spontaneous symmetry breaking involves the so-called Mexican hat potential. It really has the shape of that Latin American headdress (for the right parameter choice, see figure 6.3.1) with a local maximum in the centre and may be described by

$$V(\phi) = -a|\phi|^2 + b|\phi|^4 \tag{6.3.1}$$

for a complex $\phi = |\phi|e^{i\vartheta}$, $a, b \in \mathbb{R}$ and $b > 0$. The corresponding Lagrangian exhibits $\mathcal{U}(1)$ gauge symmetry, since it is invariant under a change of the phase ϑ.

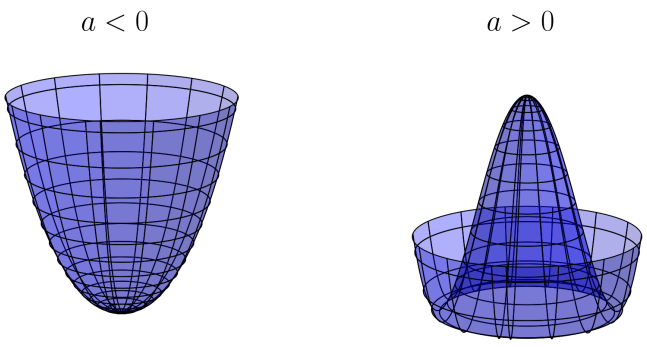

Figure 6.3.1: Mexican hat potential from equation (6.3.1) for negative and positive a

[1] Here the main idea is of course the failure of the Goldstone theorem (see below), leading to massive particles.

The equilibrium solution of such a system, i.e. the ϕ for which the minimum of the potential is attained, depends on the value of a: if it is negative, the minimum in the middle of the potential is the only solution; if it is positive, this solution becomes a local maximum and two (if we look at the vertical plane) minima of finite radius appear. The solution is therefore

$$\phi = \begin{cases} 0 & a \leq 0 \\ \sqrt{\dfrac{a}{2b}} e^{i\vartheta} & a > 0. \end{cases} \tag{6.3.2}$$

Tuning the system by increasing a from negative values, it actually shows a Pitchfork bifurcation at $a = 0$ (see figure 6.3.2). The originally stable solution in the centre becomes unstable and two new stable solutions appear at a radius that scales with the square root of the parameter a. The non-zero branch of solutions for $a > 0$ corresponds to an infinite number of realisations, since the angle ϑ can attain any value from the interval $[0, 2\pi)$, or put another way for clarity, must attain a specific value within this range. Consequently, the original $\mathcal{U}(1)$-gauge symmetry of the system is not conserved for the solution, it is spontaneously broken.

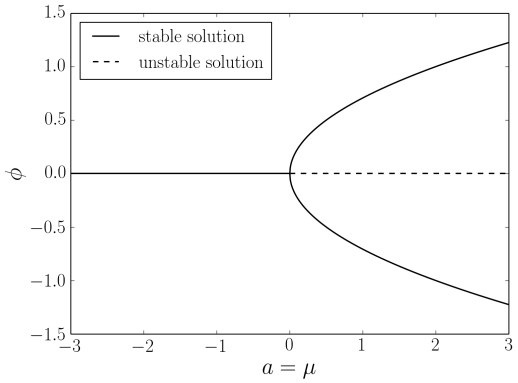

Figure 6.3.2: Pitchfork bifurcation for the Mexican hat potential; the two solution branches correspond to $\vartheta = 0$ and $\vartheta = \pi$ of equation (6.3.2)

The above notation is not chosen by chance, but in order to highlight the connection to Bose-Einstein condensates. As we shall see in section 8, the Gross-Pitaevskii equation for the condensate order parameter ϕ can be derived alternatively by starting from an energy functional containing a potential of the form (6.3.1). We identify for a homogeneous gas $a = \mu$ and $b = g/2$, yielding the known solution for the condensate density $|\phi|^2 = \mu/g$. We deduce therefore that the $\mathcal{U}(1)$-gauge symmetry is spontaneously broken for a bosonic system in the presence of a Bose-Einstein condensate. This is implied in the mean-field theories by virtue of the replacement of the field operator by a complex order parameter ϕ.

We have applied the same approach to the quasi-condensate, arguing that there exists local phase coherence. This implies that in this model, the symmetry is also broken (although only locally) and the following statements hold likewise for a quasi-condensate. A different class of theories, the number conserving approaches (see for example [87]), deal with this issue by conserving the operator character of the (quasi-)condensate.

Goldstone theorem

The Goldstone theorem [88] states that whenever a continuous symmetry is spontaneously broken, i.e. a continuous symmetry group leaves the Lagrangian but not the vacuum solution invariant [89], there must exist spinless particles (i.e. bosons) of mass zero that correspond to collective mode excitations. They were first observed in the context of BCS theory of superconductivity by Nambu [90]; that is why they are called Nambu-Goldstone bosons or

modes.

The original theorem holds for relativistic theories only, but there is an analogue of it for the non-relativistic case [91]. It is concluded there that if the interactions are of finite range, the spontaneous symmetry breaking leads to excitations with zero energy in the long-wavelength limit as the non-relativistic analogous of a vanishing mass. This means that the excitation spectrum of a Bose-Einstein condensate must be gapless.

Hugenholtz-Pines theorem

In their paper [92], Hugenholtz and Pines use Green's function techniques that were introduced by Beliaev [93, 94] in order to establish an exact relation for the chemical potential for a system of interacting bosons. Without going into much detail, we emphasize that this relation leads to the verification of the Goldstone theorem, confirming that there is no energy gap in the excitation spectrum for interacting bosons.

We have seen (table 6.1) that some of the theories we have analysed do have a gapless spectrum, namely Bogoliubov theory, Popov and Modified Popov theory, Mora-Castin theory, and others do not, like Hartree-Fock theory (both formulations) and Walser's theory. The idea of dividing these theories into two groups on the basis of their excitation spectrum was introduced by Hohenberg and Martin in [29]. In [30], this concept was adopted and already applied to some of the theories considered in this thesis. It is pointed out that it is actually a difficult task to construct a consistent theory, because two somehow contrary constraints have to be fulfilled: on the one hand, the excitation spectrum is expected to be gapless, on the other hand conservation laws (like energy, momentum, particle conservation) must be satisfied. Theories of the latter kind are called "ϕ-derivable" in [29] or "conserving", since the mentioned conservation laws are directly incorporated in their derivation. According to Griffin, the problem of finding a theory that is both gapless and consistent with conservation laws can be solved within the dielectric formalism [95]. Walser applies the same kind of argumentation to his theory: he distinguishes between thermodynamic excitations that contribute to the equilibrium, and elementary excitations resulting from the linear response to a perturbation. Only the latter have to satisfy the condition of a gapless spectrum while the thermodynamic excitations have to be consistent with conservation laws, which holds for Walser's theory. In other words, the elementary excitations are not considered to represent the Goldstone mode associated to the spontaneous symmetry breaking.

There is a theory that we have not mentioned yet but which is structurally similar. It has been proposed by Yukalov and Kleinert in [84] and has also been derived with the Hartree-Fock Bogoliubov approximation, but making use of two Lagrange multipliers. The second Lagrange multiplier is needed in order to ensure the normalisation condition $n_0 = |\phi|^2$ for the broken symmetry phase. The authors claim that in this way the theory is made self-consistent, fulfilling conservation laws and having a gapless spectrum. The resulting expressions are quite similar to those of Walser's theory (compare table 6.1), but with some opposite signs where the anomalous average m' appears and, most importantly, with a Bogoliubov kind of (thus gapless) spectrum involving also the anomalous average. Therefore it is as well IR-divergent in lower dimensions, that is why we will not address details of this theory any further.

Chapter 7

Evaluation

Having analysed the origins and the differences of the mean-field theories, we come now to the actual calculation of the integrals involved. Most of them have to be solved in a self-consistent way since the integrand itself includes often the quantity that is being calculated. In order to simplify the evaluation and interpretation, we give approximations of the integrals in the high-temperature limit. We compare the theories on the basis of the equation of state (referring to a relation of the type $n = n(\mu)$), density fluctuations and related correlation functions.

7.1 Cross-over units

As mentioned before in section 3.4, the regime that we are aiming to describe is the cross-over from a degenerate Bose gas to a quasi-condensate. We expect that the characteristic length scales of both regimes become of the same order at this point, we set therefore the phase coherence length of the one-dimensional ideal degenerate Bose gas l_ϑ (2.3.6) equal to the healing length of the quasi-condensate ξ (see chapter 8 for details). That enables us to define characteristic units:

$$\xi \simeq \frac{\hbar}{\sqrt{mgn}} = \frac{\hbar^2 n}{m k_B T} = l_\vartheta \;\Rightarrow\; n_x = \frac{1}{g}\left(\frac{m^{1/2} g k_B T}{\hbar}\right)^{2/3}. \tag{7.1.1}$$

From the zero-temperature relation we easily obtain the corresponding chemical potential:

$$\mu_x = g n_x = \left(\frac{m^{1/2} g k_B T}{\hbar}\right)^{2/3}. \tag{7.1.2}$$

Finally, since for a degenerate Bose gas the degeneracy $n\lambda_{dB}$ is large, we define a small dimensionless temperature parameter by the squared inverse of it, i.e.

$$\beta_x = \frac{2\pi}{(n_x \lambda_{dB})^2} = \left(\frac{g^2 m}{\hbar^2 k_B T} \right)^{1/3} = \frac{\mu_x}{k_B T}. \tag{7.1.3}$$

A length scale can be defined as well as

$$l_x = n_x^{-1}. \tag{7.1.4}$$

We will formulate all theories in terms of these units, yielding equations with β_x as the only free parameter. Their definition implies a cross-over temperature T_x that can be related to the Lieb-Liniger parameter γ and the quantum degeneracy temperature in the following way:

$$T_x = \sqrt{\frac{g n^3 \hbar^2}{m k_B^2}} = 2\sqrt{\gamma}\, T_d. \tag{7.1.5}$$

The cross-over occurs therefore at a reduced temperature

$$\tau = 2\sqrt{\gamma}, \tag{7.1.6}$$

which is (apart from the factor 2) the result from [65] (see section 3.4). In the same way we have

$$\beta_x = \left(\frac{\gamma^2}{\tau} \right)^{1/3}. \tag{7.1.7}$$

7.2 Numerical evaluation of self-consistent integral equations

After scaling the integrals to cross-over units, we will mention some details of how they have been evaluated numerically.

Hartree-Fock theory (dilute side)

Writing the densities and the chemical potential in terms of the units defined in (7.1.1) and (7.1.2) respectively, the integral (5.1.13) takes the following form,

$$n' = \beta_x \int_{-\infty}^{\infty} \frac{\mathrm{d}k}{2\pi} \frac{1}{e^{\beta_x (k^2/2 + 2n' - \mu)} - 1}, \tag{7.2.1}$$

where we have substituted $\frac{\hbar^2 k^2}{m \mu_x} \to k^2$ and made use of the relation $\frac{\sqrt{\mu_x}}{n_x} = \frac{\hbar}{\sqrt{m}} \beta_x$.

Since the integrand is even in k, we can change the lower integration boundary to 0 adding a factor 2. In order to treat the upper boundary numerically in a correct way, we split the integral into two parts, $\int_0^\infty(\cdots) = \int_0^1(\cdots) + \int_1^\infty(\cdots)$. For the second part we apply the substitution $x = k^{-1}$, which after swapping integration boundaries yields

$$n' = \frac{\beta_x}{\pi}\int_0^1 \mathrm{d}x \left\{ \frac{1}{e^{\beta_x(x^2/2+2n'-\mu)}-1} + \frac{x^{-2}}{e^{\beta_x(x^{-2}/2+2n'-\mu)}-1} \right\}. \tag{7.2.2}$$

The integral is now calculated using the composite Simpson rule, a numerical approximation scheme of fourth order, with step size $h \leq 5\cdot 10^{-4}$. It will be applied to all the other theories in the same way; in appendix C.3 the scheme and certain numerical subtleties are presented.

In figure 7.2.1 the results of the numerically calculated integral (7.2.2) is plotted for different values of the chemical potential against the thermal density, which is taken as the argument for the integral since it contains n' itself in the integrand. Because of that, it has to be solved self-consistently for every value of μ. These self-consistent solutions correspond to the crossing of the dashed line with the curves obtained from the integral in figure 7.2.1. Numerically, the calculation of the crossing point could be done recursively, $n'_{l+1} = f(n'_l)$, but certain conditions must be fulfilled for convergence. Because of that, we make use of the bisection method, which is comparably slow but globally convergent (details as well in appendix C.3). The choice of the starting interval has to be made in a proper way, because for n' slightly below the crossing the integral diverges (see figure 7.2.1) which causes numerical problems. If it is done correctly, a graphical representation of the equation of state, which is shown in figure 7.2.2, can be obtained. We see that on the dense side, the density approaches the asymptote $\mu = n/2$ and fails therefore to describe the quasi-condensate regime for which $\mu = n$. This is not surprising, since only a thermal gas without quasi-condensate is considered in this approach.

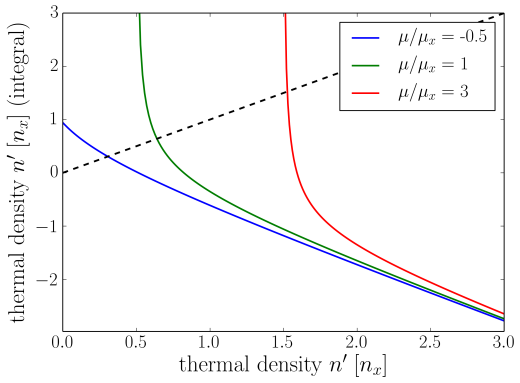

Figure 7.2.1: Numerically calculated integral (7.2.3) (Hartree-Fock theory (dilute)) vs. thermal density n' as its argument for $\beta_x = 10^{-2}$; the crossing with the dashed line corresponds to the self-consistent solution

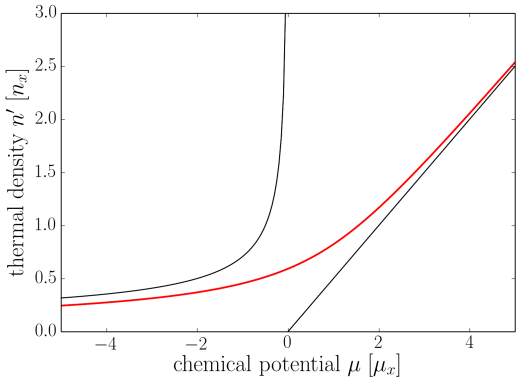

Figure 7.2.2: Numerically calculated self-consistent thermal density (Hartree-Fock theory (dilute)) and its asymptotes $n' = 1/\sqrt{-2\mu}$ (dilute side) and $n' = \mu/2$ (dense side, failing to describe the quasi-condensate regime) vs. chemical potential for $\beta_x = 10^{-2}$

Hartree-Fock theory (dense side)

In cross-over units, the thermal density is

$$n' = \beta_x \int_{-\infty}^{\infty} \frac{\mathrm{d}k}{2\pi} \frac{1}{e^{\beta_x(k^2/2+n_0)} - 1}. \tag{7.2.3}$$

We see that this integral does not need to be evaluated self-consistently. For a given value of the quasi-condensate density n_0, it can be calculated right away; the chemical potential is given by (5.1.10) in cross-over units, i.e.

$$\mu = n_0 + 2n'. \tag{7.2.4}$$

Surprisingly, for a chemical potential smaller than a certain critical value μ_c, the equations do not have a solution, whereas for larger values there are even two solution branches. This is of course not physically reasonable, there has to be an unambiguous, thus bijective relation between the chemical potential and its conjugated variable, the particle density. In order to examine which branch is the right one, we consider the compressibility. We know that for any physical system it must be positive, otherwise an increase in pressure would increase the volume as well. With some thermodynamic algebra that we leave to the appendix C.4, the compressibility may be expressed via

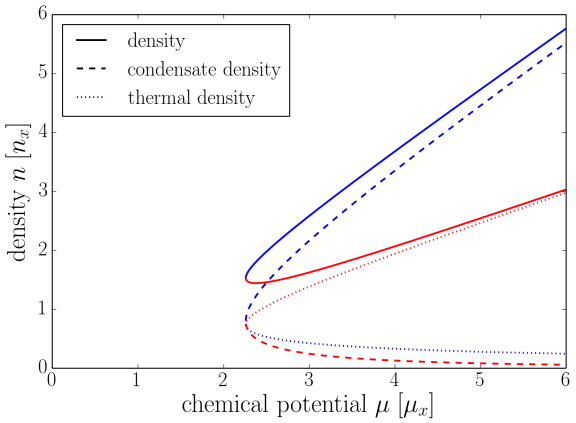

Figure 7.2.3: Both solution branches for $\beta_x = 10^{-2}$ (Hartree-Fock theory (dense)); one branch is not physically reasonable (red) since it is dominated by the thermal density

$$\kappa = -\frac{1}{V}\frac{\partial V}{\partial p}\bigg|_{T,N} = \frac{1}{n^2}\frac{\partial n}{\partial \mu}\bigg|_{V,T} \overset{!}{\geq} 0. \tag{7.2.5}$$

This relation has to be fulfilled for the whole system only, thus for the total density. We see from figure 7.2.3 that this is true for both branches (red and blue), so we cannot use this criterion here. But it has to be pointed out that the lower branch of the quasi-condensate density in figure 7.2.3 (both in red) corresponds to the upper branch of the thermal density and vice versa, such that one branch is dominated by the quasi-condensate and the other by the thermal density. For large chemical potential we expect the quasi-condensate density to be large and the thermal density to become very small, thus only the blue branch is physically reasonable and the other one has to eliminated. This means we actually can make use of the compressibility, since for the red branch of the quasi-condensate density the slope is negative. We eliminate the part of the curves where this is the case, calculating the derivative numerically with a simple finite differences scheme.

Another comment is appropriate at this point: the resemblance of the two splitting branches with the pitchfork bifurcation describing spontaneous symmetry breaking for a true condensate in figure 6.3.2 may be apparent. But this is a different situation since for the example with the Mexican hat potential, different solutions correspond to the same density. It is only the internal, not directly observable phase variable that distinguishes one solution from the other.

Modified Popov theory

Realising that $\frac{1}{e^x-1}+\frac{1}{2}=\frac{1}{2}\coth(\frac{x}{2})$, the thermal density for Modified Popov theory scaled to cross-over units may be written as

$$n' = \beta\sqrt{n_0}\int_{-\infty}^{\infty}\frac{\mathrm{d}k}{2\pi}\left\{\frac{|k|\coth\left(\frac{1}{2}\beta_x n_0|k|\left(k^2/4+1\right)^{1/2}\right)}{4\left(k^2/4+1\right)^{1/2}}-\frac{1}{2}+\frac{1}{k^2+2\mu/n_0}\right\}, \tag{7.2.6}$$

while the chemical potential is determined by (7.2.4). The are two parts of the integral that can actually be solved exactly (see appendix 7.3), the rest is evaluated numerically (see appendix C.3 for details). The easiest way of proceeding is to choose a value for the quasi-condensate density n_0 rather than the chemical potential μ and to solve (7.2.6) self-consistently replacing the chemical potential by (7.2.4). In this way we avoid having to calculate two roots which can get very complicated. Especially when both roots are close together, i.e. close to the critical point, a proper choice of the starting interval is very tedious. For the method mentioned above, this problem does not arise since for every n_0 there is only one possible self-consistent value for the thermal density.

Once the self-consistent value is obtained, we use again equation (7.2.4) to calculate the chemical potential that describes a curve with a minimum (as a function of n_0, see figure 7.2.4), resulting again in two solution branches of different densities for a given chemical potential. One of them is removed as before reestablishing bijectivity, such that we get the graphs presented in figure 7.2.5.

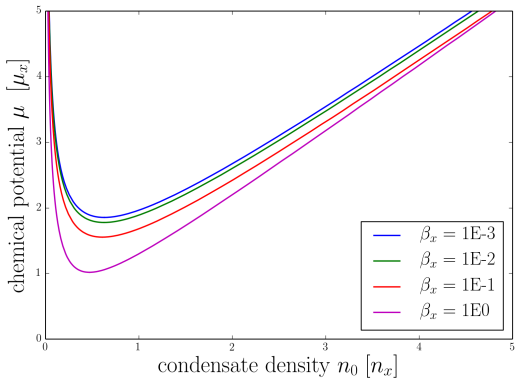

Figure 7.2.4: Chemical potential as function of the numerically calculated quasi-condensate density (Modified Popov theory) for different temperatures exhibiting a minimum which corresponds to the critical point

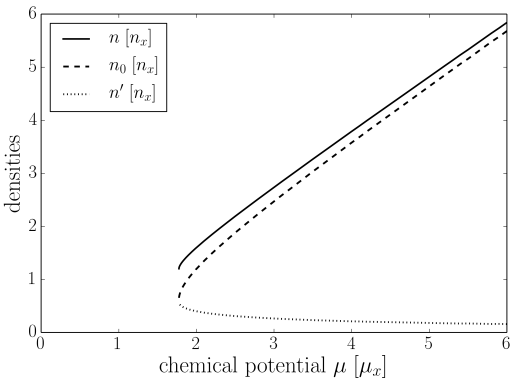

Figure 7.2.5: Numerically calculated self-consistent densities (Modified Popov theory) vs. chemical potential for $\beta_x = 10^{-2}$

Mora-Castin theory

Since the thermal density for Mora-Castin theory (scaled to cross-over units),

$$n' = \beta\sqrt{\mu} \int_{-\infty}^{\infty} \frac{\mathrm{d}k}{2\pi} \left\{ \frac{|k| \coth\left(\frac{1}{2}\beta_x \mu |k| \left(k^2/4+1\right)^{1/2}\right)}{4\left(k^2/4+1\right)^{1/2}} - \frac{1}{2} \right\}, \tag{7.2.7}$$

is equivalent to the first part of (7.2.6) (being a function of μ instead of n_0), it can be evaluated numerically in the same way. Like for Hartree-Fock theory (dense), the integral does not have to be calculated self-consistently for a given value of μ though, and there is only one solution branch (see figure 7.2.6). For small chemical potential however, the density gets negative and diverges for $\mu \to 0$. On the other side, the thermal density attains negative values for large chemical potentials (see right of figure 7.2.6). For Modified Popov theory, this does not happen, which suggests that the term stemming from the regularization of the coupling constant (5.2.13) prevents this. Mora-Castin theory exhibits thus two critical points (see as well chapter 7.3).

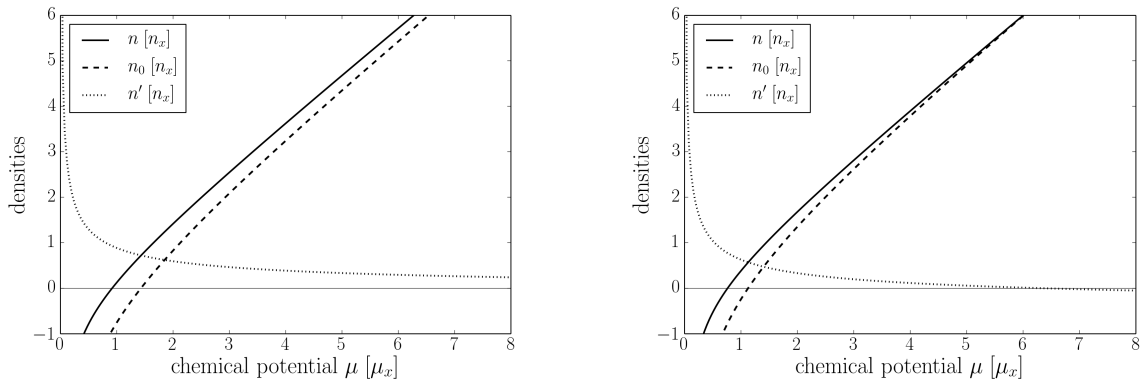

Figure 7.2.6: Numerically calculated self-consistent densities (Mora-Castin theory) vs. chemical potential for $\beta_x = 10^{-2}$ (left) and $\beta_x = 10^{-1}$ (right); for larger β_x, the second critical point at which the thermal density becomes negative is reached for smaller chemical potential.

Walser theory

Finally, we give the expressions of the thermal density and the anomalous average of Walser theory in cross-over units:

$$n' = \beta_x \sqrt{n_0} \int_{-\infty}^{\infty} \frac{dk}{2\pi} \left\{ \frac{\frac{k^2}{4} + \frac{1}{2}\left(1 - \frac{m'}{n_0}\right)}{\left[\left(\frac{k^2}{4}+1\right)\left(\frac{k^2}{4} - \frac{m'}{n_0}\right)\right]^{1/2}} \coth\left(\beta_x n_0 \left[\left(\frac{k^2}{4}+1\right)\left(\frac{k^2}{4} - \frac{m'}{n_0}\right)\right]^{1/2}\right) - \frac{1}{2} \right\} \tag{7.2.8}$$

$$m' = -\beta_x \sqrt{n_0} \int_{-\infty}^{\infty} \frac{dk}{2\pi} \frac{\frac{1}{2}\left(1 + \frac{m'}{n_0}\right)}{\left[\left(\frac{k^2}{4}+1\right)\left(\frac{k^2}{4} - \frac{m'}{n_0}\right)\right]^{1/2}} \coth\left(\beta_x n_0 \left[\left(\frac{k^2}{4}+1\right)\left(\frac{k^2}{4} - \frac{m'}{n_0}\right)\right]^{1/2}\right) \tag{7.2.9}$$

$$\mu = n_0 + 2n' + m'. \tag{7.2.10}$$

Choosing a value for the quasi-condensate density n_0, m' has to be calculated self-consistently from (7.2.9). Again there exists a bijective relation between these two quantities (see figure 7.2.7), avoiding numerical complications. The thermal density n' is obtained by calculating the integral (7.2.8) numerically, and eventually the chemical potential μ from (7.2.10). Numerical details are given in appendix C.3 and figure 7.2.8 shows the results. It is actually the only theory for which thermal and quasi-condensate density are not equal at the critical point, but for higher chemical potential, due to the non-vanishing anomalous average.

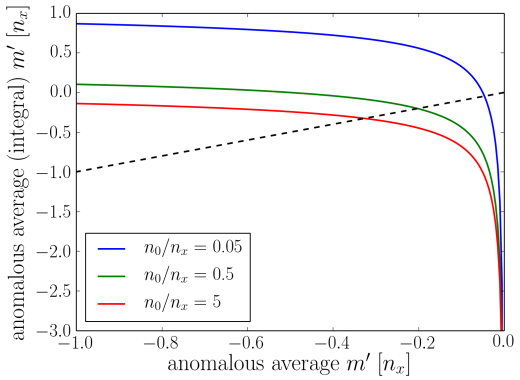

Figure 7.2.7: Numerically calculated integral (7.2.9) (Walser theory) vs. anomalous average m' as its argument for $\beta_x = 10^{-2}$; the crossing with the dashed line corresponds to the self-consistent solution

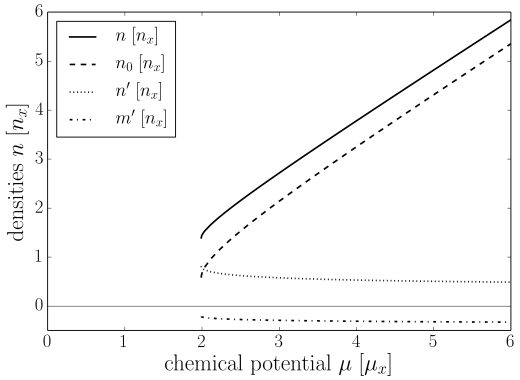

Figure 7.2.8: Numerically calculated self-consistent densities (Walser theory) vs. chemical potential for $\beta_x = 10^{-2}$

7.3 High-temperature expansions and critical points

We have seen that it is possible to solve the self-consistent equations by calculating the integrals numerically; this is quite costly in terms of computer performance. In order to reduce the computational effort and also to get a clearer picture of the structure of the equations and therefore the underlying physics, we provide simple approximations of the integrals. The cross-over region being the regime that we want to focus on, we consider the temperature or, more precisely, the degeneracy as explained in 7.1, to be relatively high $\beta_x \ll 1$. This allows us to get expansions in powers of β_x.

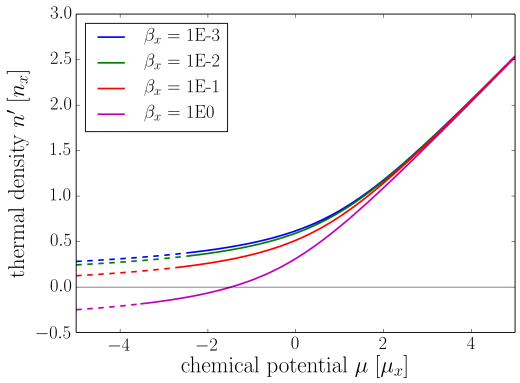

Figure 7.3.1: High-temperature approximation (7.3.2) (Hartree-Fock theory (dilute)) evaluated numerically with the bisection method (dashed) and exactly with Cardan formulae (solid)

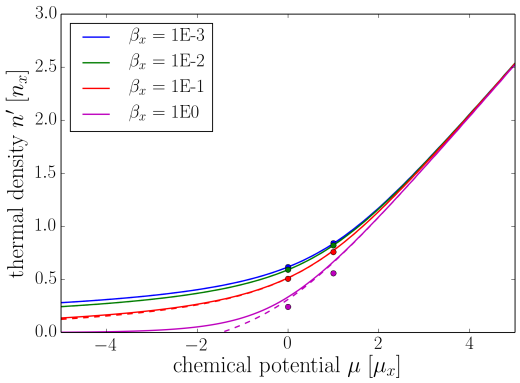

Figure 7.3.2: Numerically calculated density (solid) of Hartree-Fock theory (dilute) compared to its high-temperature approximation (dashed) with cross-over points from table 7.2 and equation (7.3.4)

Having a close look at the integrals of both Hartree-Fock theories, we see that they are quite similar to those appearing in section 2 of the ideal gas. As a matter of fact, we can use the results already obtained by identifying (7.2.1) and (7.2.4) as Bose-Einstein integrals (apart from prefactors), which gets clear if we apply the substitution $\beta k^2/2 = x$,

$$n' = \frac{1}{\pi}\sqrt{\frac{\beta_x}{2}}\int_0^\infty \mathrm{d}x \frac{x^{-1/2}}{e^\alpha e^x - 1} = \sqrt{\frac{\beta_x}{2\pi}}\, g_{1/2}\left(e^{-\alpha}\right), \tag{7.3.1}$$

where $\alpha_{HF^-} = \beta_x(2n' - \mu)$ or $\alpha_{HF^+} = \beta_x n_0$ for Hartree-Fock theory (dilute) and (dense), respectively. Since β_x is small and hence α as well (densities $\sim \mathcal{O}(1)$ near cross-over), the Bose function can be expanded with (A.1.4), yielding:

$$n' = \sqrt{\frac{\beta_x}{2\pi}}\left(\sqrt{\frac{\pi}{\alpha}} + \zeta(1/2) - \zeta(-1/2)\alpha + \mathcal{O}(\alpha^2)\right). \tag{7.3.2}$$

These formulas can be evaluated in the same way as the integral equations before, i.e. with the bisection method (not necessary for Hartree-Fock theory (dense) of course). Alternatively, it is actually possible for Hartree-Fock theory (dilute) to get an exact analytic expression (considering contributions up to $\mathcal{O}(\sqrt{\beta_x})$) for the self-consistent solution. For that, (7.3.2) is transformed into an equation cubic in n', which can be solved with the Cardan formulae. Although this is not really of practical use for the equation of state since it is not applicable for the whole parameter range, it is a good way of validating our numerical methods (see figure 7.3.1). In appendix C.5 it is explained how the solution can be obtained. The high-temperature expansions provide a very good approximation for small values of β_x (see figure 7.3.2). For larger $\beta_x \geq 1$, the approximation is not satisfying as expected.

For the other theories, the expansion is more involved. The hyperbolic cotangent $\coth(x)$ appearing in the integrals cannot be expanded right away because there is a finite difference between it and its small-β_x approximation $1/x$ for large x, leading to an UV-convergence

problem for the next order in the expansion. We will leave it to the appendix C.6 to show that with some appropriate additions and subtractions the integrals can be split into convergent parts in the high-temperature limit. The resulting expressions have a similar structure: an expansion in β_x with coefficients a_1, a_2 involving zeta-functions (see table 7.1). For Modified Popov theory (equation (C.6.15)) and Walser theory (anomalous average, equation (C.6.36)), the calculation of the correction of order $\mathcal{O}(\beta_x^{1/2})$ is done numerically. In both cases, the result is approximately a multiple of $\zeta(-1/2)/\sqrt{2\pi}$ and we replace therefore the coefficients by these values (for the other theories, the coefficients have been calculated exactly), such that we have for all theories

$$a_1 = \frac{\zeta(1/2)}{\sqrt{2\pi}} \approx -0.58260, \qquad a_2 = -\frac{\zeta(-1/2)}{\sqrt{2\pi}} + \mathcal{O}(10^{-5}) \approx 0.08294. \tag{7.3.3}$$

Theory	thermal density n'
ideal Bose gas	$\frac{1}{\sqrt{-2\mu}} + a_1\beta_x^{1/2} - 2a_2\mu\beta_x^{3/2}$
Hartree-Fock (dilute)	$\frac{1}{\sqrt{2(2n'-\mu)}} + a_1\beta_x^{1/2} + a_2(2n'-\mu)\beta_x^{3/2}$
Hartree-Fock (dense)	$\frac{1}{\sqrt{2n_0}} + a_1\beta_x^{1/2} + a_2 n_0\beta_x^{3/2}$
Modified Popov	$\frac{1}{2\sqrt{n_0}} + a_1\beta_x^{1/2} + \frac{1}{2}\frac{n_0}{\sqrt{2\mu}}\beta_x + a_2 n_0\beta_x^{3/2}$
Mora-Castin	$\frac{1}{2\sqrt{\mu}} + a_1\beta_x^{1/2} + a_2\mu\beta_x^{3/2}$
Walser	$\left(1+\sqrt{\frac{n_0}{-m'}}\right)\frac{1}{4\sqrt{n_0}} + a_1\beta_x^{1/2} + a_2(n_0+m')\beta_x^{3/2}$ $m' = \left(1-\sqrt{\frac{n_0}{-m'}}\right)\frac{1}{4\sqrt{n_0}} + 2a_2(n_0+m')\beta_x^{3/2}$

Table 7.1: Small-β_x expansion of the thermal density for different mean-field theories up to order $\mathcal{O}(\beta_x^{5/2})$ (with colours denoting different orders of β_x)

The approximations all reproduce the results obtained by numerical integration with very good accuracy; for example, for Hartree-Fock theory (dense), the numerically calculated accuracy (relative deviation averaged over the region of the plots) is of order $\mathcal{O}(10^{-5})$ for $\beta_x = 10^{-3}$ and $\mathcal{O}(10^{-3})$ for $\beta_x = 10^{-1}$. As expected, for higher $\beta_x \geq 1$, the approximations get worse, especially for smaller values of the chemical potential (see figures 7.3.2, 7.3.3, 7.3.4; for similar figures of Mora-Castin theory and Hartree-Fock theory (dense) see appendix C.6). Since on the dense side of the cross-over the curve approaches the quasi-condensate limit $\mu = n$ (cross-over units) independently of the theory[1] and the actual β_x, the approximations are more accurate in this regime.

The way we have treated the equations of Hartree-Fock theory can be applied to the ideal Bose gas as well. Table 7.1 shows that the approximation that we have made before in section 2.3

[1] Apart from Hartree-Fock theory (dilute) of course.

for the degenerate regime actually corresponds to the zero-th order of the high-temperature expansion. For β_x sufficiently small, it yields good results (see figure C.6.2 in appendix C.6). The structural resemblance to the mean-field theories, especially with Mora-Castin theory, becomes apparent.

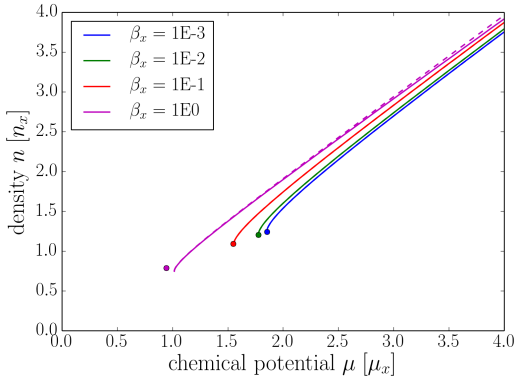

Figure 7.3.3: High-temperature approximation (dashed) with critical points (dots) compared to numerically calculated integrals (Modified Popov theory)

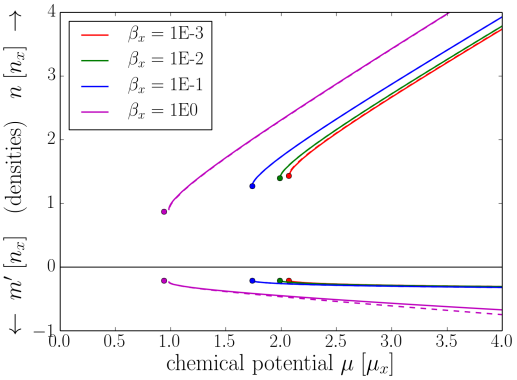

Figure 7.3.4: Numerically calculated density and anomalous average (Walser theory) compared to its high-temperature approximations (dashed) with critical points (dots)

We can make use of the above expansions in order to easily get approximations of characteristic values for the corresponding theory. Above all, the points where some theories stop to work, i.e. the critical points, are of interest. The slope of the density, that is the compressibility, gets infinite at these points, which allows us to obtain their values (in practice we use the quasi-condensate density or the anomalous average to calculate the slope, see appendix C.7). For the ideal Bose gas, the critical point is actually $\mu_c = 0$, since the density diverges there. Mora-Castin theory works for all positive values $\mu > 0$, but the density attains negative values for small chemical potentials and therefore we consider the point where $n_c = 0$ as the critical point. As a matter of fact, Mora-Castin theory has a second critical point above which (in terms of higher chemical potential) the thermal density becomes negative (see appendix C.7; in table 7.2 both critical points - the lower and the upper one - are given). Hartree-Fock theory (dilute) does not exhibit a critical point, but we can compute the cross-over density $n(\mu = 0)$ instead (see appendix C.5 for details). All results are summarized in table 7.2 and we observe from figures 7.3.3 and 7.3.4 that they yield good approximations for small $\beta_x \leq 10^{-1}$.

Theory	critical points	
	chemical potential μ_c	density n_c
ideal Bose gas	0	∞
Hartree-Fock (dilute)	≈ 0	$\overbrace{2^{-2/3}}^{\approx 0.63} + \frac{2}{3} a_1 \beta_x^{1/2}$
Hartree-Fock (dense)	$\overbrace{3 \cdot 2^{-1/3}}^{\approx 2.38} + 2 a_1 \beta_x^{1/2}$	$\overbrace{2^{2/3}}^{\approx 1.59} + a_1 \beta_x^{1/2}$
Modified Popov	$\overbrace{3 \cdot 2^{-2/3}}^{\approx 1.89} + 2 a_1 \beta_x^{1/2} + \mathcal{O}(\beta_x)$	$\overbrace{2^{1/3}}^{\approx 1.26} + a_1 \beta_x^{1/2} + \mathcal{O}(\beta_x)$
Mora-Castin (lower)	$2^{-2/3} + a_1 \beta_x^{1/2}$	0
(upper)	$(4a_1^2 \beta_x)^{-1} \left(1 + a2/(4a_1^2)\right)^{-2} + \mathcal{O}(\beta_x)$	μ_{c2}
Walser	$\approx 2.11 + 2 a_1 \beta_x^{1/2}$	$\approx 1.45 + a_1 \beta_x^{1/2}$

Table 7.2: Critical points (cross-over point for Hartree-Fock (dilute)) of different mean-field theories up to order $\mathcal{O}(\beta_x^{3/2})$ (with colours denoting different orders of β_x; see appendix C.7 for details); for Mora-Castom theory, both upper and lower critical values are given; for Walser theory, the critical anomalous average is $m_c' \approx -0.21 + \mathcal{O}(\beta_x^{3/2})$.

As a matter of fact, we have defined the cross-over units in a way that the cross-over occurs obviously at $\mu_{\text{co}} = n_{\text{co}} = 1$ (see section 7.1). In order to obtain the cross-over density of Hartree-Fock theory, we should therefore rather take the density at $\mu = 1$. This can be done in very similar way as showed in appendix C.5 for $\mu = 0$, yielding the approximate result

$$n_{\text{co}} \approx 0.85 + \frac{2}{3} a_1 \beta_x^{1/2}. \tag{7.3.4}$$

We have used expressions of the ideal Bose gas in order to define these units however. If we want to estimate where the cross-over takes place by considering mean-field data only (thus taking interactions into account), we may calculate the crossing of the asymptotes of the curves that we consider correct for the corresponding regime, that is the quasi-condensate limit on the dense side and Hartree-Fock theory (dilute) on the dilute side. We plug therefore the quasi-condensate relation $n = \mu$ into $n = 1/\sqrt{2(2n - \mu)}$. This yields

$$n_{\text{co}} = \mu_{\text{co}} = 2^{-2/3} \approx 0.63, \tag{7.3.5}$$

which is lower than what the definition of the units implies. It is of the same order though, affirming that we do describe the cross-over from a degenerate Bose gas to a quasi-condensate.

We want to refer quickly to the analogy with spontaneous symmetry breaking again in order to shade some light on the nature of the critical points. For a true condensate, there exists a phase transition at which the condensate density starts to grow (abruptly) from zero, corresponding

to the bifurcation seen for spontaneous symmetry breaking. Similar to that, one could argue that for the mean-field theories the quasi-condensate density just drops to zero at the critical point. We know that in one dimension there is no phase transition though, and we observe as well that the critical quasi-condensate density predicted by the mean-field theories is in fact non-zero (except for Mora-Castin theory (by definition)). The critical points can still be seen as a reasonable approximation for the point where the cross-over takes place, but the quasi-condensate density should be continued smoothly for smaller chemical potential. Formally, the reason for the critical points is that the chemical potential behaves close to this point for all theories (exhibiting a critical point) like

$$\mu \sim \frac{a}{\sqrt{n_0}} + bn_0, \tag{7.3.6}$$

which obviously has a minimum $n_0 > 0$ (with $a, b > 0$ some coefficients depending on the theory).

7.4 Correlation functions

Correlation functions are key elements of understanding any complex system, quantifying the relation between different parts or aspects of it. We have seen already in chapter 3 that they are of great importance when it comes to deciding if BEC actually has occurred and in which regime the system is in. The special case of $z = z'$ of the first order correlation function is the density that we have analysed in the previous chapter, its analogue of the second order correlation function are density fluctuations.

7.4.1 First order correlation function

The first order spatial correlation function may be written with the splitting (4.0.1) of the field operator as

$$g_1(z, z') = \langle \Psi^\dagger(z)\Psi(z')\rangle = \phi(z)\phi(z') + \langle \delta\psi^\dagger(z)\delta\psi(z')\rangle. \tag{7.4.1}$$

For a homogeneous system, only the difference of the two arguments is important. We can set one of them to zero without loss of generality and write

$$g_1(z) = n_0 + \underbrace{\langle \delta\psi^\dagger(0)\delta\psi(z)\rangle}_{n'(z)}. \tag{7.4.2}$$

The expectation value on the right hand side can be calculated in the same way as the thermal density n', only that the integral now includes an additional exponential e^{ikz}. Since the rest of the integrand is even in k, only the (also even) real part of it survives the integration from

$-\infty \to \infty$. The distance z appearing in the correlation functions is scaled to cross-over units using (7.1.4). We end up with integrals of the form (we give that of Walser theory)

$$n'(z) = \beta_x \sqrt{n_0} \int_{-\infty}^{\infty} \frac{dk}{2\pi} \left\{ \frac{\frac{k^2}{4} + \frac{1}{2}\left(1 - \frac{m'}{n_0}\right)}{\left[\left(\frac{k^2}{4}+1\right)\left(\frac{k^2}{4} - \frac{m'}{n_0}\right)\right]^{1/2}} \coth\left(\beta_x n_0 E(k)\right) - \frac{1}{2} \right\} \cos\left(\beta_x \sqrt{n_0} k z\right). \tag{7.4.3}$$

This procedure corresponds to the Hartree-Fock Bogoliubov and therefore the symmetry breaking approach. Fixing the phase of the condensate eliminates its influence on the first order correlation function, as can be seen from equation 7.4.2. In lower dimensions, phase fluctuations play a crucial role though, it is therefore not expected that 7.4.2 can capture the physics of a quasi-condensate. For Mora-Castin and Modified Popov theory, the authors derive other expressions for $g_1(z)$, relating it directly to phase fluctuations. In [79], $g_1(z)$ is associated to phase fluctuations of the quasi-condensate only; the relation that we have already found in section 3.2 (equation (3.3.5)) therefore reads (for a homogeneous system in Modified Popov theory) for large distances z

$$g_1(z) = n_0 e^{-\langle[\vartheta(0)-\vartheta(z)]^2\rangle/2}. \tag{7.4.4}$$

The exponent is evaluated using equation (5.2.7), which has to be renormalised in the same way as done for the density and the chemical potential, yielding

$$\langle[\vartheta(0) - \vartheta(z)]^2\rangle = \int_{-\infty}^{\infty} \frac{\mathrm{d}k}{2\pi} \left\{ \left[\frac{g}{E(k)} \coth(\beta E(k)/2) + \frac{g}{2\epsilon(k) + 2\mu} \right] (1 - \cos(kz)) \right\}. \tag{7.4.5}$$

The factor involving the cosine actually cancels the IR-divergence here. The whole correlation function scaled to cross-over units eventually reads

$$g_1(z) = n_0 \exp\left(-\frac{\beta_x}{2\sqrt{n_0}} \int_{-\infty}^{\infty} \frac{\mathrm{d}k}{2\pi} \left\{ \left[\frac{\coth\left(\beta_x n_0 \sqrt{k^2(k^2+1)}\right)}{\sqrt{k^2(k^2+1)}} - \frac{1}{k^2 + \frac{\mu}{2n_0}} \right] (1 - \cos(2\beta_x \sqrt{n_0} k z)) \right\} \right). \tag{7.4.6}$$

Mora and Castin derive a similar expression in [27], although their treatment is much more involved. They leave the density inside the expectation value $\langle \Psi^\dagger(0)\Psi(z)\rangle$ and expand it up to second order in the density fluctuations δn. The exponential involving the phase difference is treated exactly, expanding it in an infinite series, taking the thermal expectation value of all terms using Wick's theorem and then summing up the resulting series exactly. Finally, they include corrections stemming from the third order Hamiltonian H_3, which amounts to replacing the (quasi-)condensate density n_0 by the complete density n. For large distances, they can

reproduce previous findings [19] and their result can be related to standard Bogoliubov theory. $g_1(z)$ therefore involves an integral similar to (4.3.4) whose IR-divergence is again cancelled by a cosine factor; in cross-over units it reads

$$g_1(z) = n \exp\left(-\frac{\beta_x \sqrt{\mu}}{n} \int_{-\infty}^{\infty} \frac{\mathrm{d}k}{2\pi} \left\{ \frac{k^2/2+1}{2\sqrt{k^2(k^2/4+1)}} \coth\left(\frac{\beta_x \mu}{2} \sqrt{k^2(k^2/4+1)} \right) \right\} (1 - \cos(\beta_x \sqrt{\mu} k z)) \right). \tag{7.4.7}$$

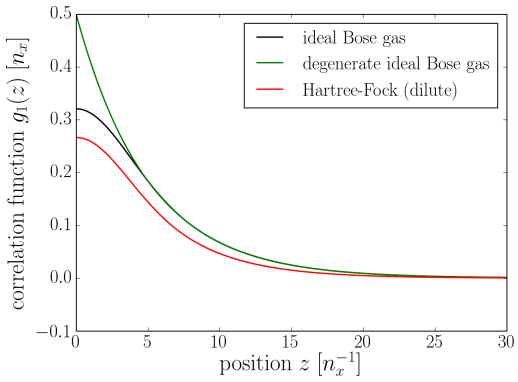

Figure 7.4.1: First order correlation function $g_1(z)$ of Hartree-Fock theory (dilute) compared to the ideal Bose gas at $\mu = -2\mu_x$ and $\beta_x = 10^{-1}$

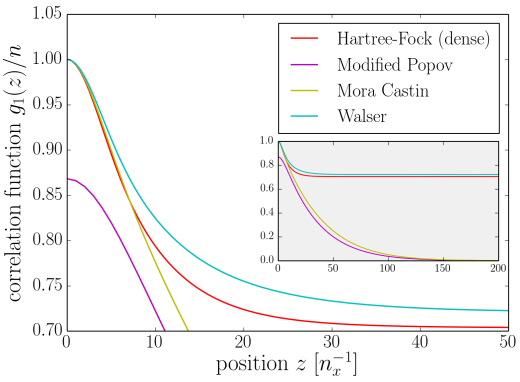

Figure 7.4.2: Normalised first order correlation function $g_1(z)/n$ for different mean-field theories at $\mu = 2.1\,\mu_x$ and $\beta_x = 10^{-1}$; for $z \to \infty$ it approaches n_0/n for Hartree-Fock and Walser theory, whereas for Mora-Castin and Modified Popov theory it approaches zero, predicting respectively the presence or absence of a true quasi-condensate

The numerical calculation is done for all theories using the self-consistent values of the densities and chemical potential obtained earlier. It turns out that the correlation function (2.3.5) of the degenerate ideal Bose gas is actually a good approximation of the ideal Bose gas' result obtained numerically (see lhs of figure 7.4.1). While it reproduces almost exactly the same curve for large distances, it gives higher values near zero and a non-vanishing slope at the origin. That is why the density of the degenerate gas is higher as we have seen already when we examined the high-temperature expansions (see figure C.6.2).

The correlation length of the degenerate gas, which in cross-over units actually is $l_\vartheta = 1/(\sqrt{-2\mu}\beta_x) = n/\beta_x$, underestimates therefore the typical length scale of the decay (see figure 7.4.3). For the mean-field theories using the HFB approach for the determination of $g_1(z)$, this length is obtained by calculating numerically (bisection method) the drop off to $1/e$ of $(g_1(z) - n_0)/n'$, whereas for Mora-Castin $g_1(z)/n$ and for Modified Popov theory $g_1(z)/n_0$ is taken. We observe that for Hartree-Fock theory (dilute) it scales like the degenerate Bose gas with $\sim n/\beta_x$ (see inlay of figure 7.4.3) and coincides with the ideal Bose gas result, with an off-set being the only difference between these two and the degenerate gas.

The mean-field theories show two different types of behaviour with respect to the spatial dependence of $g_1(z)$ for large distances. For the first group of theories (Hartree-Fock (dense) and Walser), it approaches the value n_0, whereas for the second group (Mora-Castin and

Modified Popov) it vanishes in the limit $z \to \infty$ (see figure 7.4.3). According to criterion (3.3.8), the first group predicts therefore the presence of a true condensate, which we know does not exist in one-dimensional homogeneous systems. The second group is capable of describing this fact, only a quasi-condensate exists and hence there is no long-range order. It must be emphasized though that the behaviour of the second group should not be put on a equal footing with that of the ideal Bose gas (or Hartree-Fock theory (dilute)) for which $g_1(z \to \infty)$ vanishes, too. This is of course due to the fact that there is only thermal density for these theories and consequently $n_0 = 0$.

As we have seen before, it is the different treatment of phase fluctuations that is responsible for the different behaviour of $g_1(z)$. For the first group, phase fluctuations are excluded from g_1 by means of the symmetry breaking approach, whereas for the second group the phase is incorporated in the exponential with some extra effort. The phase coherence is only local in the quasi-condensate, which means that its coherence properties can only be captured on this length scale by the symmetry breaking approach. The similar decay of g_1 (of the two different groups) near the origin (see figure 7.4.2) affirms this.

The density of Mora-Castin theory is negative for $\mu < \mu_c$ and therefore the exponential in equation (7.4.7) leads to an increasing correlation function ($g_1(z > 0)/|n| > 1$). Because of this, we plot only values beyond the critical point in figure 7.4.3. We observe that Mora-Castin and Modified Popov theory are the only ones that can capture the fact that condensation actually enhances coherence and thus the coherence length should increase with growing quasi-condensate density. Contrary to that, the correlation length decreases for Hartree-Fock and Walser theory (see rhs of figure 7.4.3, plotting against chemical potential or density is almost equivalent here). For the latter, the approach of $g_1(z)$ to a non-zero plateau for large distances corresponds to an infinite phase correlation length of the true condensate that is predicted. The decay of $g_1(z)$ characterises therefore only the thermal part of the gas, which manifests in linear scaling of the coherence length with the thermal density (not shown).

Completing this subsection, we may conclude that Mora-Castin and Modified Popov theory are able to describe the phase coherence properties of an one-dimensional quasi-condensate. For the latter, $g_1(0)$ does not yield the whole, but only the quasi-condensate density. The difference between them is negligible for a "fully quasi-condensed" system though and originates, as seen from Mora-Castin theory, from not taking higher orders of the Hamiltonian into account.

7.4.2 Equation of state

As we have seen before, the first order correlation function g_1 at zero distance yields the density as a function of the chemical potential, in this context called the equation of state. We have already analysed it in detail for the different theories in section 7.2 and therefore we focus on the comparison of the results here.

Hartree-Fock theory (dilute) is the only one that is actually capable of producing results for the cross-over region (figure 7.4.5). For large negative chemical potential, it approaches the ideal Bose gas solution and can therefore be considered reasonable in this regime because in a very dilute system the particles hardly interact with each other. But since it does not take

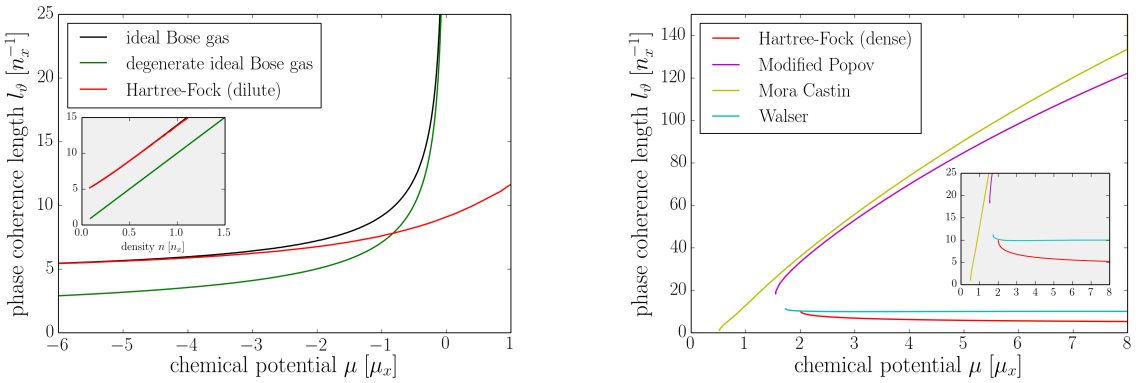

Figure 7.4.3: Phase coherence length vs. chemical potential for $\beta_x = 10^{-1}$; on the dilute side (left), Hartree-Fock theory (dilute) approaches the ideal Bose gas results, the degenerate gas is shifted by a constant to lower values; on the dense side (right) the length decreases for growing chemical potential for Hartree-Fock (dense) and Walser theory, for Mora-Castin and Modified Popov theory it increases

the particles in the quasi-condensate into account, it is in the strict sense applicable to the dilute side only, which manifests in a wrong slope on the dense side. As a matter of fact, it is the factor 2 that appears within the Hartree-Fock approximation that leads to the asymptote $\mu \sim n/2$.

All mean-field theories that do not neglect the condensed particles exhibit a critical point below which there is no density defined or, in case of Mora-Castin theory, the density attains negative values (and finally diverges). We want to emphasize again that this critical point has no physical origin since there is no phase transition in one-dimensional systems which is confirmed by the exact solution of Yang Yang (see section 3.4). The reason for this is the violation of the initial assumption that the field operator describing the quasi-condensate can be replaced by a complex number. Approaching the cross-over in fact amounts to increasing the healing length ξ and decreasing the phase coherence length l_ϑ, until $l_\vartheta \gg \xi$ is not satisfied anymore. But this condition was the basis of the justification of the symmetry breaking approach that has been applied. It is therefore natural that the mean-field theories are not capable of quantifying the quasi-condensate density in this region.

Still all these theories work reasonably well in the quasi-condensate regime. The density approaches the asymptote $n = \mu$, the thermal fraction of the density goes to zero whereas the quasi-condensate fraction reaches one in this limit (see figure 7.4.4). In order to get a full description of the cross-over in the mean-field approach, it seems therefore natural to combine different theories, namely Hartree-Fock theory (dilute) with another mean-field theory for the dense side. The choice of the most appropriate theory may be made on the basis of how close its results are to those of the exact theory of Yang Yang or, as we are going to do in part III, those of the stochastic model. We might as well decide by examining how close the mean-field theory in consideration comes to Hartree-Fock theory (dilute). For that, we calculate the jump between the densities at the corresponding critical point using Cardan formulae. This yields in lowest order

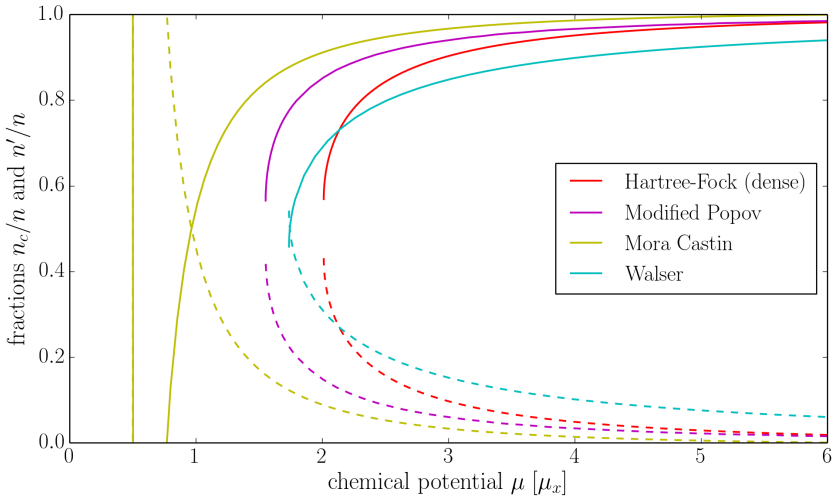

Figure 7.4.4: Quasi-condensate fraction n_0/n (solid) and thermal fraction n'/n (dashed) for different mean-field theories for $\beta_x = 10^{-1}$

$$\Delta n(\mu_c) \approx \begin{cases} 0.256\, n_x & \text{Hartree-Fock (dense)} \\ 0.122\, n_x & \text{Modified Popov} \\ 0.230\, n_x & \text{Walser.} \end{cases} \tag{7.4.8}$$

In this way of thinking, the best theory would be of course that of Mora-Castin. There is no jump in the density, the two curves cross each other more or less at the cross-over which is another argument for its suitability. The actual crossing point can be calculated by equating the two equations of state, but due to the self-consistence condition it is difficult to get a reasonably good (universal) approximation of it. For the example that we have chosen for most of the calculations, $\beta_x = 10^{-1}$, the crossing is approximately at $\mu \approx 1.10\,\mu_x$ and $n \approx 0.80\,n_x$.

7.4.3 Second order correlation function

The second order correlation function (3.3.6) is an important quantity that permits to identify the regime of the Bose gas in consideration. Moreover, it is closely related to density fluctuations and it is linked to the structure factor $S(k)$, which is an important quantity that can be measured in scattering experiments, via

$$S(k) = \int_L \mathrm{d}z\, \left(g_2(z) - n^2\right) e^{-ikz}. \tag{7.4.9}$$

Its evaluation is carried out again by separating the field operator and assuming Gaussian statistics for the thermal contribution. In this way moments of odd numbers of operators vanish, leading for a homogeneous gas eventually to

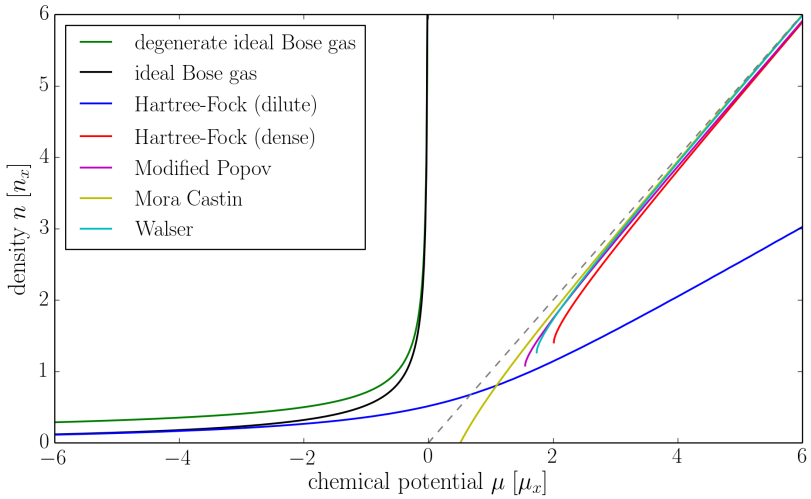

Figure 7.4.5: Equation of state for different mean-field theories and the ideal Bose gas for $\beta_x = 10^{-1}$

$$g_2(z) = \langle \Psi^\dagger(0)\Psi(0)\Psi^\dagger(z)\Psi(z)\rangle = n^2 + 2n_0 \,\mathrm{Re}\,\big(\overbrace{\langle \delta\psi^\dagger(0)\delta\psi(z)\rangle}^{n'(z)} + \overbrace{\langle \delta\psi(0)\delta\psi(z)\rangle}^{m'(z)}\big) + |\langle \delta\psi^\dagger(0)\delta\psi(z)\rangle|^2 + |\langle \delta\psi(0)\delta\psi(z)\rangle|^2. \tag{7.4.10}$$

It contains terms that are similar to n' with an additional space dependence (an additional factor $\cos(kz)$), just as we have seen it for the first order correlation function, and terms similar to m' as well (we use therefore the notation $n'(z)$ and $m'(z)$ in table 7.3). For the calculation of $g_2(z)$ these higher moments are taken into account depending on the theory in a similar way we have described before in 6.2. For Mora-Castin and Modified Popov theory, the treatment differs again a bit from the Hartree-Fock Bogoliubov approach. The calculus in discrete space of the former gives rise to a result in which $n'^2(z)$ is not present and n_0 is replaced by n as for $g_1(z)$ (if compared to the expression that would correspond to using equation (7.4.10)). For Modified Popov theory, the anomalous average is taken into account (although for the calculation of the density it is neglected, see 6.2) for the evaluation of $g_2(z)$ in [79], but it is identified with the quadratic contribution of the phase fluctuations and therefore eliminated in order to remove the IR-divergences. The result is therefore equal to that corresponding to the HFB treatment of equation (7.4.10) with $m'(z) = 0$. In table 7.3 all results are summarised.

Theory	$g_2(z)$	$g_2(0)/n^2$	density fluctuations $\delta^2 n$
ideal Bose gas	$n'^2 + \lvert n'(z)\rvert^2$	2	n'^2
Hartree-Fock (dilute)	$n'^2 + \lvert n'(z)\rvert^2$	2	n'^2
Hartree-Fock (dense)	$n^2 + 2n_0 \operatorname{Re} n'(z) + \lvert n'(z)\rvert^2$	$2 - \frac{n_0^2}{n^2}$	$2n_0 n' + n'^2$
Modified Popov	$n^2 + 2n_0 \operatorname{Re} n'(z) + \lvert n'(z)\rvert^2$	$2 - \frac{n_0^2}{n^2}$	$2n_0 n' + n'^2$
Mora-Castin	$n^2 + 2n \operatorname{Re} n'(z)$	$2 - \frac{n_0 - n'}{n}$	$2n_0 n' + 2n'^2$
Walser	$n^2 + 2n_0 \operatorname{Re}(n'(z) + m'(z)) + \lvert n'(z)\rvert^2 + \lvert m'(z)\rvert^2$	$2 - \frac{n_0^2 - (2n_0 + m')m'}{n^2}$	$2n_0(n' + m') + n'^2 + m'^2$

Table 7.3: Second order correlation function and density fluctuations of different mean-field theories

Comparing (7.4.10) to the expression of $g_1(z)$ (7.4.2), we can establish a relation between the two correlation functions:

$$g_2(z) = n^2 - n_0^2 + g_1^2(z) + 2n_0 \operatorname{Re} m'(z) + |m'(z)|^2. \tag{7.4.11}$$

For the degenerate ideal Bose gas we identify

$$g_2(z) = n^2 + g_1^2(z) = n^2 \left(1 + e^{-2|z|/l_\vartheta}\right), \tag{7.4.12}$$

which is a reasonable approximation for the ideal Bose gas in this regime when it comes to the examination of the length scale of density correlations (see figures 7.4.6 and 7.4.9), but the deviation of absolute values of $g_2(z)$ is now bigger since densities are squared. Hartree-Fock theory approaches the ideal Bose gas result in the dilute system once again. We see that the density correlation length is of the same order as the phase correlation length for these theories, a fact that may be observed already from equation (7.4.11). From there it is obvious that if the terms involving $m'(z)$ are neglected as is done for all theories except for that of Walser, the only spatial dependence of $g_2(z)$ stems from $g_1(z)$ and therefore a similar behaviour, above all a similar length scale of correlations, is expected in that case[2]. The correlation length is obtained numerically by calculating - in a first attempt - the length of the decay of $(g_2(z) - n^2)/(g_2(0) - n^2)$ to $1/e$.

The numerical evaluation for Mora-Castin and Walser theory has to be done carefully now since the cosine causes strong oscillations in the limit $x \to 0$ (where x is the integration variable, see figure 7.4.7). They stem from the second part of the integral (in terms of the splitting of the integration interval as in (7.2.2)) and thus from the UV-limit. For these two

[2]This holds of course not for Mora-Castin and Modified Popov theory, since $g_1(z)$ is evaluated in a different way and therefore relation (7.4.11) is not correct

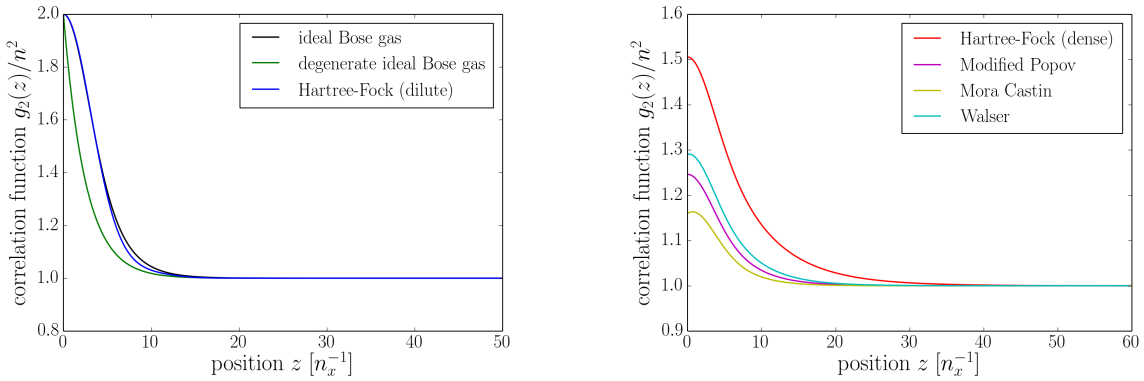

Figure 7.4.6: Normalised second order correlation function $g_2(z)$ of different mean-field theories for $\beta_x = 10^{-1}$; for large z it approaches a 1 for all theories, whereas at $z = 0$ different densities lead to values between 1 and 2 for the mean-field theories (right, $\mu = 2.1\,\mu_x$), proving that this is the cross-over from the decoherent to the quasi-quasi-condensate regime; ideal Bose gas and Hartree-Fock (dilute) describe the decoherent regime as expected (left, $\mu = -2\,\mu_x$)

theories, $g_2(z)$ at large distances z is not smaller than $g_2(0)$ for chemical potentials above a certain value ($\mu \gtrsim 6.31\,\mu_x$ for Mora-Castin and $\mu \gtrsim 7.34\,\mu_x$ for Walser theory with $\beta_x = 10^{-1}$). This can be observed from the integrands of the integrals involved ($n'(z)$ for Mora-Castin and $n'(z) + m'(z)$ for Walser theory) in figure 7.4.7 for Mora-Castin theory (and in appendix C.9.1 for Walser theory) as well. The maximum of $g_2(z)$ is not at $z = 0$ any more and $g_2(0) < 1$, which means that the particles do not stick together as one would expect for bosons. This behaviour is called anti-bunching and is normally related to fermions. Walser found a similar behaviour [81] for a trapped gas: $g_2(0) < 1$, but without a local maximum close to the origin as we have observed (see figure C.9.1 in the appendix). According to the paper, this is a sign of "sub-Poissonian statistics".

We know that in the Tonks-Girardeau regime, the bosons effectively behave as if they were fermions and thus an anti-bunching effect can be expected. For this $\gamma \geq \sqrt{\tau}$ is needed, which translates with equation (7.1.7) into the condition $\beta_x \geq 1$. Having chosen $\beta_x = 0.1$, we are in fact not that far from the strongly-interacting regime and the observed effect may be interpreted as a sign that we are getting close to it. Nevertheless, it is not expected that the mean-field approach is capable of describing the physics of strong interaction. We attribute the anti-bunching therefore to an inconsistency of the theories. This is especially obvious for Mora-Castin theory, because the point where $g_2(\infty)$ becomes bigger than $g_2(0)$ coincides exactly with the critical point at which the thermal density becomes negative. Walser theory does not exhibit a similar critical point, but here the negative anomalous average is responsible for the anti-bunching. For smaller values of β_x, this phenomenon is less influential and sets in for much higher chemical potentials[3], which suggest that the validity of the theories is beyond $\beta_x < 10^{-1}$.

[3]For Mora-Castin theory, the deviation of the maximum's location from $z = 0$ gradually increases with μ, being present already for small values. On the other hand, $g_2(\infty) > g_2(0)$ holds only above the mentioned critical value of μ.

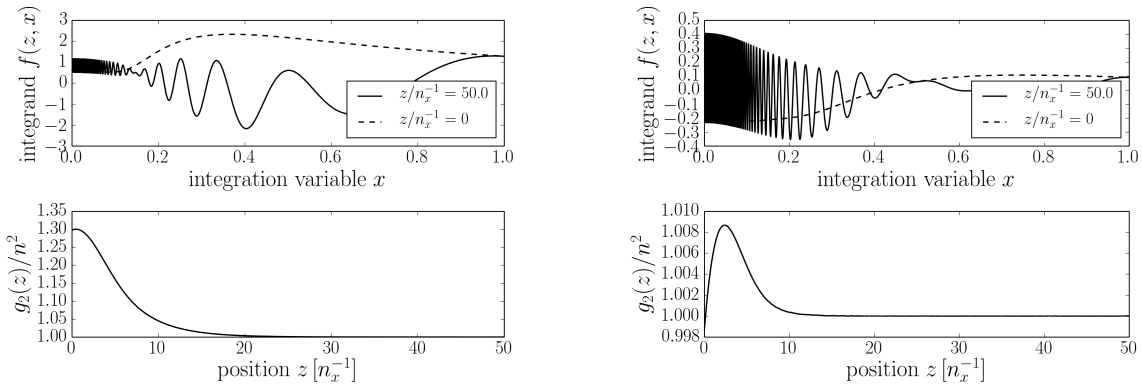

Figure 7.4.7: Integrand of $n'(z)$ and second order correlation function for $\mu = 1.60\,\mu_x$ (left) and $\mu = 6.48\,\mu_x$ (right) for Mora-Castin theory; $g_2(\infty) > g_2(0)$ above the critical value $\mu_{c2} \approx 6.31$ ($\beta_x = 10^{-1}$)

Consequence of the anti-bunching effect - applying the criterion for the determination of the length scale of the decay mentioned above - is a diverging correlation length for large chemical potential (see figure 7.4.8). Since we have argued that this does not have a physical reason, we modify the criterion in an appropriate way, namely by calculating the length of the decay of $(g_2(z) - n^2)/max(g_2(z) - n^2)$ from its maximum's location to $1/e$. In this way, the density correlation decreases for all theories with growing density (or chemical potential, see figure 7.4.9).

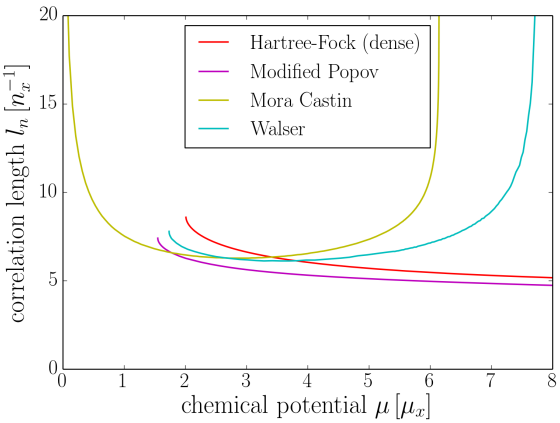

Figure 7.4.8: Diverging correlation length for Mora-Castin and Walser theory due to the anomalous behaviour of the correlation function, making it necessary to modify the way the length is determined ($\beta_x = 10^{-1}$)

Finally we notice that for all theories, $g_2(z)/n^2$ approaches one in the limit $z \to \infty$. Mathematically, this is a consequence of the Riemann-Lebesque lemma [96], which states that for a L^1-integrable function $f(k)$ the Fourier transform at infinity tends to zero, i.e.

$$\lim_{x\to\infty} \int_a^b \mathrm{d}k\, f(k) e^{ikx} \to 0 \tag{7.4.13}$$

for arbitrary boundaries a and b. For the mean-field theories, the integrals $n'(z)$ and $m'(z)$ are of this kind, such that at infinity it remains only $g_2(\infty) = n^2$. Again the approach of a non-zero plateau for large distances corresponds to an infinite density correlation length of the quasi-condensate; in this case it is physically reasonable though, since density fluctuations are suppressed. The length scale obtained from the decay to this plateau explained above rather characterises the small scale correlation described by the healing length and as such, scales approximately as $l_n \sim n^{-1/2}$.

Comparing the length scales of the two correlation functions (figures 7.4.3 and 7.4.9), we observe that taking the asymptotes[4] yields a rough estimate of $l_\vartheta \simeq l_n \approx 10\, n_x^{-1}$ at the cross-over (for $\beta_x = 10^{-1}$). This affirms the initial assumption that both characteristic length scales are of the same order at the cross-over. In fact, this is the scale of the phase-coherence length of the degenerate ideal Bose gas, $l_\vartheta = n/\beta_x \approx 10, n_x^{-1}$ with $n \approx 1$ at the cross-over.

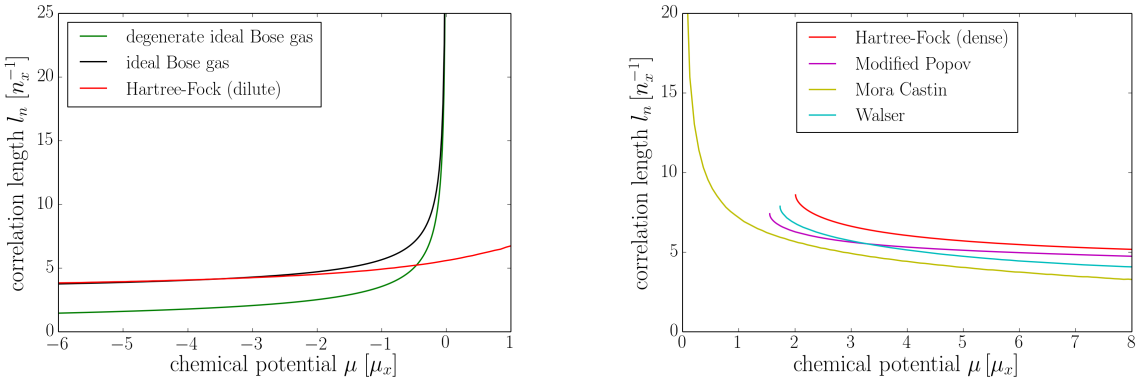

Figure 7.4.9: Density correlation length vs. chemical potential ($\beta_x = 10^{-1}$); on the dilute side (left), Hartree-Fock theory (dilute) approaches the ideal Bose gas results, the degenerate gas is shifted by a constant to lower values; on the dense side (right), the length decreases for the all mean field theories with growing chemical potential (applying the Modified criterion)

7.4.4 Density fluctuations

Density fluctuations can be extracted from the 2^{nd}-order correlation function via

$$\delta n^2 = \langle n^2 \rangle - n^2 = g_2(0) - n^2. \tag{7.4.14}$$

Suppressed density fluctuations manifest therefore in a normalised 2^{nd}-order correlation function $g_2(0)/n^2$ tending to one or the "Mandel parameter"[5] $Q = \delta n^2/n$ tending to zero which is the case for all mean-field theories on the dense side of the cross-over (except for Hartree-Fock theory (dilute), see figure 7.4.10). Hartree-Fock theory (dilute) and the ideal Bose gas exhibit large density fluctuations and thus $g_2(0)/n^2$ is two as expected for the decoherent regime where no (quasi)-condensate is present. In fact, the deviation of $g_2(0)$ from 2 is a measure of the violation of Wick's theorem and thus Gaussian statistics. We can conclude therefore that in the quasi-condensate regime, all mean-field theories (except for Hartree-Fock theory (dilute)) behave according to non-Gaussian statistics. Since we have assumed Gaussian statistics for the thermal part of the gas, it is in fact the quasi-condensate only that is non-Gaussian.

Comparing figure 7.4.10 (right) to figure 7.4.8, it gets clear that the density fluctuations become negative for Mora-Castin and Walser theory at the same point where the second order

[4] Namely the low-μ asymptotes, but without the region very close to the cross-over since we know that the slope there may not be correct (see slope of equation of state in figure 7.4.5 for example).

[5] In its original formulation [97], the Mandel parameter is defined for the particle number N and as such a measure for the deviation from Poissonian statistics, for which $\delta N^2 = N$.

correlation length diverges. For Mora-Castin theory this point actually is the second critical point where the thermal density becomes negative, whereas for Walser theory the (negative) anomalous average is responsible for both phenomena.

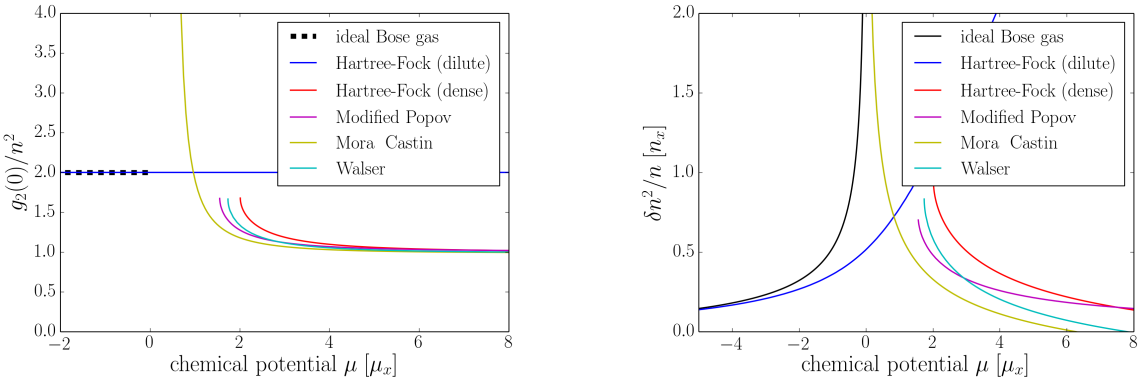

Figure 7.4.10: Normalised second order correlation function $g_2(0)/n^2 = \delta n^2/n^2 + 1$ (left) and Mandel parameter $Q = \delta n^2/n$ (right) for different mean-field theories and the ideal Bose gas for $\beta_x = 10^{-1}$

Another interesting feature is the almost exact match of the critical fluctuations, that is the fluctuations at the critical point of the corresponding theory. If we consider the approximations of the critical points from table 7.2, we obtain up to $\mathcal{O}(\beta_x^{3/2})$

Theory	critical density fluctuations $\delta n_c^2/n^2$	
	$\beta_x = 10^{-1}$	$\beta_x = 10^{-2}$
Hartree-Fock (dense)	0.680	0.731
Modified Popov	0.657	0.725
Walser	0.662	0.720

Although these critical points do not have a physical meaning, it may underline the importance of density fluctuations to the failure of the theories. In fact for Mora-Castin theory, the smallness of density fluctuations was a fundamental assumption in the derivation of the theory which is obviously not fulfilled getting close to the cross-over (see figure 7.4.10).

Part III

Stochastic modelling

Chapter 8

The Gross-Pitaevskii equation

Since the Stochastic Gross-Pitaevskii equation (SGPE), that we want to analyse in chapter 9, is in some sense a finite temperature generalisation of the Gross-Pitaevskii equation (GPE), we dedicate this chapter to the properties of the latter. A Fortran code has been set up in order to study it numerically and get used to the methods of the code used for the SGPE (which was supplied by Cockburn [98]).

The Gross-Pitaevskii equation (GPE) [99, 100] is a non-linear Schrödinger equation for a classical field $\phi(\mathbf{r},t)$ that has been widely used to describe the properties of a pure (quasi-)condensate. It neglects thermal excitations and is therefore limited to the zero (or low) temperature case. Particle interaction is taken into account in Hartree approximation through an effective potential created self-consistently by the particles, it is therefore a mean-field theory for the ground state of a system of interacting bosons. Since all particles are in the same quantum state in this case and considered to be independent of each other (they are only coupled to the mean-field), they can be described by a single wave function $\phi(\mathbf{r},t)$, which is linked to the single particle wave function $\varphi_0 = 1/V^{1/2}$ through $\phi = N_0^{1/2}\varphi_0$, yielding the (quasi-)condensate density $n_0 = |\phi|^2$.

In chapter 6.1 we have seen that it can be derived from the Heisenberg equation of motion (6.1.1) for the field operator $\Psi(\mathbf{r},t)$, replacing it by the classical field $\phi(\mathbf{r},t)$ and thus neglecting contributions from excitations, i.e. thermal density and anomalous average in the context of mean-field theory, completely. Preserving an external potential $U(\mathbf{r})$ in the general case, it reads

$$i\hbar\frac{\partial}{\partial t}\phi(\mathbf{r},t) = \left(-\frac{\hbar^2\nabla^2}{2m} + U(\mathbf{r}) - \mu + g\left|\phi(\mathbf{r},t)\right|^2\right)\phi(\mathbf{r},t). \tag{8.0.1}$$

The stationary equation may alternatively be obtained by minimising the energy functional $\delta\mathcal{E} = 0$,

$$\mathcal{E}[\phi(\mathbf{r},t)] = \int_V \mathrm{d}\mathbf{r} \left\{ \frac{\hbar^2}{2m}|\nabla\phi(\mathbf{r},t)|^2 + U(\mathbf{r})|\phi(\mathbf{r},t)|^2 - \mu|\phi(\mathbf{r},t)|^2 + \frac{g}{2}|\phi(\mathbf{r},t)|^4 \right\}, \tag{8.0.2}$$

underlining the relation of Bose-Einstein condensation to spontaneous symmetry breaking (see section 6.3).

8.1 Analytical approaches

For a homogeneous system, an expansion in plane waves and a Bogoliubov transformation yield the known quasi-particle solution that we have seen in chapter 6.1. That is plausible because we know that the GPE arises in the context of Bogoliubov theory (see equation (6.1.1)).

If the conditions of the local density approximation are fulfilled (see 9.4), these solutions are valid for an inhomogeneous system with non-zero trapping potential as well. In the following, it is considered to be harmonic, thus (we focus on the one-dimensional case from now on)

$$U(z) = \frac{m}{2}\omega_z^2 z^2. \tag{8.1.1}$$

If interactions between the particles are neglected, the trapped solutions are just those of the quantum harmonic oscillator, that is a Gaussian for the ground state[1]. The density profile will presumably be wider than that if the particles repel each other ($g > 0$). A first idea of how a typical density profile of an interacting (quasi-)condensate in a trap looks like can be obtained from the Thomas-Fermi approximation. If the interaction is considered to be strong, the kinetic part can be neglected and we have the solution

$$n(z) = \frac{1}{g}\left(\mu - U(z)\right)\,\theta(R_F - |z|), \tag{8.1.2}$$

where $\theta(x)$ is the Heavyside step function and $R_F = \sqrt{\frac{2\mu}{m\omega_z^2}}$ the Thomas-Fermi radius. The density profile has therefore roughly the shape of the inverted trapping potential (see figure 8.2.1).

The solution (8.1.2) can be rewritten in terms of the Thomas-Fermi radius as

$$n = \frac{\mu}{g}\left(1 - \left(\frac{z}{R_F}\right)^2\right). \tag{8.1.3}$$

[1]The ground state solution is strictly valid only for a chemical potential corresponding to the ground state energy, i.e. $\mu = \hbar\omega_z/2$. The characteristic length scale is the harmonic oscillator length for all solutions though.

Since it has to be normalised to the particle number N, an explicit expression for the chemical potential can be obtained:

$$\mu = \frac{3}{2}\frac{gN}{R_F} \;\Rightarrow\; \mu = \left(\frac{3}{2}gN\sqrt{\frac{m\omega_z^2}{2}}\right)^{2/3} \tag{8.1.4}$$

Integrating over N yields the total energy of the gas, which shows that the chemical potential is not exactly equal to the average energy per particle, i.e.

$$\mu = \frac{5}{3}\frac{E}{N}. \tag{8.1.5}$$

The Thomas-Fermi approximation works very well, as we shall see comparing it to the numerically obtained solution in the next section (see figure 8.2.1). At zero temperature, the kinetic energy of the particles can in fact be neglected; the good agreement of the Thomas-Fermi solution proves therefore that the conditions for the local density approximation (see section 9.4) are satisfied at zero temperature, i.e., that the system behaves locally as if it was homogeneous with the corresponding homogeneous equation of state. The small deviation from the numerical result at the edges of the (quasi-)condensate is only due to the required smoothness of the function.

We also want to define a characteristic length scale for the (quasi-)condensate. For that we consider a stationary system subject to an infinitely high potential on one side and no potential in the rest of the system ((quasi-)condensate "next to a wall"), i.e.

$$U(z) = \begin{cases} \infty & z < 0 \\ 0 & z \geq 0. \end{cases} \tag{8.1.6}$$

For $z \to \infty$ the system is thus homogeneous and we have $\mu = g|\phi_\infty|^2$, where $|\phi_\infty|^2$ is the density very far from the wall. Hence we have to solve the equation

$$\frac{\hbar^2}{2m}\frac{d^2\phi}{dz^2} + g\left(|\phi_\infty|^2 - |\phi|^2\right)\phi = 0, \qquad \phi(0) = 0 \wedge \phi(\infty) = \phi_\infty, \tag{8.1.7}$$

which yields the solution (see figure 8.1.1)

$$\phi(z) = \phi_\infty \tanh\left(\frac{z}{\sqrt{2}\xi}\right), \qquad z \geq 0 \tag{8.1.8}$$

proving that the typical length scale on which the (quasi-)condensate attains its bulk value, that is on which it restores its original density in the presence of a perturbation, is the healing length

$$\xi = \frac{\hbar}{\sqrt{2mgn_\infty}}. \tag{8.1.9}$$

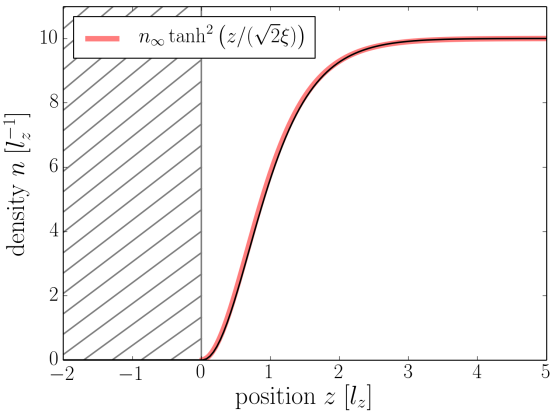

Figure 8.1.1: Healing of the (quasi-)condensate at a hard wall with $\mu = 1\hbar\omega_z$ and $g = 0.1\hbar\omega_z l_z$ (l_z - harmonic oscillator length, see (8.2.1)); the numerical solution from imaginary time evolution matches almost exactly the theoretical solution of equation (8.1.8).

It is actually the length scale on which kinetic and interaction effects become of the same order (setting $\epsilon(k) = gn$ yields the same length scale) and therefore as well roughly the size of solitonic solutions of the GPE. For repulsive interaction, thus $g > 0$ what we consider in this thesis, there exist dark solitons only. These strongly localised and stable solutions are a "lack" of density propagating in non-zero background (hence the denomination dark) that have the shape of the solution (8.1.9) (continued symmetrically on the other side of the wall). Due to the balance of non-linear and dispersive effects, they maintain their original shape during their propagation even when they interact with other solitons. Various experiments have proven their existence in Bose-Einstein condensates [101][102]. These solutions can be derived exactly using the integrability of the equation by means of inverse scattering theory, which has been applied in [103] to the non-linear Schrödinger equation. This is a GPE without trapping and chemical potential that arises apart from Bose-Einstein condensation in the context of non-linear optics [104], water waves and other fields.

The dark soliton solution of the homogeneous Gross-Pitaevskii equation looks as follows [105]:

$$\phi(z,t) = \sqrt{n}\left\{\sqrt{1-\left(\frac{v}{c}\right)^2}\tanh\left[\sqrt{1-\left(\frac{v}{c}\right)^2}\frac{z-vt}{\sqrt{2}\xi}\right] + i\frac{v}{c}\right\}. \tag{8.1.10}$$

Since there is a phase shift across the soliton, it is actually a topological defect of the system. The propagation speed v, the phase shift $\Delta\varphi$ and the shape of the soliton are highly dependent on each other. The faster the soliton propagates, the shallower it is and the smaller is the phase shift. At the maximum velocity c, the Bogoliubov speed of sound (4.1.21), its phase shift and density dip are zero, making it indistinguishable. The other limiting case is a stationary black soliton with phase shift of π and a density dip going down to zero.

8.2 Numerical approaches

The numerical treatment of the of SGPE follows the same way as for the GPE, that is why we mention the main aspects already here. First of all, the equation has to be made dimensionless and as we consider generally inhomogeneous systems with an harmonic potential, it is natural to formulate the theory in harmonic oscillator units. We therefore scale

$$z \to \frac{z}{l_z}, \qquad \phi \to \phi\, l_z^{1/2}, \qquad t \to \omega_z t, \qquad g \to \frac{g}{\hbar\omega_z l_z}, \qquad \mu \to \frac{\mu}{\hbar\omega_z} \tag{8.2.1}$$

with the harmonic oscillator length $l_z = \sqrt{\frac{\hbar}{m\omega_z}}$. In terms of these units, the GPE takes the form

$$i\,\frac{\partial}{\partial t}\phi(z,t) = \left(-\frac{\partial_z^2}{2} + \frac{z^2}{2} - \mu + g\,|\phi(z,t)|^2\right)\phi(z,t). \tag{8.2.2}$$

This equation is numerically integrated using the Crank-Nicholson scheme [106], a consistent finite difference method of second order that is unconditionally stable in terms of Von-Neumann stability [107]. Still it is required that the temporal and spatial step sizes fulfil the condition $\Delta t/\Delta x^2 \leq 1/2$ for spurious oscillations not to occur. Since the method is implicit in time - in fact the time average of the spatial derivative is taken - the matrix equation

$$M\phi^{m+1} = \Omega(\phi^m) \tag{8.2.3}$$

has to be inverted. It is derived from the discretised version of the GPE (details are presented in appendix D.1)

$$\left[1 + \frac{i\Delta t}{2}\left(\frac{\delta_z^2}{2} + V_j - \mu + g|\phi_j^{m+1/2}|^2\right)\right]\phi_j^{m+1} = \left[1 - \frac{i\Delta t}{2}\left(\frac{\delta_z^2}{2} + V_j - \mu + g|\phi_j^{m+1/2}|^2\right)\right]\phi_j^m, \tag{8.2.4}$$

where $j = 1, ..., N_x$ and $m = 1, ..., N_t$ are spatial and temporal indices, respectively and δ_z^2 is the finite difference scheme of the second derivative. The $m + 1/2$ in the interaction term indicates a time average (it is the only time-dependent term that enters the matrices), which is taken into account in practice by solving the matrix equation for ϕ'^{m+1} with ϕ^m in the interaction term on both sides of equation (8.2.3) and taking the average of the obtained solution and ϕ^m, i.e. $(\phi^m + \phi'^{m+1})/2$, to solve for the final ϕ^{m+1}.

We identify $\Omega(\phi^m) = M^*\phi^m$, with the matrix generally taking the form

$$M = \begin{pmatrix} b_1 & c_1 & & & & a_1 \\ a_2 & b_2 & c_2 & & & \\ & a_3 & b_3 & c_3 & & \\ & & \ddots & \ddots & \ddots & \\ & & & a_{N_x-1} & b_{N_x-1} & c_{N_x-1} \\ c_{N_x} & & & & a_{N_x} & b_{N_x} \end{pmatrix} \tag{8.2.5}$$

where

$$a_j = \begin{cases} 0 & i = 1 \\ -\frac{i\Delta t}{4\Delta z^2} & \text{else} \end{cases}, \quad c_j = \begin{cases} 0 & i = N_x \\ -\frac{i\Delta t}{4\Delta z^2} & \text{else} \end{cases}, \quad b_j = 1 + \frac{i\Delta t}{2}\left(\frac{1}{\Delta z^2} + V_j - \mu + g|\phi_j^{m+1/2}|^2\right). \tag{8.2.6}$$

The final form of the matrix M depends still on the boundary conditions. The code developed by Cockburn [98] for the SGPE applies zero boundary conditions, whereas for the purpose of the present thesis periodic boundary conditions had to be implemented. This is necessary because with the mean-field approach we have analysed the thermodynamic limit, which with a finite system size can only be modelled by a closed ring. For zero boundary conditions $\phi(\pm L/2, t) \equiv 0$ (where L is the length of the system), the matrix (8.2.5) is tridiagonal with $c_1 = a_{N_x} = \Omega_1 = \Omega_{N_x} = 0$ set to zero. The standard tridiagonal matrix algorithm can be used, making the calculation very fast since only $\mathcal{O}(N_x)$ operations are needed.

If we use periodic boundary conditions, the matrix is not completely tridiagonal any more since we have $M_{1N_x} = a_1 = M_{N_x 1} = c_{N_x} = -\frac{i\Delta t}{4\Delta z^2}$. But it can be reduced to a tridiagonal form, such that for the solution the tridiagonal matrix algorithm has to be applied twice (see appendix D.1), which is still much faster than using Gaussian elimination ($\mathcal{O}(N_x^3)$ operations).

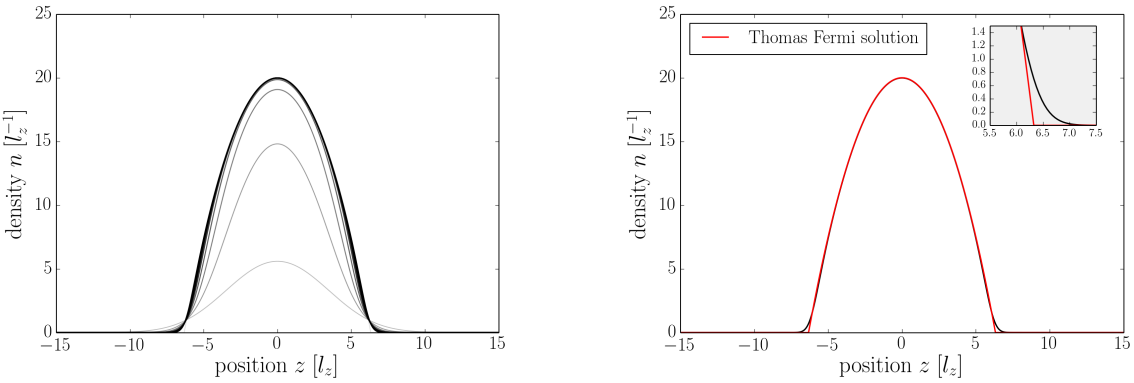

Figure 8.2.1: Equilibrium solution of the GPE with harmonic potential and zero-boundary conditions for $\mu = 20\hbar\omega_z$ and $g = 1\hbar\omega_z l_z$, obtained by numerical integration in imaginary time; the density profile converges to its final solution (left, time step $\delta\tau = 0.05\omega_z^{-1}$ between snapshots, linewidth increasing with time), which deviates from the Thomas Fermi approximation only on the edges of the (quasi-)condensate (right).

In order to get equilibrium solutions of the differential equation numerically, we can make use of imaginary time evolution. Substituting $\tau = it$, we have $-\partial_\tau \phi = H\phi$ and for a linear Hamiltonian

$$\phi(\tau) = e^{-H\tau}\phi(0). \tag{8.2.7}$$

We expand the initial state $\phi(0)$ in eigenstates of the Hamiltonian ϕ_i ordered by their energy $H\phi_i = E_i\phi_i$. With τ tending to infinity, all exited states decay and one is left with the ground state:

$$\lim_{\tau\to\infty} \phi(\tau) = \lim_{\tau\to\infty} \sum_{i=0}^{\infty} c_i e^{-E_i\tau}\phi_i = \lim_{\tau\to\infty} c_0 e^{-E_0\tau}\phi_0. \tag{8.2.8}$$

The convergence to the final solution can be observed for the density profile in figure 8.2.1(left), while the evolution of the total energy and particle number are displayed in figure 8.2.2. In imaginary time, the Hamiltonian acts as a source term that populates the system from any non-zero initial condition. The final solution is very close to the Thomas-Fermi approximation, as we have analysed already in the previous section.

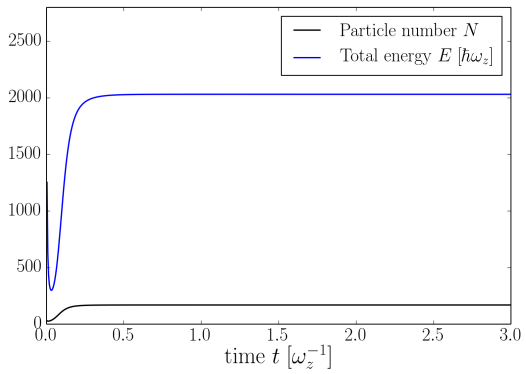

Figure 8.2.2: Energy and particle number conservation of the ground state of the GPE (same parameters as in figure 8.2.1); the equilibrium solution is obtained in imaginary time and after $t = 2\omega_z^{-1}$ the evolution is carried out in real time

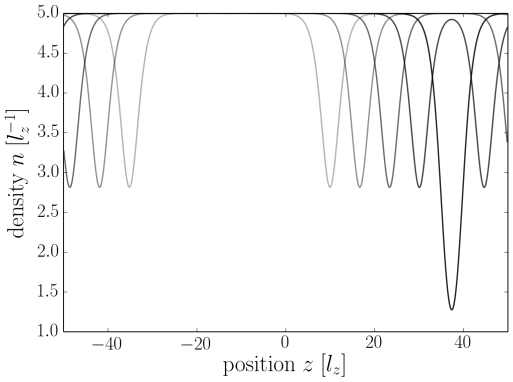

Figure 8.2.3: Two solitons propagating at $v = 0.75c$ in a homogeneous (quasi-)condensate with periodic boundary conditions ($\mu = 0.5\hbar\omega_z$, $g = 0.1\hbar\omega_z l_z$, $N_x = 2000$, $\delta t = 5\omega_z^{-1}$ between snapshots)

The equilibrium states found by imaginary time propagation can be used as initial states for dynamical simulations. For example we can put a soliton in a homogeneous system and see how it behaves. For that we simply multiply the equilibrium solution with the rhs of equation (8.1.10) (without the factor $\sqrt{n}$) for some velocity $0 \leq v \leq c$. The main objective behind that was the validation of the implementation of the periodic boundary conditions, making use of the soliton's stability. We analyse its behaviour when it passes from "one side to the other" - there is of course no difference between the two "sides" since physically we model a closed ring; therefore the soliton should not notice any change at the boundary of the numerical system. Although it might be difficult to see from the figures (8.2.3), the soliton moves in the trap from one side to the other without noticeable loss of amplitude. Additionally, we plot the collision of two solitons in a homogeneous system, as it can be observed as well in figure 8.2.3, in a 3d plot involving a time axis.

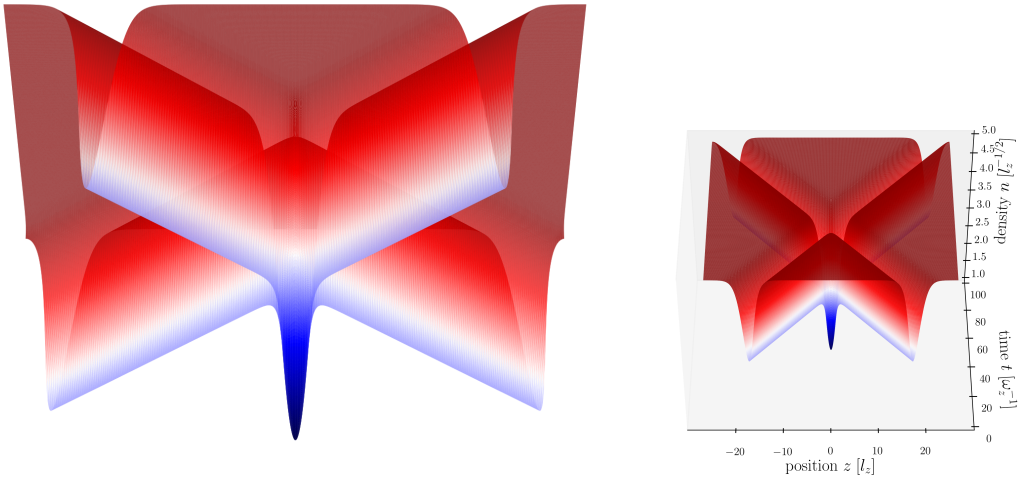

Figure 8.2.4: 3d plot of two solitons colliding in a homogeneous (quasi-)condensate (left: seen from below, time runs from front to back as in the right figure which shows the same seen from above; parameters as in figure 8.2.3) obtained from numerical integration of the GPE; they emerge unchanged from the collision maintaining exactly their original shape.

Chapter 9

The Stochastic Gross-Pitaevski equation

The Gross-Pitaevskii equation has been very successful in describing both equilibrium and dynamical properties of a Bose-Einstein (quasi-)condensate for very low temperatures. On the other hand, it is a quite simple model and it seems therefore natural to generalise it in order to incorporate finite temperature effects. There exists a wide range of theories that have been set up for this purpose (a short overview can be found in [108], detailed comparison in [109]). One type of approaches treats the (quasi-)condensate classically and separates it from the thermal cloud, with both parts of the system interacting via mean-fields and particle exchange. In the most popular version, which is named "ZNG" due to early works of Zaremba, Nikuni and Griffin [110], the thermal cloud obeys a quantum Boltzmann equation [111]. Apart from techniques related to the Truncated Wigner method [112][113], that we leave apart here since it not able to fully describe thermal effects, there is the approach of the Stochastic Gross-Pitaevskii equation (SGPE) which goes beyond the mean-field description. This is a Langevin equation for a complex field that includes the (quasi-)condensate and the highly occupied, low lying modes[1]. The dynamics of the coupling to the thermal cloud is considered in a detailed way, following from the independent works of Stoof [114][115] on one side, and Gardiner and Davis [116][117] on the other.

Although the ZNG equations already are quite suitable to reproduce a lot of experimental findings, only the SGPE is capable of fully capturing the behaviour of systems with large phase fluctuations (see for example [118][119]). We know that this is the case in low-dimensional systems and because of that we choose this technique in order to provide a possibility of validating the results obtained from the mean-field theories. For numerical evaluation of the equation, we use the code developed by Cockburn [98].

[1] In one dimension, the complex field includes the quasi-condensate, whose definition is not completely clear in this context. It could be assumed that the quasi-condensate actually contains the low-lying modes, but we do not adopt this picture here.

9.1 Derivation

We adopt the approach of Stoof and co-workers to the SGPE [25][120] and follow in the derivation to a large extent the steps of [98]. This method describes the whole matter field in terms of the Wigner (quasi-) probability distribution function $P[\Psi^*, \Psi, t]$ (see appendix D.2) for the order parameter Ψ that characterises the state of the complete system. A Fokker-Planck equation is derived for Ψ within the Keldysh non-equilibrium formalism [121], and in the following the probability distribution is split into a product of two distributions $P[\Psi^*, \Psi, t] = P_0[\Phi^*, \Phi, t]P_1[\psi^*, \psi, t]$. $\Phi(\mathbf{r}, t)$ contains not only the (quasi-)condensate, but also low lying thermal modes which is one of the main differences to the ZNG formalism as mentioned before; $\psi(\mathbf{r}, t)$ represents the thermal cloud. Integration over the contribution of these modes in the Fokker-Planck equation leads to a quantum Boltzmann equation (see appendix D.2)

$$\frac{\partial f}{\partial t} + (\nabla_{\mathbf{p}}\epsilon) \cdot (\nabla f) - (\nabla\epsilon) \cdot (\nabla_{\mathbf{p}} f) = \mathcal{C}_{12}[f] + \mathcal{C}_{22}[f] \tag{9.1.1}$$

for the Wigner distribution f of the thermal cloud, which can be used to get the expectation value of the particle density of the thermal cloud (assuming that higher moments of ψ are not relevant):

$$n_t(\mathbf{r}, t) = \int \frac{\mathrm{d}\mathbf{p}}{(2\pi\hbar)^3} f(\mathbf{r}, \mathbf{p}, t). \tag{9.1.2}$$

$\mathcal{C}_{12}$ and $\mathcal{C}_{22}$ in equation (9.1.1) are collision integrals that describe scattering processes between low-lying modes and thermal cloud, and within the thermal cloud, respectively.

The dynamics of the low-lying modes are described by a Fokker-Planck equation, that is obtained by integrating out the contribution of the thermal cloud from the original equation for Ψ and reads

$$\begin{aligned} i\hbar\frac{\partial}{\partial t}P_0[\Phi^*, \Phi, t] = &\int_V \mathrm{d}\mathbf{r}\, \frac{\delta}{\delta\Phi^*}\Big[\left(H_{GP} + iR(\mathbf{r}, t)\right) \Phi^*\, P_0[\Phi^*, \Phi, t]\Big] \\ &- \int_V \mathrm{d}\mathbf{r}\, \frac{\delta}{\delta\Phi}\Big[\Big(H_{GP} - iR(\mathbf{r}, t)\Big) \Phi\, P_0[\Phi^*, \Phi, t]\Big] \\ &- \int_V \mathrm{d}\mathbf{r}\, \frac{\hbar}{2}\frac{\delta^2}{\delta\Phi\delta\Phi^*}\Sigma^K(\mathbf{r}, t) P_0[\Phi^*, \Phi, t], \end{aligned} \tag{9.1.3}$$

where $H_{GP} = -\frac{\hbar^2\nabla^2}{2m} + U(\mathbf{r}) - \mu + g\,|\Phi(\mathbf{r}, t)|^2$. Dissipation is described by the term involving

$$R(\mathbf{r},t) = 4\pi g^2 \int \frac{\prod_{i=2}^{4} \mathrm{d}\mathbf{p}_i}{(2\pi\hbar)^6}\, \delta(\mathbf{p}_2-\mathbf{p}_3-\mathbf{p}_4)\, \delta(\epsilon_c+\epsilon_2-\epsilon_3-\epsilon_4)\, [f_2(f_3+1)(f_4+1) - (f_2+1)f_3f_4]\,, \tag{9.1.4}$$

where the f_is are Wigner functions of the thermal cloud and $\epsilon_i = \epsilon(k_i) + U(\mathbf{r}) + 2g|\Phi|^2$ is the Hartree-Fock energy. The counterpart of that, the fluctuations, are characterised by the Keldysh self-energy:

$$\Sigma^K(\mathbf{r},t) = -\frac{4\pi i}{\hbar} g^2 \int \frac{\prod_{i=2}^{4} \mathrm{d}\mathbf{p}_i}{(2\pi\hbar)^6}\, \delta(\mathbf{p}_2-\mathbf{p}_3-\mathbf{p}_4)\, \delta(\epsilon_c+\epsilon_2-\epsilon_3-\epsilon_4)\, [f_2(f_3+1)(f_4+1) + (f_2+1)f_3f_4] \tag{9.1.5}$$

In order to solve this system of equations, it is necessary to make further simplifications because the dependence of R and Σ^K on Φ via $\epsilon_c = -\frac{\hbar^2\nabla^2}{2m} + U(\mathbf{r}) + g\,|\Phi|^2$ yields multiplicative noise. If the processes that lead to thermalisation in the thermal cloud take place on a much faster timescale than the scattering between the two subsystems, it can be assumed that the thermal cloud is in equilibrium. In this case, the quantum Boltzmann equation does not have to be solved since the Wigner function may be replaced by Bose-Einstein distribution. Furthermore, it is possible to apply the fluctuation-dissipation relation for the thermal cloud:

$$iR(\mathbf{r},t) = -\frac{1}{2}\hbar\Sigma^K(\mathbf{r},t)\, \left(1 + 2N_{BE}(\epsilon_c-\mu)\right)^{-1} \simeq -\frac{\hbar}{4}\Sigma^K(\mathbf{r},t)\, \beta\, (\epsilon_c-\mu) \tag{9.1.6}$$

For the highly-occupied modes, it has been assumed that the Rayleigh-Jeans distribution is a reasonable approximation, such that $\left(1 + 2N_{BE}(\epsilon_c-\mu)\right)^{-1} \simeq 1/2\,\beta(\epsilon_c-\mu)$. In this way, the Langevin equation that is obtained from the Fokker-Planck equation (9.1.3), takes the following form with the damping term in the pre-factor:

$$i\hbar\frac{\partial}{\partial t}\Phi(\mathbf{r},t) = \left(1 - i\gamma(\mathbf{r},t)\right)\left[-\frac{\hbar^2\nabla^2}{2m} + U(\mathbf{r}) - \mu + g\,|\Phi(\mathbf{r},t)|^2\right]\Phi(\mathbf{r},t) + \eta(\mathbf{r},t). \tag{9.1.7}$$

The (dimensionless) damping term

$$\gamma(\mathbf{r},t) = \frac{i\hbar}{4}\beta\Sigma^K(\mathbf{r},t) \tag{9.1.8}$$

is related to the amplitude of the fluctuations, which are modelled by Gaussian white noise, via

$$\langle\eta(\mathbf{r},t)\eta(\mathbf{r}',t')\rangle = 2k_BT\gamma(\mathbf{r},t)\,\delta(\mathbf{r}-\mathbf{r}')\,\delta(t-t'). \tag{9.1.9}$$

How both are incorporated into the numerical time stepping algorithm is explained in appendix D.1. As for any stochastic simulation, the fluctuations are modelled by generating pseudo-random numbers from a distribution obeying (9.1.9).

The results of a single run will exhibit a considerable amount of noise (see figure 9.2.1 for an example with comparably little noise), depending on the parameter choice. The higher the temperature, the stronger are the fluctuations (see equation (9.1.9)), requiring more simulations to be run for the averaging. In general, we perform ensemble averages of about 10^3 to 10^4 single runs, which are very well suited for parallel computing. The high-throughput computing facility *CONDOR* at Newcastle university, that comprises more than one thousand distributed working stations, provided the perfect infrastructure for these simulations.

We finish this section concluding that the SGPE (9.1.7) is a generalised Gross-Pitaevskii equation for the field $\Phi(\mathbf{r}, t)$. It characterises not only the (quasi-)condensate, but not the whole system either as mentioned before. Low-lying, highly occupied modes are included in it, contrary to the clear separation of the (quasi-)condensate from the rest of the system applied in the mean-field approach. The higher modes of the system that are considered to be in equilibrium, act as a heat bath of a certain temperature that "feeds" particles into the system (or absorbs them depending on the parameters and initial conditions). Since these modes are sparsely occupied, the density that is not considered in Φ is small and may therefore be neglected.

One of the tricky questions in this context is where to draw the line between system and thermal cloud. For consistency, it has to be ensured that for all modes that are taken into account for Φ, the classical approximation of (9.1.6) is approximately fulfilled. All other modes have to be separated, which is done in practice by tuning the momentum cut-off inherent in the space discretisation of the numerical implementation of the equation. How to choose this cut-off will be examined in more detail in section 9.5.

9.2 Growth to equilibrium

The SGPE is capable of describing both equilibrium and dynamical properties of a weakly interacting Bose gas. For comparison with mean-field results, we focus here mainly on the static case, but we want to emphasize that the equation is not limited to that. One of its strengths is actually the description of non-equilibrium processes like the growth of a (quasi-)condensate from a thermal gas, which was the first application of the theory in [25]. Starting from an initial condition Φ, particles scatter from the thermal cloud into the system until the equilibrium solution is reached (see figure 9.2.1). This works formally a bit like imaginary time propagation that we have applied to the GPE (see (8.2.7)), it is based on a completely different physical background though (or, more precisely, there is a physical meaning of it, contrary to imaginary time evolution). It is the damping term in the prefactor that is responsible for the growth, but fluctuations are vital for starting the process when still no (quasi-)condensate (nor low-lying modes) are present [114].

The rate at which particles are fed into the system depends on the strength of the damping term,

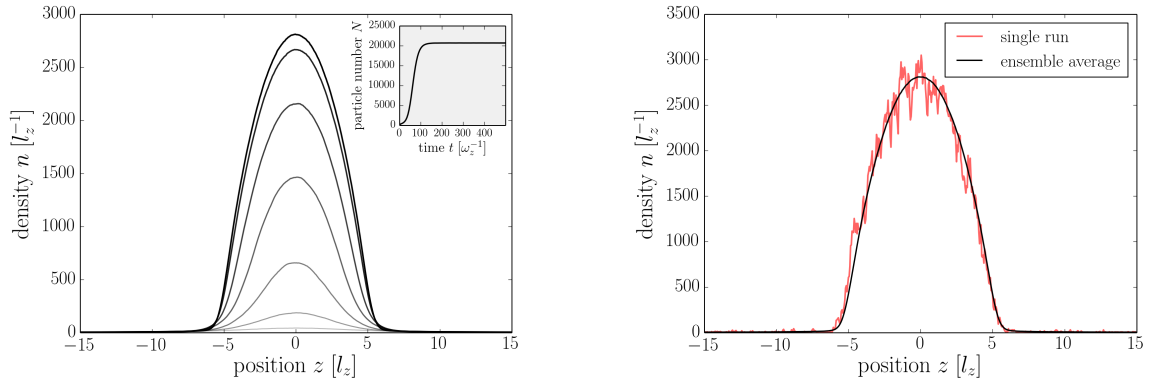

Figure 9.2.1: Growth from zero to the equilibrium solution of the SGPE (left) obtained numerically at $T = 100\,\mathrm{nK}$, $\omega_\perp = 754\,\mathrm{Hz}$, $\omega_z = 220\,\mathrm{Hz}$ and $\mu = 15\,\hbar\omega_z$ by averaging over 10^4 single runs in order to reduce the noise (right).

that is on $\gamma(\mathbf{x}, t)$. In order to reproduce the exact dynamics, all details of its determination have to be taken into account, including its spatial and temporal dependence. But since only the equilibrium is of interest to us now, we may neglect this and simplify matters by considering constant and uniform values of γ (this is of course trivially fulfilled for static and homogeneous systems). We want to examine if we can even take higher values than the "correct" one, accelerating our simulations in this way, without changing noticeably the equilibrium properties of the obtained solution (as stated in [98]).

In [98], the value of γ obtained from spatial averaging is compared to an approximation introduced in [122] in the context of vortex formation, given by

$$\gamma_{\mathrm{bare}} = \kappa \frac{4mk_BT}{\pi} \left(\frac{a_s}{\hbar}\right)^2 . \tag{9.2.1}$$

$\kappa = 3$ is a factor that was matched to the experimental data originally, whereas in [98] it turns out that equation (9.2.1) yields a good approximation to the exact expression (9.1.8) for $\kappa \approx 1$ for temperature $T \leq 400\mathrm{nK}$. We take it therefore as a reference for a simulation at $T = 20\mathrm{nK}$ that is carried out for a wide range of γ, comparing the particle number to that obtained with γ_{bare} (see figure 9.2.2). On one hand, we observe that a larger γ accelerates the convergence to equilibrium drastically. On the other hand, it has in fact a small influence on the equilibrium particle number, which grows with decreasing damping rate. For large γ, this is almost not noticeable (see matching of the curves for $10^{-4} \leq \gamma \leq 10^{-1}$ in figure 9.2.2 (c)), whereas for smaller values close to γ_{bare} is gets quite obvious. Without focusing on the reasons for that, we observe that the deviation from the equilibrium solution obtained with γ_{bare} (independently of the choice of κ) still does not exceed 1.5% of the total value for any γ examined here. In order to get feasible simulation times (for γ_{bare} about 10^8 time steps are required for convergence for the chosen parameters), we neglect this difference and take $\gamma \sim 10^{-3} \ldots 10^{-1}$ for our simulations, bearing in mind that the obtained density is slightly too low. A correction of this *a posteriori* would require a detailed analysis of the parameter dependence of this effect, so we abstain from doing this.

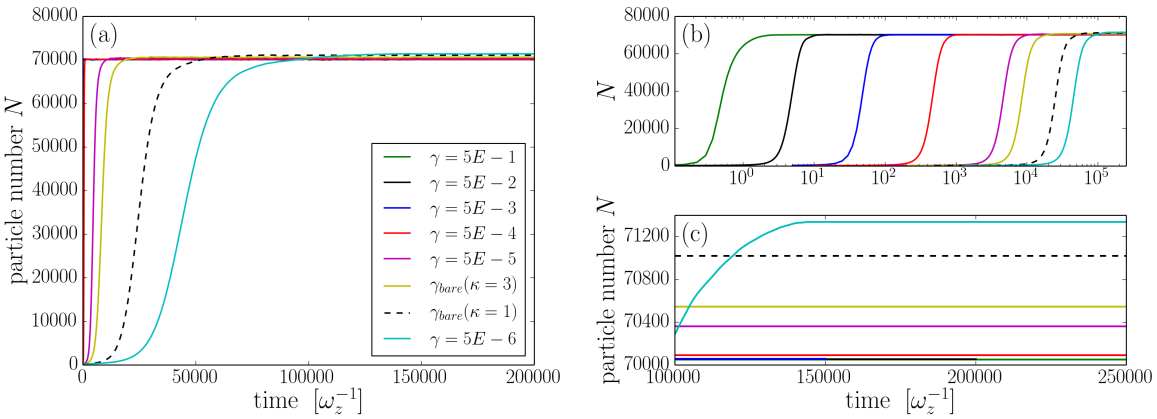

Figure 9.2.2: Growth of particle number to equilibrium for different values of the damping rate γ, obtained numerically from the SGPE for a system with $T = 20\,\mathrm{nK}$, $\omega_\perp = 2\pi \cdot 32\,\mathrm{Hz}$, $\omega_z = 2\pi \cdot 9\,\mathrm{Hz}$ and $\mu = 22.1\,\hbar\omega_z$ and $\gamma_{\mathrm{bare}} = \kappa \cdot 0.91 \cdot 10^{-5}$; larger γ accelerate the convergence (a), the convergence time is in fact directly proportional to the inverse of the damping rate (b); the equilibrium particle number is practically independent of γ for $10^{-4} \leq \gamma \leq 10^{-1}$, below that it attains larger values (c) (time averaging over the last time steps (about 100) has been applied additionally here)

9.3 Density profiles and (quasi-)condensate fraction

A lot of effort has been made in the course of the development of the SGPE and related approaches in order to incorporate finite temperature effects. We compare therefore the density profiles obtained from the SGPE for different temperatures to those of the GPE in order to see its effect. From figure 9.3.1 we observe that up to $T/T_c = 0.003$ there is practically no difference to the zero-temperature solution. Only above that value, the temperature starts to spread the wings of the profile, since this is where the thermal atoms reside mostly. This leads as well to a reduction of the profile's peak height.

In order to examine this in more detail, it is necessary to determine the fraction of the gas that is actually (quasi-) condensed and which contributes to the thermal density. The solution of the SGPE yields results for the below cut-off density $\Phi(z,t)$ of the gas, contrary to mean-field theories, which directly give independent quantities for the condensate and the thermal part of the gas. Further analysis of $\Phi(z,t)$ is therefore needed. One approach that is potentially able of identifying the quasi-condensate density is inspired by the mean-field assumption that the thermal part of the gas obeys Gaussian statistics. The (quasi-)condensate can therefore be defined as the part of the gas that violates Wick's theorem, which states for a Gaussian field

$$\langle|\psi(z)|^4\rangle = 2\langle|\psi(z)|^2\rangle^2 + |\langle\psi^2(z)\rangle|^2. \tag{9.3.1}$$

In the original formulation of the definition [123, 124], that has been applied for example in [125], the anomalous average is neglected, identifying the quasi-condensate density as

$$n_{qc}(z) = \sqrt{2\langle|\psi(z)|^2\rangle^2 - \langle|\psi(z)|^4\rangle}. \tag{9.3.2}$$

The anomalous average is in fact very small (taking it into account yielded practically the

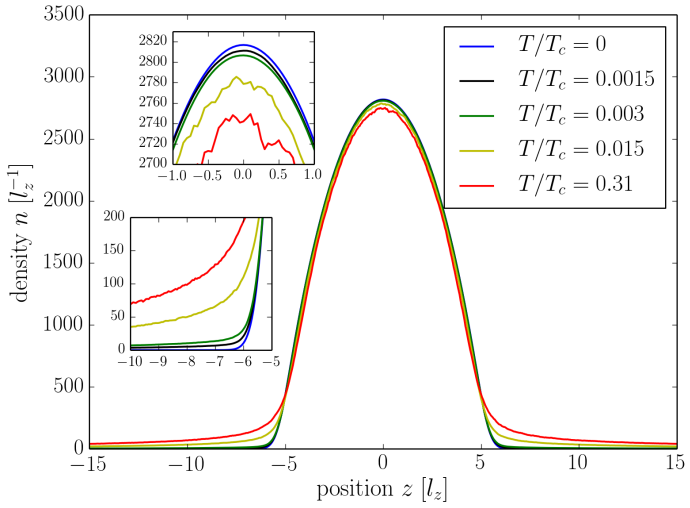

Figure 9.3.1: Broadening of the density profiles for finite temperatures (corresponding to $T \approx 0.002 \ldots 0.43$) compared to the GPE result (parameters as in figure 9.2.1)

same quasi-condensate density for the simulations of figure 9.3.2).

Apart from that, in a trap there can even exist a true condensate, which additionally to being density coherent as the quasi-condensate is phase coherent. It may be calculated making use of the Penrose-Onsager criterion [7] for condensation that we mentioned in section 3.2. In this approach, the condensate density n_{po} is identified with the largest eigenvalue of the single-particle density matrix [31], which is obtained by numerically diagonalising the matrix $\langle \Phi(z_j, t^m)\Phi(z_{j'}, t^m)\rangle$ from the simulations. An approximate form of this has been introduced in [31] as well, combining the Landau criterion of condensation (3.3.8), the definition of $g_1(0, z)$ in Modified Popov theory for a homogeneous gas (7.4.4) and the expression for the quasi-condensate density (9.3.2) in order to construct

$$\tilde{n}_{po} = n_{qc} e^{-\langle [\vartheta(0)-\vartheta(z)]^2\rangle/2} \approx \sqrt{2n^2(z) - g_2(z)}\, g_1(0, z). \tag{9.3.3}$$

It is expected to hold only for large distances z, which is affirmed by the simulations carried out in [31] and in the frame of this thesis, as shown in figure 9.3.2. The higher the temperature, the larger is the value of z from which upward the approximation yields good agreement though. Closer to the trap centre, its gives larger values and reaches the quasi-condensate level at the very centre.

Furthermore, the quasi-condensate density is always larger than the density of the Penrose-Onsager mode, since not the whole gas is phase coherent for the given parameters. Both do conserve the typical Thomas-Fermi like shape of the condensate, characteristic for the GPE. Thermal densities may be calculated by determining the difference of the corresponding condensate density to the total density n. Due to their kinetic energy, the "thermal particles" tend to populate the wings of the trap and thus their density is higher there (just like the excited states of the harmonic oscillator). In the middle of the trap however, the condensed part of the gas dominates and therefore the thermal density is lower there (independently

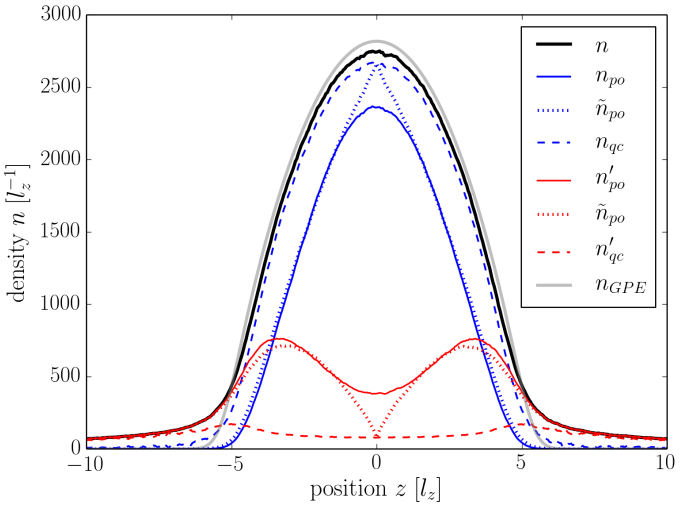

Figure 9.3.2: Densities of the Penrose-Onsager mode n_{po}, its approximation $\tilde{n}_{po}$ from equation (9.3.3), the quasi-condensate from (9.3.2) and the corresponding thermal densities (parameters as in figure 9.2.1 with $T \approx 0.43\,T_\vartheta \approx 0.31\,T_c$)

of the definition of the condensate density). For the comparison with mean-field results, we have to use the quasi-condensate density, since for the homogeneous system there is no phase coherent part of the gas, as pointed out before.

9.4 Local density approximation

We have already mentioned the local density approximation (LDA) in the course of this thesis; now we want to take a closer look at it since it will help us bridging the gap between the equation of state, as a typical mean-field result, and the density profiles obtained from the SGPE just as from experiments.

Essential for the approximation is the observation that the trapping potential $U(z)$ enters in the same way in a general Hamiltonian as the chemical potential. They both can therefore be combined in one quantity, the so-called local chemical potential,

$$\mu_{\mathrm{loc}} = \mu - U(z). \tag{9.4.1}$$

The main assumption of the LDA is that the gas can locally be regarded as if it was homogeneous, but with a chemical potential following from (9.4.1). In this case, it can be treated analytically in the same way - above all, the wave function can (locally) be expanded in plane waves - and all results that we have obtained thus far for a homogeneous gas hold as well. Thus a density profile can be translated into an equation of state, and vice versa. For example, we can take the density profile obtained from the GPE from figure 8.2.1 and convert it into the corresponding equation of state (see figure 9.4.1). Not surprisingly, we get the quasi-condensate limit $\mu = gn$ on the dense side and no density on the dilute side, since there

are no thermal excitations present.

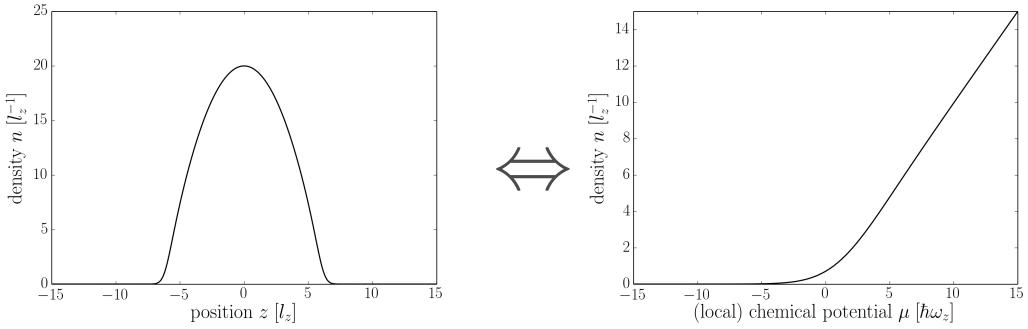

Figure 9.4.1: Equivalence of the density profile (left) and the equation of state (right) in the local density approximation for the numerical equilibrium solution of the GPE (parameters as in figure 8.2.1)

Thus the whole range of regimes that appear when the equation of state is passed from negative to positive chemical potential, hence the cross-over from a thermal degenerate Bose gas to a quasi-condensate, can be observed in the density profile starting from the wings approaching the centre of the trap.

But is this approximation justified? In order to get an answer, we want to examine the conditions which have to be fulfilled for the LDA. For the gas to be locally homogeneous, we need that the typical length scale of the variation of the density profile is much larger than the scale on which the gas reacts to perturbations, that is the healing length ξ. As we have seen in the previous section, the Thomas-Fermi solution is a good approximation of a density profile even for finite temperature. We take therefore the Thomas-Fermi radius as the length scale of the density profile. This yields a condition for the axial trapping frequency[2]:

$$\omega_z \ll \frac{1}{\hbar}\sqrt{2\mu\,(\mu - U(z))}. \tag{9.4.2}$$

At the same time we know that $\mu - U(z)$ is bounded,

$$\mu - U(R_F) = 0 \leq \mu - U(z) \leq \mu = \mu - U(0). \tag{9.4.3}$$

Hence we expect the LDA to be generally fulfilled for small trapping potential, above all in the quasi-condensate regime, where $\omega_z \ll \frac{\mu}{\hbar}$ is required (this is actually equivalent to $R_F \gg l_z$). In [72] it is argued that this a reasonable assumption for typical experimental realisations of a one-dimensional Bose gas. The further we get to the edge of the quasi-condensate though, the smaller the local chemical potential gets, making it more and more difficult to fulfil condition (9.4.2). Using the link to the equation of state, the LDA will therefore deviate most strongly from the correct solution in the cross-over region. Further away from the trap centre, the density profile varies quite slowly in space, such that the LDA can be justified again.

[2]This reasoning is not completely rigorous, since we do assume the validity of the LDA already implicitly using the Thomas-Fermi approximation and the healing length $\xi = \hbar/(\sqrt{2m\mu_{\mathrm{loc}}})$

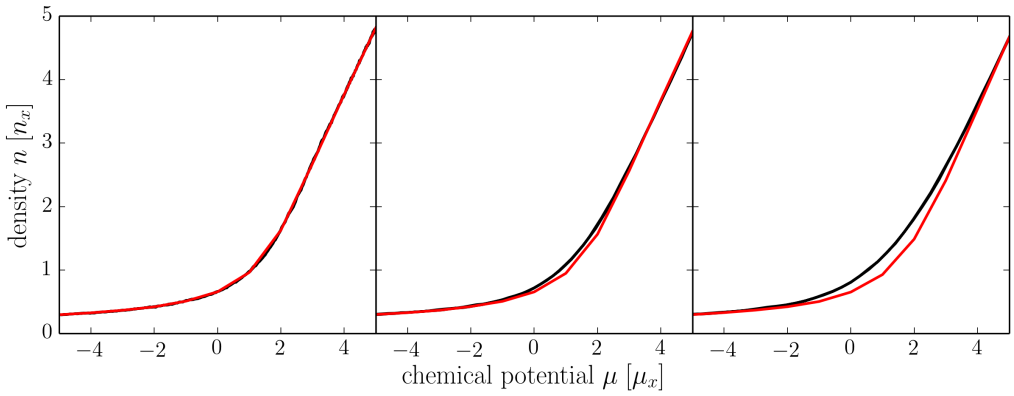

Figure 9.4.2: Equation of state ($\beta_x = 10^{-1}$) obtained from a trapped gas in LDA (black) compared to its homogeneous result (red) from the SGPE for increasing axial trapping frequency from left to right ($\omega_z = 9.09, 36.4, 52.4\,\mathrm{Hz}$); very good agreement is found in the quasi-condensate regime and the ideal gas limit, whereas the deviation gets bigger close to the cross-over and for higher ω_z.

Higher temperatures tend to broaden the density profile (see figure 9.3.1), decreasing its slope in the cross-over region. Consequently, the LDA will work better in this case. This is affirmed by the simulations that we have performed. For the same parameters we compare in figure 9.4.2 the equation of state obtained from a system confined by a harmonic potential applying the LDA to that obtained from homogeneous systems with periodic boundary conditions. For the latter we determine the density by spatial averaging of the ensemble averaged density profile. In this way, we don't need as many single runs ($\sim 10^3$) as for a trapped system ($\sim 10^4$). As expected, the approximation yields good agreement in the quasi-condensate and the ideal gas limit, but deviates close to the cross-over. The strength of the deviation depends above all on the axial trapping frequency, as expected.

For the upcoming comparison of the results obtained with the SGPE to those of the mean-field theories, we will therefore make use of the LDA as long as it is justified, since with one simulation the whole equation of state can be calculated. In the cross-over region we have to stick to the homogeneous systems, requiring one ensemble of single runs for every data point.

One last comment has to be made in this regard. Although we have seen that the LDA works reasonably well, we have to be very careful with its usage. Above all, the correspondence between homogeneous and trapped systems breaks down completely in the regime where for the trapped system a true condensate with suppressed phase fluctuations exists, which is not possible for a homogeneous system. The density (profile) is admittedly the same for a quasi- and a true condensate, but the phase coherence properties are different [64].

9.5 Parameter choice and cut-off

The numerical implementation of the SGPE used in this thesis has been developed in a way that makes it easy to choose all parameters such that they are physically reasonable and close to experiments. That is why experimental parameters are entered in SI-units (except for the chemical potential), whereas the calculation itself is carried out in harmonic oscillator units.

The comparison with mean-field theories formulated in terms of cross-over units is therefore a non-trivial task because various conditions have to be fulfilled (we label harmonic oscillator and cross-over units by a *ho* and *co* subscript, respectively; no subscript means SI units).

On one hand, it has to be assured that the system in consideration is in fact (quasi-) one-dimensional, i.e. that transverse modes of the system are not excited

$$k_B T, \mu \ll \hbar\omega_\perp. \tag{9.5.1}$$

For the first condition, we introduce the factor $f_1 = \hbar\omega_\perp/(k_B T) \gg 1$. With the definition of the cross-over temperature parameter $\beta_x \ll 1$ (7.1.3) and the effective one-dimensional coupling constant

$$g = \frac{g_{3d}}{2\pi l_\perp^2} = 2\hbar\omega_\perp a_s \tag{9.5.2}$$

this leads to the condition

$$\omega_\perp = \frac{\beta_x^3 \omega_{\mathrm{lim}}}{f_1} \ll \beta_x^3 \omega_{\mathrm{lim}}, \tag{9.5.3}$$

where e.g. $\omega_{\mathrm{lim}} = \frac{\hbar}{4a_s^2 m} \approx 365\,\mathrm{MHz}$ for sodium ($a_s = 2.75\,\mathrm{nm}$, $m = 3.82 \cdot 10^{-26}\,\mathrm{kg}$). For a given value of β_x we have therefore

$$T = \frac{\hbar\omega_{\mathrm{lim}}}{k_B} \frac{\beta_x^3}{f_1^2}. \tag{9.5.4}$$

We have thus an inverted temperature dependence of β_x due to the dependence of the coupling strength on the transverse trapping frequency.

The second condition of (9.5.1) is then automatically fulfilled, since we have with $\mu_x = \beta_x k_B T$

$$\frac{|\mu|}{\hbar\omega_\perp} = |\mu_{co}| \frac{\beta_x k_B T}{\hbar\omega_\perp} = |\mu_{co}| \frac{\beta_x}{f_1} \ll 1 \tag{9.5.5}$$

and $\mu_{co} \leq \mathcal{O}(1)$ for our purposes.

On the other hand we have to make sure that the cut-off that comes along with the discretisation of space is chosen in a way that all relevant processes are still taken into account. Thus the grid spacing Δz must be smaller than the characteristic length scales of the system, which are the healing length and the thermal wavelength:

$$\Delta z < \min(\lambda_{dB}, \xi). \tag{9.5.6}$$

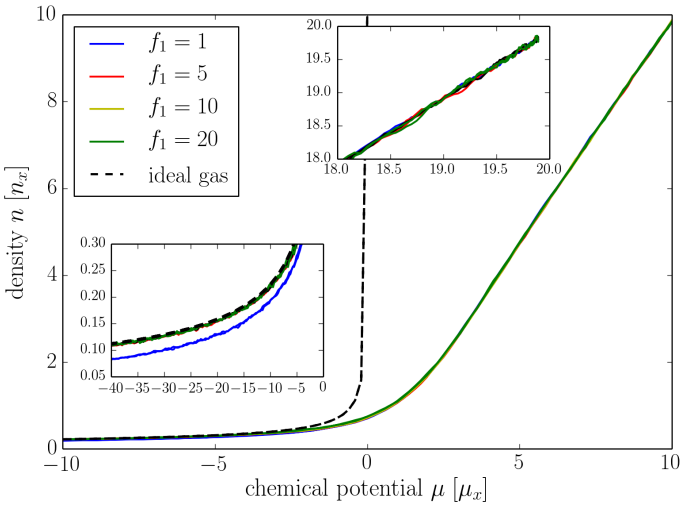

Figure 9.5.1: Equation of state in cross-over units obtained from a trapped gas in LDA for different ratios f_1 of transverse trapping to thermal energy ("1d-ness"); parameter ranges $T \approx 700 \ldots 2\,\mathrm{nK}$, $\omega_\perp \approx 91385 \ldots 4570\,\mathrm{Hz}$, $\omega_z = 3640 \ldots 9\,\mathrm{Hz}$

We observe that for our purposes, the healing length will generally be larger than the thermal wavelength. Approximating $gn \leq |\mu|$ in the healing length and proceeding as in equation (9.5.5), we have

$$\frac{\lambda_{dB}}{\xi} \sim \sqrt{\frac{gn}{k_B T}} \leq \sqrt{\frac{|\mu|}{k_B T}} = \sqrt{|\mu_{co}|\beta_x} < 1. \tag{9.5.7}$$

We can focus consequently on the thermal wavelength. For this purpose, we introduce another factor $f_2 = \lambda_{dB}/\Delta z \gg 1$. With Δz in harmonic oscillator units (as it enters in the code), this translates into the relation

$$\omega_z = \frac{k_B T}{2\pi\hbar} \Delta z_{ho}^2 \, f_2^2. \tag{9.5.8}$$

In order to fix all parameters, we still have to choose the two factors we have introduced. For f_1 this is rather straightforward; we need that condition (9.5.1) is fulfilled and that the temperature attains values that are still close to experiments, which limits f_1 from above. As a matter of fact, we have found that the results obtained for f_1 between 1 and 20 practically do not differ on the dense side of the cross-over (see figure 9.5.1). However, on the dilute side different densities are obtained, which we exploit to determine f_2. In this limit, the solution should approach the degenerate ideal Bose gas result; not the one we have seen for the thermodynamic limit though, but for a finite system size. Hence the integral from equation (2.3.1) has to be calculated with a cut-off determined by f_2, yielding

$$n = \frac{1}{\pi\hbar\beta} \sqrt{\frac{2m}{-\mu}} \arctan\left(\sqrt{\frac{E_{\mathrm{cut}}}{-\mu}} \right). \tag{9.5.9}$$

For values $f_1 > 5$ we get already a reasonable agreement, for $f_1 > 10$ there is practically no improvement any more (see figure 9.5.1). For the temperature not to get too low, we choose therefore $f_1 = 10$.

For f_2 it is a bit more complicated, because determining its value amounts to the decision of which modes are taken into the system (see end of section 9.1), since

$$f_2 = \sqrt{\frac{E_{cut}}{k_B T}}, \tag{9.5.10}$$

where $E_{cut} = \hbar^2/(2m\Delta z^2)$ is the UV energy cut-off introduced by the grid. On one side, we want to take as many modes as possible into account, otherwise the density of the thermal cloud gets "lost". This and the need to capture relevant length scales require a large cut-off. On the other side, the assumption of the whole system being still describable classically requires a low cut-off.

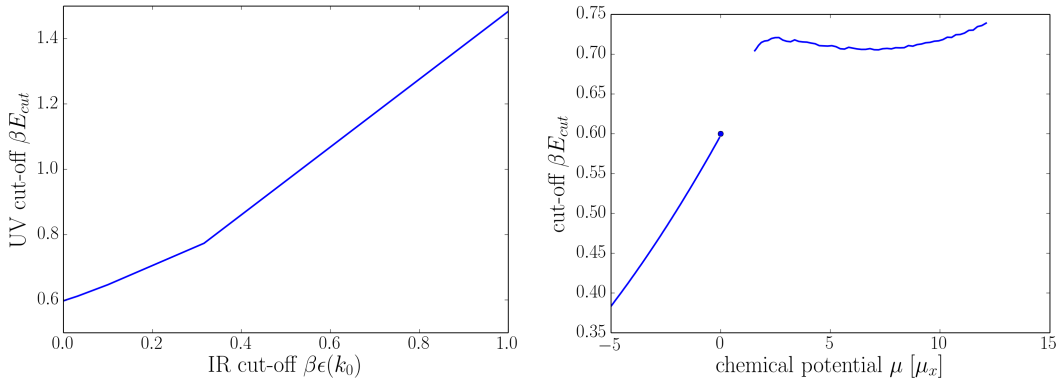

Figure 9.5.2: Cut-off determination by comparing BE to RJ distribution as explained in the text; ideal gas in the canonical ensemble (left and dot in right figure), the grand canonical ensemble (right, dilute side) and Modified Popov theory (right, dense side) yield the consistent result $\lim_{\mu\to 0} \beta E_{\mathrm{cut}} = 0.6$

We have made attempts to actually determine the cut-off from qualitative arguments (rather than just matching the result to other data). In the course of the derivation of the SGPE (in the version we are using), the Bose-Einstein (BE) distribution is replaced by the classical Rayleigh-Jeans (RJ) distribution. We know that the latter gives higher values in the high momentum limit, it is therefore reasonable to calculate the cut-off such that the integrated RJ distribution yields the same densities as the BE distribution integrated up to infinity.

In principle, we prefer a parameter independent cut-off for matters of simplicity (LDA would not be possible otherwise). That is why we have performed such a calculation for the ideal gas within the canonical ensemble. This is a bit tricky, because both integrals are - surprisingly - IR divergent. This may be worked around by introducing a small IR cut-off k_0, because the RJ distribution is in fact the low momentum approximation of the BE distribution and thus they give both the same result in this limit. The UV cut-off has to be determined consequently such that

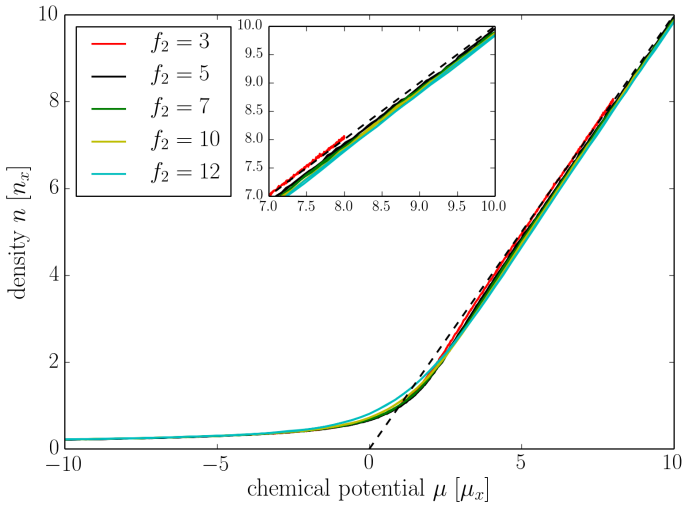

Figure 9.5.3: Equation of state in cross-over units obtained numerically from a trapped gas in LDA for different cut-off ratios f_2 compared to the quasi-condensate limit; parameter ranges: $T = 7\,\mathrm{nK}$, $\omega_\perp = 9139\,\mathrm{Hz}$, $\omega_z = 0.4 \ldots 52\mathrm{Hz}$

$$\frac{1}{x_0} - \frac{1}{\sqrt{\beta E_{\mathrm{cut}}}} = \int_{x_0}^{\infty} \frac{\mathrm{d}x}{e^{x^2} - 1}, \tag{9.5.11}$$

where $x_0 = \sqrt{\beta\epsilon(k_0)}$. In order to get the exact result, we have to take the limit $x_0 \to 0$. This is quite difficult numerically, it helps to convert the above integral into Bose-Einstein integral form though (appendix A.1). Eventually, we obtain the result $\beta E_{\mathrm{cut}} = 0.6$ (see figure 9.5.2). For comparison, we repeat the calculation within the grand-canonical ensemble, which is less involved since the chemical potential regularizes the integrals. We find a small linear dependence of the cut-off from the chemical potential and in the limit $\mu \to 0$ we recover 0.6. Eventually, we use Modified Popov theory as an example of a mean-field theory in order to get results for the dense side, recovering the same cut-off in the limit $\mu \to 0$; hence the obtained result seems to be somehow universal[3]. Unfortunately, it is not suited for our purposes, as f_2 is required to be larger than one.

For that reason, we have to stick to analysing the results that different cut-offs yield. Contrary to f_1, we find that the density is practically independent from the cut-off choice in the ideal gas limit, and differs in the quasi-condensate limit and the cross-over region. Small values of f_2 give densities $n > \mu$ already for small chemical potentials (see inlay of figure 9.5.3). We choose therefore the smallest value of f_2 that still gives an asymptote $n \sim \mu$ in this limit. From the same figure we estimate this value to be $f_2 = 5$.

[3]This is underlined by the fact that the result, although in the grand canonical ensemble calculated for a specific temperature, is temperature independent.

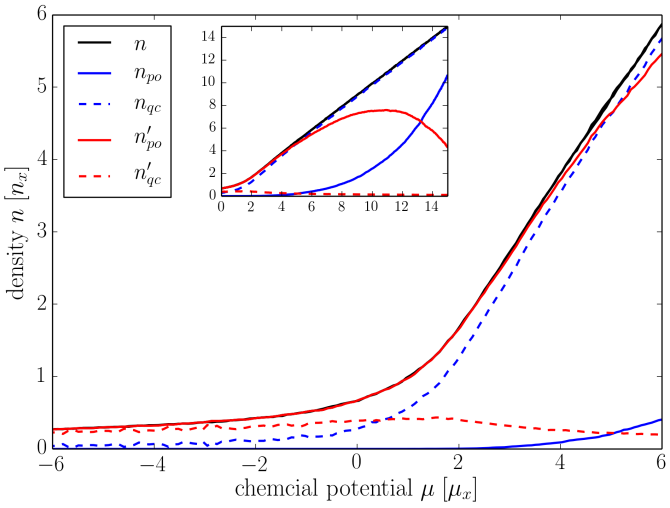

Figure 9.6.1: Equation of state obtained from the SGPE ($T = 7\,\mathrm{nK}$, $\omega_\perp = 9139\,\mathrm{Hz}$, $\omega_z = 9\mathrm{Hz}$,$\mu = 150\,\hbar\omega_z \approx 15\,\mu_x$) with the total density n, quasi-condensate density n_{qc} and Penrose-Onsager mode n_{po} and the corresponding thermal densities $n'_{qc/po} = n - n_{qc/po}$ (same quantities in the inset)

9.6 Equation of state and comparison to mean-field theories

We notice that for our choice for the factors $f_1 = 10$ and $f_2 = 5$, we can apply the LDA without changing the result noticeably (see section 9.4). We will therefore calculate the equation of state from the density profile of a trapped Bose gas with

$$T = 7\,\mathrm{nK}, \qquad \omega_\perp = 9139\,\mathrm{Hz}, \qquad \omega_z = 9\,\mathrm{Hz}, \qquad \mu = 150\,\hbar\omega_z \approx 15\,\mu_x. \tag{9.6.1}$$

We have now prepared everything for a comparison of the results that we have obtained from the different approaches. Prior to that, we present the equation of state of SGPE for the chosen parameters along with Penrose-Onsager mode, quasi-condensate density (9.3.2) and the corresponding thermal densities in figure 9.6.1. The quasi-condensate density behaves as we would expect it: it grows from zero on the dilute side until reaching $n_{qc} \simeq n$ on the dense side. The thermal density that is linked to it, remains almost constant up to cross-over from where on it decreases until reaching zero for high chemical potentials. As we have argued before, these two quantities are actually those that we can obtain from the homogeneous mean-field theories (thus $n_{qc} \equiv n_0$ and $n'_{qc} \equiv n'$). The Penrose-Onsager mode corresponds to a true, phase coherent condensate, which cannot exist in an one-dimensional homogeneous Bose gas. That is why this quantity is of no relevance for us here; nevertheless we observe a slightly different behaviour especially around the cross-over region (compared to the quasi-condensate).

Finally, we compare the densities that we have obtained for the mean-field theories with those of the SGPE. As expected, the SGPE density approaches the degenerate ideal Bose gas limit, the influence of the cut-off seems to have a negligible influence (since the curve of the degenerate gas plotted in figure 9.6.2 corresponds to the thermodynamic limit). The only theory that is able to capture the physics of the (non-degenerate) ideal Bose gas is

therefore Hartree-Fock theory (dilute), which fails on the dense side though. The SGPE is the only one that actually can describe the cross-over and the quasi-condensate limit correctly. Remarkably, for the region close to the cross-over, Hartree-Fock theory (dense), although being the most simple of the theories, gives densities that are closer to the SGPE result than all other mean-field theories. Having said that, it must be pointed out that this may not be a good criterion, remembering that the SGPE result is dependent on the parameters, above all the cut-off. At the end, we have just chosen values for the factors f_1 and f_2, and with a different choice maybe another mean-field theory would give better matching than Hartree-Fock. In section 7.4.2 we have argued that Mora-Castin theory is in that sense unique that it has a crossing with Hartree-Fock theory (dilute). Here we realize that it yields quite high (quasi-condensate) densities in the cross-over region, whereas the thermal density is very low (see as well figure 9.6.3 around $\mu = 2\,\mu_x$).

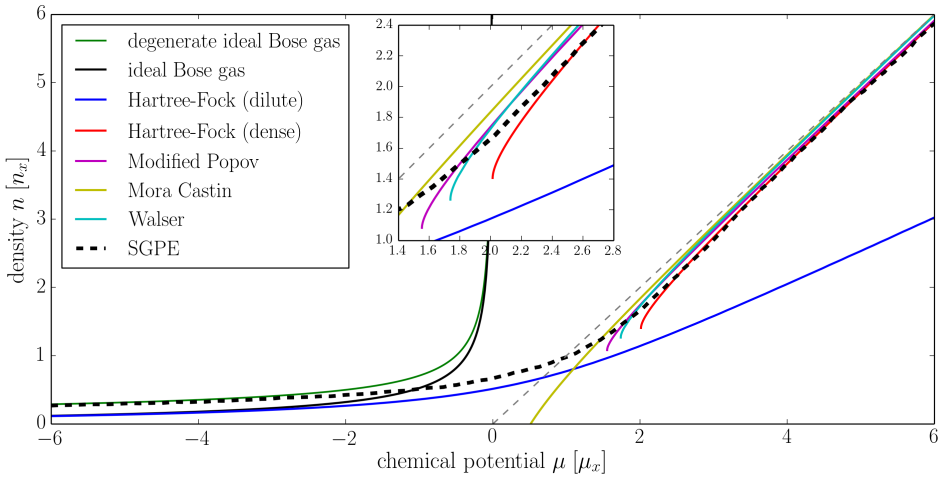

Figure 9.6.2: Equation of state obtained for different mean-field theories, the SGPE and the ideal Bose gas for $\beta_x = 10^{-1}$

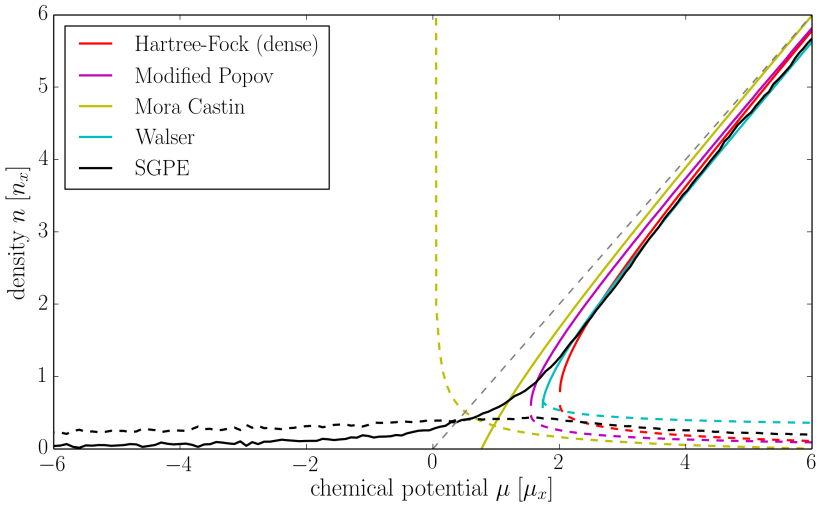

Figure 9.6.3: Quasi-condensate (solid) and thermal density (dashed) for different mean-field theories and the SGPE for $\beta_x = 10^{-1}$

For completeness, we finish this chapter applying the LDA the other way around, creating density profiles from the equation of state of the mean-field theories (figure 9.6.4). This does not provide really new insights, but shows that the mean-field theories are in principle capable of describing a Bose gas in a trap, given that the conditions for the LDA are fulfilled.

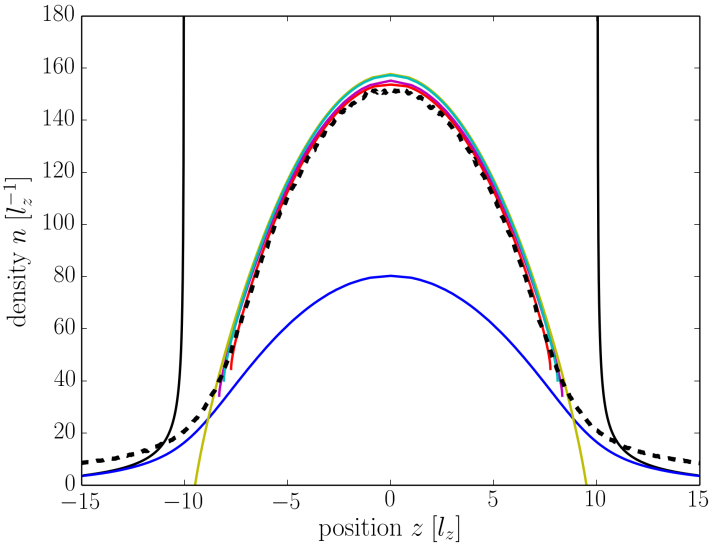

Figure 9.6.4: Density profiles obtained in LDA from the mean-field theories, corresponding to the equation of state from figure 9.6.2 (but with $\mu = 50\hbar\omega_z$ instead; colours as in figure 9.6.2).

9.7 Correlation functions

Finally we have a quick look an the correlation functions. The first order correlation function of a homogeneous gas obtained from the SGPE decays exponentially and reaches zero as expected for a quasi-condensate. The decay is in fact a bit faster than for Mora-Castin and Modified Popov theory (see figure 9.7.1).

Density fluctuations have as well been calculated with the SGPE for a trapped gas using the LDA with the parameters from the previous section. On the dense side of the cross-over, or equivalently in the trap centre, $g_2(0)$ reaches the coherent value of one. On the dilute side, or in the wings of the trap, it approaches the decoherent value two. The cross-over from one regime to the other can easily be identified (see figure 9.7.2). The SGPE seems to work as well on the dilute side of the cross-over, although the impact of the fluctuations is much bigger, resulting in a quite noisy curve.

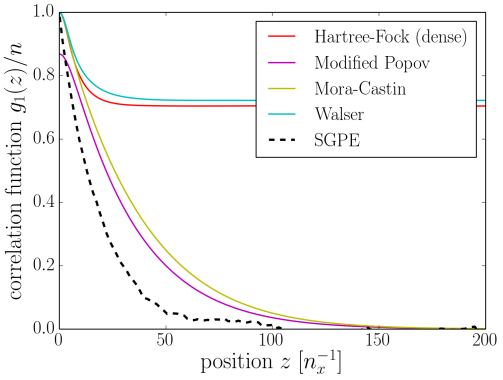

Figure 9.7.1: First order correlation function $g_1(z)$ obtained from the SGPE for a homogeneous gas (parameters as in section 9.6) for $\mu = 2.1\,\mu_x$ and $\beta_x = 10^{-1}$ compared to mean-field results

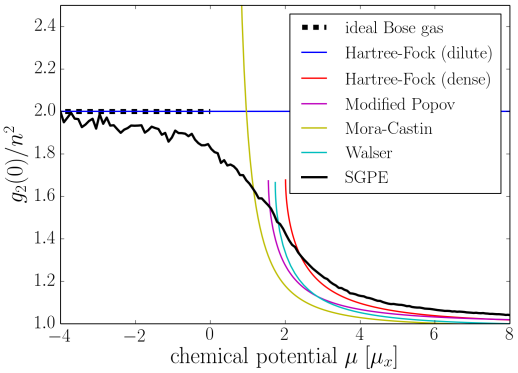

Figure 9.7.2: Second order correlation function $g_2(0)$ obtained from the SGPE for a trapped gas using the LDA (parameters as in section 9.6) compared to mean-field results for $\beta_x = 10^{-1}$

Chapter 10

Summary and outlook

In this thesis the one-dimensional interacting Bose-Einstein quasi-condensate has been examined making use of various mean-field approaches on one side, and a stochastic model on the other. Results obtained from both methods have been compared within their common scope of validity.

The description of an interacting Bose gas with mean-field theory is a tricky task in lower dimensions. Long-wavelength quantum fluctuations destroy long-range order and therefore the formation of a proper condensate is impossible in the thermodynamic limit. The existence of the latter is the basis of the mean-field treatment in the sense of Bogoliubov theory though, since only a macroscopically occupied ground state justifies the replacement of the corresponding field operator by a complex number. In this way the phase of the (quasi)-condensate is fixed, the original $\mathcal{U}(1)$-gauge symmetry spontaneously broken and by this means phase fluctuations excluded from the description of the gas. In three dimension or generally in the presence of a true condensate, this is no problem since there exists long-range order with respect to the phase and thus phase fluctuations are not important in general. For the quasi-condensate in lower dimensions, only density fluctuations are suppressed, but the phase fluctuates. The application of the symmetry breaking approach is still justifiable though in the quasi-condensate regime, which we have referred to as the dense side of the cross-over, because the phase coherence length l_ϑ is much larger than the healing length ξ. Viewed on the scale of the latter characteristic length, the gas exhibits some kind of local phase coherence which makes the introduction of the order parameter characterising low-lying modes possible.

This approach has the following consequences:

- True condensate and quasi-condensate have the same properties with respect to the density of the gas. For this reason, the equation of state, the second order correlation function $g_2(z)$ and density fluctuations can be described properly with the mean-field approach on the dense side of the cross-over. This includes an asymptote of $n \sim \mu$ for large μ, a density correlation length decreasing with density and suppressed density fluctuations $\delta n^2 \to 0$ in the quasi-condensate limit. Approaching the cross-over from this limit, the density fluctuations grow until reaching $\delta n^2 \approx 0.7\, n^2$ at the critical

points, coming close to the degenerate, completely Gaussian ideal Bose gas (or thermal interacting gas described by Hartree-Fock theory (dilute)) limit of $\delta n^2 = n^2$.

- Phase coherence properties of a quasi-condensate can only be captured on the length scale of the local phase coherence, if additional effort is made in order to incorporate phase fluctuations in the first order correlation function as for Modified Popov and Mora-Castin theory. Therefore the standard Hartree-Fock Bogoliubov approach mistakenly predicts the presence of a true condensate even in one dimension.

- The theories leave their range of validity approaching the cross-over from the dense side. The assumption of local phase coherence based on the condition $l_\vartheta \gg \xi$ gets violated close to the cross-over, which we have seen from explicitly calculating correlation lengths over a wide range of accessible values of the chemical potential. This violation manifests in critical points beyond which the theories do not work, or in the case of Mora-Castin theory, the density gets negative.

All mean-field theories (for the dense side of the cross-over) reviewed in this thesis except for Mora-Castin theory (that is, Hartree-Fock (dense), Modified Popov and Walser theory) make use of the condition ($l_\vartheta \gg \xi$) in the course of their derivation. Mora-Castin theory, however, is based on the assumption $\delta n \ll n_0$, where δn are density fluctuations around the mean-field. The failure of this theory close to the cross-over is therefore due to the violation of this condition.

Characteristic quantities of these theories are given in terms of self-consistent integral equations. In this work, these equations have been scaled to characteristic units of the cross-over, leaving the dimensionless temperature-interaction strength parameter $\beta_x = \mu_x/k_BT$ as the only free parameter. This parameter is typically small $\beta_x \ll 1$, making it possible to give high-temperature expansions of the integrals in powers of β_x. This reduces the numerical effort of solving the self-consistent equations drastically and gives an easy access to estimates of the critical points. Correlation functions, the equation of state and density fluctuations have been calculated for the dense side of the cross-over. Although a description beyond the mentioned critical points, and therefore a description of the cross-over itself, is not possible, mean-field theory can be used for the whole range of the cross-over by combining different theories. Hartree-Fock theory in the formulation for the dilute side does not show a critical point, but since it does not include a (quasi-)condensate, it gives an incorrect asymptote on the dense side. Still it works fine on the dilute side, which makes it possible to combine it with one of the other theories on the dense side in order to obtain a complete description of the cross-over from the degenerate Bose gas to the quasi-condensate. For most of the theories, the resulting curve is not continuous but exhibits a jump in the density at the critical point. In the case of Mora-Castin theory however, there is a crossing and thus the resulting curve is, although not smooth, continuous (which makes it the most obvious choice for this procedure). Together with the high-temperature expansions, this provides a powerful tool for calculating the equation of state or, equivalently, density profiles with the local density approximation, of a finite temperature Bose gase in one dimension with little numerical effort.

For Mora-Castin and Walser theory, an "anti-bunching" behaviour in the density fluctuations has been found. This effect is negligible for $\beta_x \leq 10^{-2}$, but quite obvious for the the parameter

value in consideration $\beta_x = 10^{-1}$. This is admittedly quite close to the strongly interacting Tonks-Girardeau regime (for which $\beta_x \geq 1$), but a mean-field approach is not expected to be capable of describing the physics of fermionisation. It rather suggests that these theories are less suited in this parameter range. That is particularly clear for Mora-Castin theory, which predicts negative thermal densities for chemical potentials larger than a (second) critical value that scales with the inverse of β_x (for $\beta_x = 10^{-1}$ it is thus quite small $\mu_{c2} \approx 6.31\,\mu_x$).

Furthermore, the theories have been compared qualitatively adopting a scheme introduced by Griffin [30]. They all are structurally similar (which becomes most apparent in the high-temperature expansions in table 7.1) and differ in the way higher moments of the quantum field are taken into account. It has been found that considering more hydrodynamic fields (higher moments of the quantum field) does not necessarily imply an improved description of the gas. The simplest theory considered, Hartree-Fock theory (dense), yields in fact quite similar results as Walser theory, which takes account of all second-order averages including the anomalous average. Moreover, the latter is not able to capture the phase coherence properties of a quasi-condensate either. Within the mentioned comparison, the theories have as well been analysed according to their excitation spectra. The Goldstone (and Hugenoltz-Pines) theorem requires a gapless spectrum for the excitations associated to the spontaneous symmetry breaking, but on the other hand fundamental conservation laws have to be fulfilled. The two theories mentioned above (Hartree-Fock (dense) and Walser) do not have a gapless spectrum though; Walser justifies this by relating the Goldstone mode to a different kind of excitations.

In the second part of this thesis, we have evaluated the Stochastic Gross-Pitaevskii equation in the version of Stoof *et al.* [25, 120] numerically using a code developed by Cockburn [98]. The SGPE is a non-linear Langevin equation for a complex field that includes the (quasi-)condensate and low-lying excitations up to a cut-off that is determined by the spacing of the numerical grid. The field is coupled to a thermal cloud whose dynamics are described by a quantum Boltzmann equation. For simplicity, thermal equilibrium within this cloud and high occupation of the field modes is assumed in order to make use of the classical Rayleigh-Jeans distribution. That is why the SGPE results approach the degenerate (classical) ideal Bose gas on the dilute side of the cross-over.

We have analysed the influence of the strength of the coupling γ between the field and the heat bath and found that the equilibrium properties are practically unaffected over many orders of magnitude of γ. Density profiles of harmonically trapped gases have been calculated, and the quasi-condensate, Penrose-Onsager mode and associated thermal densities have been determined. The density profiles have been converted to the equation of state of a homogeneous Bose gas making use of the local density approximation. We analysed the validity of the latter by comparing the equations of state obtained in LDA from a trapped gas to those obtained from a whole range of homogeneous systems with periodic boundary conditions. It has been found that the approximation gives slightly wrong results in the cross-over region, depending above all on the axial trapping frequency ω_z.

For the comparison with mean-field results, it was a particularly difficult task to determine the parameters used for the simulations. Especially the UV cut-off introduced by the grid was not easy to determine and was chosen in the end such that expected results in the ideal Bose gas and quasi-condensate limits are obtained. We found good agreement, in terms of equation

of state, first order correlation function and density fluctuations, between the two approaches beyond the critical points of the mean-field theories. The SGPE is capable of describing the cross-over region and the dilute side as well, although fluctuations are very strong in this latter regime. The numerical effort for these results is huge compared to the mean-field approach, because ensemble averages of more than 1000 single runs have to be taken. On the other hand, the SGPE is not limited to equilibrium properties, in fact its strength is the correct description of dynamical processes in trapped Bose gases (see for example [25, 126]).

It turned out to be rather difficult to decide on the basis of results obtained in this thesis, which of the mean-field theories is the most appropriate for the description of a quasi-condensate. When it comes to phase coherence properties, it is clear that only Mora-Castin and Modified Popov theory give correct results. But coherence properties with respect to density and the equation of state itself is described by all mean-field theories (except for Hartree-Fock theory (dilute)) qualitatively in the same way. On the far dense side of the cross-over, they all yield very similar results. The comparison with the SGPE cannot really be taken as a benchmark theory here, because its results depend on the parameter choice, especially the on cut-off choice. In order to finally answer that question, a comparison with the exact solution of the Yang-Yang equations would be necessary.

Further comparison could as well be undertaken with other non-perturbative theories, like the thermal field theory (TFT) developed by Castin [45]. In the limit of high temperatures, he derives a classical field theory, evaluating the corresponding classical path integrals by means of an analogy with quantum mechanics in imaginary time. In the work of Polster [127], the path integrals are associated to the solution of a Fokker-Planck equation. This method allows the description of the full cross-over and gives easy access to statistical properties of the gas. We have compared the equations of state obtained by Polster to our results in the appendix D.3. We found good agreement with the SGPE data for $\beta_x = 10^{-1}$ (see left of figure D.3.1). For the strict comparison with mean-field results we need smaller values of β_x though, because the classical approximation corresponds to the limit $\beta_x \to 0$. We observed for $\beta_x = 10^{-3}$ that Hartree-Fock theory (dilute) approaches the TFT level on the dilute side, while on the dense side all mean-field theories are in rather good agreement with the TFT. Hartree-Fock theory (dense) seems to deviate more than the other theories though. A more detailed analysis, including coherence properties, is necessary here.

Apart from that, the temperature dependence of characteristic quantities could be another way of investigation for the mean-field theories. In this thesis we mainly restricted ourselves to constant β_x for our calculations. Superfluidity in a one-dimensional ring trap would be an interesting field of research for the SGPE. A further comparison with mean-field theory (and as well the TFT) is possible via the calculation of the superfluid fraction of the gas, which can be obtained from equilibrium properties [128].

Appendices

Appendix A

Bose-Einstein integral

A.1 Expansion of the Bose-Einstein integral

We come across different forms of the Bose-Einstein integral $g_n(z)$, which is also known as polylogarithm or Jonquière's function $\mathrm{Li}_n(z)$:

$$g_n(z) = \frac{1}{\Gamma(n)} \int_0^\infty \frac{x^{n-1}\,\mathrm{d}x}{z^{-1}e^x - 1} \tag{A.1.1}$$

The integral can be treated in the following way:

$$\int_0^\infty \frac{x^{n-1}\,\mathrm{d}x}{z^{-1}e^x - 1} = \int_0^\infty \mathrm{d}x\, ze^{-x} \left(1 - ze^{-x}\right)^{-1} x^{n-1} = \int_0^\infty \mathrm{d}x\, ze^{-x} \sum_{k=0}^\infty \left(ze^{-x}\right)^k x^{n-1} \tag{A.1.2}$$

Applying the substitution $y := x(k+1)$ makes the gamma function appear:

$$g_n(z)\Gamma(n) = \sum_{k=0}^\infty z^{k+1} \int_0^\infty \mathrm{d}x\, e^{-x(k+1)} x^{n-1} = \sum_{k=0}^\infty \frac{z^{k+1}}{(k+1)^n} \underbrace{\int_0^\infty \mathrm{d}y\, e^{-y} y^{n-1}}_{\Gamma(n)} \tag{A.1.3}$$

We thus have

$$g_n(z) = \sum_{k=1}^\infty \frac{z^k}{k^n}, \tag{A.1.4}$$

which is a Dirichlet series. It converges absolutely for $\mathrm{Re}\, n > 1$ if $f_k = z^k$ is a bounded series or in this case equivalently, if the sum $\sum_{k=1}^{\infty} f_k$ is convergent. Since this is the geometric series, we deduce that the sum (A.1.4) converges absolutely for $z < 1$ on the half plane $\mathrm{Re}(n) > 1$.

In [35], the Mellin transform of this sum is taken. The inverse transformation is carried out by integration over the complex plane using residue calculus, which yields with $z = e^{-\alpha}$:

$$g_n(e^{-\alpha}) = \frac{\Gamma(1-n)}{\alpha^{1-n}} + \sum_{k=0}^{\infty} \frac{(-1)^n}{n!} \zeta(n-k)\, \alpha^k \tag{A.1.5}$$

This holds for all $n \in \mathbb{R}$ and is convergent for $|\alpha| \leq 2\pi$ if $n \geq 1$. If $n < 1$, it diverges for $\alpha \to 0$, but in this case we can use the original expression (A.1.4) which can be identified as the Riemann Zeta function:

$$g_n(1) = \sum_{k=1}^{\infty} \frac{1}{k^n} = \zeta(n). \tag{A.1.6}$$

This sum is divergent for $n \leq 1$. But the Riemann Zeta function can be analytically continued[1] and given a value even in this case; this will be important in many calculations in this thesis.

The sum in (A.1.5) converges quite rapidly for $\alpha \leq 1$ and can thus be truncated after a few terms in this case. Zeta and Gamma function have the following values for half-integer arguments [129]:

$n \to$	$-3/2$	$-1/2$	$1/2$	$3/2$	$5/2$
$\zeta(n)$	-0.02549	-0.20789	-1.46035	2.61238	1.34149
$\Gamma(n)$	$\frac{4}{3}\sqrt{\pi}$	$-2\sqrt{\pi}$	$\sqrt{\pi}$	$\frac{1}{2}\sqrt{\pi}$	$\frac{3}{4}\sqrt{\pi}$

A.2 Heat capacity of the ideal Bose gas above T_c

We follow the steps of [34] for the calculation of the heat capacity of the ideal Bose gas above the condensation temperature. It yields an equation explicit in temperature and improves the result given by London already in 1938 [3].

First of all, we use the expansion (A.1.5) in the expressions for the energy and the pressure given in 2.1.12 and (2.1.13), respectively. As we are interested in an approximation around the critical point, we expand the Bose-Einstein functions for $|\mu| \ll 1$, thus for $\alpha = -\beta\mu \ll 1$:

$$g_{3/2}(\alpha) \simeq \Gamma(-1/2)\, \alpha^{1/2} + \zeta(3/2) \tag{A.2.1}$$

$$g_{5/2}(\alpha) \simeq \Gamma(-3/2)\, \alpha^{3/2} + \zeta(5/2) + \zeta(3/2)\, \alpha \simeq \zeta(5/2) + \zeta(3/2)\, \alpha. \tag{A.2.2}$$

[1] More precisely, the Riemann Zeta function is defined by the Dirichlet series (A.1.6) only for $n > 1$.

From (A.2.1), (2.1.6) with $N - N_0 \equiv N$ and (2.1.9) we obtain an expression for α:

$$\alpha = \left(\frac{g_{3/2} - \zeta(3/2)}{\Gamma(-1/2)}\right)^2 = \left(\frac{\frac{N\lambda_{dB}^3}{g_s V} - \zeta(3/2)}{\Gamma(-1/2)}\right)^2 = \left(\frac{\zeta(3/2)}{2\sqrt{\pi}}\left[1 - \left(\frac{T_c}{T}\right)^{3/2}\right]\right)^2. \tag{A.2.3}$$

The internal energy (2.1.11) can now be written as:

$$E = \frac{3}{2}Nk_BT\frac{g_{5/2}(\alpha)}{g_{3/2}(\alpha)} \simeq \frac{3}{2}Nk_BT\frac{\zeta(5/2) + \zeta(3/2)\,\alpha}{\zeta(3/2) + \Gamma(-1/2)\,\alpha^{1/2}} \tag{A.2.4}$$

For small α this can be expanded and eliminating α with (A.2.3), we obtain:

$$E \simeq \frac{3}{2}Nk_BT\left\{a_1 + a_2\left(\frac{T_c}{T}\right)^{3/2} + a_3\left(\frac{T_c}{T}\right)^3\right\} \qquad T > T_c \tag{A.2.5}$$

where the three coefficients are given by:

$$a_1 = 3\frac{\zeta(5/2)}{\zeta(3/2)} - \frac{\zeta^2(3/2)}{4\pi} \approx 0.997 \tag{A.2.6}$$

$$a_2 = \frac{\zeta^2(3/2)}{2\pi} - 3\frac{\zeta(5/2)}{\zeta(3/2)} \approx -0.454 \tag{A.2.7}$$

$$a_3 = \frac{\zeta(5/2)}{\zeta(3/2)} - \frac{\zeta^2(3/2)}{4\pi} \approx -0.030. \tag{A.2.8}$$

From there it is easy to calculate the pressure and the heat capacity:

$$p = \frac{2E}{3V} \simeq \frac{Nk_BT}{V}\left\{a_1 + a_2\left(\frac{T_c}{T}\right)^{3/2} + a_3\left(\frac{T_c}{T}\right)^3\right\} \qquad T > T_c \tag{A.2.9}$$

$$C_V = \left.\frac{\partial E}{\partial T}\right|_V \simeq Nk_B\left\{\frac{3}{2}a_1 - \frac{3}{4}a_2\left(\frac{T_c}{T}\right)^{3/2} - 3\,a_3\left(\frac{T_c}{T}\right)^3\right\} \qquad T > T_c \tag{A.2.10}$$

Appendix B

Bogoliubov theory

B.1 Zero-point energy in one dimension

The integral which has to be calculated is:

$$\Delta E_0 = \frac{L}{4\pi} \int_{-\infty}^{\infty} \mathrm{d}k \left\{ \left(\frac{\hbar^2 k^2}{2m} \left(\frac{\hbar^2 k^2}{2m} + 2g|\phi|^2 \right) \right)^{1/2} - \frac{\hbar^2 k^2}{2m} - g\,|\phi|^2 \right\}. \tag{B.1.1}$$

With the substitution $x^2 := \hbar^2 k^2/(4mg|\phi|^2)$ this can be written as:

$$\begin{aligned} \Delta E_0 &= \frac{L}{2\pi} \frac{\sqrt{2m}}{\hbar} \left(2g|\phi|^2\right)^{3/2} \int_0^{\infty} \mathrm{d}x \left\{ \left(x^2 \left(x^2 + 1 \right) \right)^{1/2} - x^2 - \frac{1}{2} \right\} \\ &= \frac{L}{2\pi} \frac{\sqrt{2m}}{\hbar} \left(2g|\phi|^2\right)^{3/2} \left(\frac{\left(x^2+1\right)^{3/2}}{3} - \frac{x^3}{3} - \frac{x}{2} \right) \Bigg|_0^{\infty} \end{aligned} \tag{B.1.2}$$

The value of the integral is $-1/3$ since in the large x-limit the leading term is $\frac{1}{8x}$ and thus the contribution of the upper bound is zero. Hence we obtain the result for the correction of the ground state energy density for the Bogoliubov theory in one dimension due to the zero-point energy:

$$\frac{\Delta E_0}{L} = -\frac{1}{6\pi} \frac{\sqrt{2m}}{\hbar} \left(2g|\phi|^2\right)^{3/2}. \tag{B.1.3}$$

B.2 Thermodynamics in one dimension

The energy contribution of the excitations in one dimension can be calculated with the corresponding expression of the ideal Bose gas (2.1.11) using the Bogoliubov dispersion relation instead of that for free particles. This is justified for low temperatures, for which the Bose-Einstein distribution can be approximated by the Boltzmann distribution. We apply the substitution $x^2 = \hbar^2 k^2 \beta^2 g n_0 / m$:

$$\frac{E - E_0}{L} \simeq \frac{1}{2\pi} \int_{-\infty}^{\infty} \mathrm{d}k \, E(k) e^{-\beta E(k)} = \frac{\sqrt{2}\xi}{\lambda_{dB}^2 \beta^2 g n_0} \int_0^{\infty} \mathrm{d}x \, x \left(x^2 + 4(\beta g n_0)^2 \right)^{1/2} e^{-\frac{x}{(2\beta g n_0)} \left(x^2 + 4(\beta g n_0)^2 \right)^{1/2}} \tag{B.2.1}$$

For small temperatures and thus large β, we can neglect $x^2 \ll 4(\beta g n_0)^2$, the integral is dominated by the low-x contribution anyway due to the exponential. We therefore have:

$$\frac{E - E_0}{L} \simeq \frac{2^{3/2}\xi}{\lambda_{dB}^2 \beta} \int_0^{\infty} \mathrm{d}x \, x e^{-x} = \frac{2^{3/2}\xi}{\lambda_{dB}^2 \beta}. \tag{B.2.2}$$

Appendix C

Finite temperature mean-field theories

C.1 Divergences of Popov theory

The integral of the thermal density can be written as

$$n' = \int_{-\infty}^{\infty} \frac{\mathrm{d}\mathbf{k}}{(2\pi)^d} \left\{ \frac{\epsilon(k) - E(k)}{2E(k)} + \frac{\epsilon(k)}{E(k)} N_{BE}(E(k)) + \frac{gn_0}{E(k)} \left(N_{BE}(E(k)) + \frac{1}{2} \right) \right\}. \qquad \text{(C.1.1)}$$

Writing $E(k) = \sqrt{a^2k^4 + bk^2}$ and $\epsilon(k) = ak^2$, we have in the IR-limit the expansions

$$E(K) \sim \sqrt{b}k + \frac{a^2}{2}k^3, \quad N_{BE}(E(K)) \sim \frac{k_BT}{\sqrt{b}k + \frac{a^2}{2}k)} \ (T \neq 0) \qquad \text{(C.1.2)}$$

This yields the following limits:

1. $\lim\limits_{k\to 0} \dfrac{\epsilon(k) - E(k)}{2E(k)} k^{d-1} = \lim\limits_{k\to 0} \left(\dfrac{ak^d}{2\sqrt{b}} - \dfrac{k^{d-1}}{2} \right) = \begin{cases} 0 & d \geq 2 \\ -1/2 & d = 1 \end{cases}$

2. $\lim\limits_{k\to 0} \dfrac{\epsilon(k)}{E(k)} N_{BE}\, k^{d-1} = \lim\limits_{k\to 0} \dfrac{ak_BT}{2b} k^{d-1} = \begin{cases} 0 & d \geq 2 \\ \dfrac{k_BT}{2gn_0} & d = 1 \end{cases}$

3. $$\lim_{k\to 0}\frac{gn_0}{E(k)}\left(N_{BE}+\frac{1}{2}\right)k^{d-1}=\lim_{k\to 0}\left(\frac{gn_0k_BT}{b}k^{d-3}+\frac{gn_0}{2\sqrt{b}}k^{d-2}\right)$$
$$=\lim_{k\to 0}\begin{cases}\frac{m}{\hbar^2}k_BT & d=3\\ \frac{m}{\hbar^2}\frac{k_BT}{k}+\frac{\sqrt{gn_0m}}{2\hbar} & d=2\\ \frac{m}{\hbar^2}\frac{k_BT}{k^2}+\frac{\sqrt{gn_0m}}{2\hbar}\frac{1}{k} & d=1.\end{cases}$$

We observe that the last term is IR-divergent for all temperatures in 1d and for all $T\neq 0$ in 2d (assuming that $\lim_{k\to 0}\frac{0}{k}=0$). For the UV-limit we have

$$E(K)\sim ak^2+\frac{b}{2a},\qquad N_{BE}(E(K))\sim e^{-\beta(ak^2+b/2a)}\to 0 \tag{C.1.3}$$

and therefore:

1. $$\lim_{k\to\infty}\frac{\epsilon(k)-E(k)}{2E(k)}k^{d-1}=\lim_{k\to\infty}-\frac{b}{4a^2}k^{d-3}=\begin{cases}-\frac{gn_0m}{\hbar^2} & d=3\\ 0 & d\leq 2\end{cases}$$

2. $$\lim_{k\to\infty}\frac{\epsilon(k)}{E(k)}N_{BE}\,k^{d-1}=0$$

3. $$\lim_{k\to\infty}\frac{gn_0}{E(k)}\left(N_{BE}+\frac{1}{2}\right)k^{d-1}=\lim_{k\to\infty}\frac{gn_0}{2a}k^{d-3}=\begin{cases}\frac{gn_0m}{\hbar^2} & d=3\\ 0 & d\leq 2\end{cases}$$

Since the first and the last term compensate, there is no UV-divergence in any dimension. If the last term is subtracted though, as is done in the Modified Popov theory, the integral is UV-divergent in three dimensions (compensated by renormalising the coupling constant in Modified Popov theory).

C.2 Diagonalisation of Hartree-Fock Bogoliubov Hamiltonian

The diagonalisation of the full Hamiltonian is carried out in the same way as we have done for the Bogoliubov theory in section 4.1, taking higher orders of the quantum field into account though. Additionally to the Hamiltonian up to second order that has been considered before ((4.1.2) - (4.1.3)), the Hamiltonian of third and fourth order are incorporated:

$$H_3 = g \int_V \mathrm{d}\mathbf{r} \left(\phi \, \delta\psi^{\dagger 2} \delta\psi + h.c. \right) \tag{C.2.1}$$

$$H_4 = \frac{g}{2} \int_V \mathrm{d}\mathbf{r} \, \delta\psi^{\dagger 2} \delta\psi^2. \tag{C.2.2}$$

We approximate these higher order terms by ordering the operators pairwise similar to Wick's theorem and approximate quadratic terms by their expectation value (see self-consistent quadratic approximation in [30]):

$$\delta\psi^{\dagger 2} \delta\psi \simeq 2n' \delta\psi^\dagger + m'^* \delta\psi \tag{C.2.3}$$

$$\delta\psi^{\dagger 2} \delta\psi^2 \simeq m' \delta\psi^{\dagger 2} + m'^* \delta\psi^2 + 4n' \delta\psi^\dagger \delta\psi. \tag{C.2.4}$$

The third order Hamiltonian in this approximation reads therefore

$$H_3 = g \int_V \mathrm{d}\mathbf{r} \left\{ \left(2n'\phi + m'\phi^* \right) \delta\psi^\dagger + h.c. \right\}. \tag{C.2.5}$$

Taking a closer look at the first order Hamiltonian (4.1.2), we observe that the integrands of H_1 and H_3 sum up to give the generalised Gross-Pitaevskii equations (6.1.5) and consequently vanish, $H_1 + H_3 = 0$. Using again (6.1.5), the ground state energy is obtained:

$$E_0 = \int_V \mathrm{d}\mathbf{r} \left(\frac{g}{2} n_0 + 2g'_n + gm' \right) n_0 = -g n_0 V \left(\frac{n_0}{2} + 2n' + m' \right). \tag{C.2.6}$$

We are left with the part of Hamiltonian that has to be diagonalised ($n = n_0 + n'$ and $m = m' + n_0$):

$$H_2 + H_4 = \int_V \mathrm{d}\mathbf{r} \left\{ \delta\psi^\dagger \left(h_0 - \mu + 2gn \right) \delta\psi + \frac{g}{2} \left(m \delta\psi^{\dagger 2} + m^* \delta\psi^2 \right) \right\}. \tag{C.2.7}$$

Comparing that to the original second order Hamiltonian (4.1.3), we see that we can use the results obtained there if we promote

$$h_0 + gn_0 \to h_0 - \mu + 2gn, \qquad \phi^2 \to m, \tag{C.2.8}$$

recovering the findings of (6.1.12) - (6.1.17). Additionally, we can calculate the correction of the ground state energy as we have done in B.1.

$$\frac{\Delta E_0}{L} = \frac{1}{4\pi}\int_{-\infty}^{\infty} \mathrm{d}k \left\{ \left[\left(\epsilon(k) - 2m'\right)\left(\epsilon(k) + 2g|\phi|^2\right)\right]^{1/2} - \epsilon(k) - g\left(n_0 - m'\right)\right\}$$
$$= \frac{gn_0\xi}{\sqrt{2}\pi}\int_0^{\infty} \mathrm{d}x \left\{ \left[\left(x^2 - \frac{m'}{n_0}\right)\left(x^2+1\right)\right]^{1/2} - x^2 - \frac{1}{2}\left(1 - \frac{m'}{n_0}\right)\right\} \tag{C.2.9}$$

C.3 Numerical integration

All numerical calculations concerning the mean-field theories have been carried in Python.

Composite Simpson rule

For the numerical evaluation of all integrals considered in this thesis we use the composite Simpson rule. The integration interval (a, b) is split into $2N$ steps of length $h = (b-a)/2N$, defining the grid points $x_n = a + nh$. The integral is then approximated by

$$\int_a^b \mathrm{d}x\, f(x) = \frac{h}{3}\left(f(a) + f(b) + 2\sum_{n=1}^{N-1} f(x_{2n}) + 4\sum_{n=1}^{N} f(x_{2n-1})\right) + \mathcal{O}(h^4). \tag{C.3.1}$$

For all calculations we have $N = 1000$, $(a, b) = (0, 1)$, therefore $h = 5 \cdot 10^{-4}$ and an accuracy of $\mathcal{O}(10^{-7})$.

Small-x approximations

Due to limitations originating from the finite accuracy of any computational calculus, we get some problems for small values of the integration variable x (generally we have expressions of the kind $0 \cdot \infty$ causing overflows). This especially occurs for the gapless theories, but as well for the part of the integrals that come from the transformation that maps the integration interval $(1, \infty)$ to $(0, 1)$. Consequently we have to make use of the approximations mentioned in the following.

For both Hartree-Fock theories (dilute and dense side), the second part of the integrals (7.2.2) and (7.2.3) has the limit

$$\lim_{x\to 0} \frac{x^{-2}}{e^{\beta_x(x^{-2}/2 + const.)} - 1} = \lim_{x\to 0} \frac{e^{-\beta_x/(2x^2)}}{x^2} = \lim_{x\to\infty} \frac{x^2}{e^{\beta_x x^2/2}} \to 0, \tag{C.3.2}$$

but computationally this causes problems. Therefore it is approximated with 0 for small values $x \leq 1 \cdot 10^{-4}$.

For Modified Popov theory (and equivalently for Mora-Castin theory since they contain similar expressions), we approximate for small $x \leq 5 \cdot 10^{-4}$

$$\frac{x\coth\left(\frac{1}{2}\beta_x n_0 k\left(x^2/4+1\right)^{1/2}\right)}{4\left(x^2/4+1\right)^{1/2}} \simeq \frac{1}{2\beta_x n_0}+\frac{\beta_x n_0}{24}x^2 \tag{C.3.3}$$

and for $\arg\left[\coth(\cdots)\right] \geq 700$, $\coth(\cdots) \approx 1$ and with that

$$\frac{\coth\left(\frac{1}{2}\beta_x n_0 x^{-1}\left(x^{-2}/4+1\right)^{1/2}\right)}{4x^3\left(x^{-2}/4+1\right)^{1/2}} \simeq \frac{1}{2x^2\left(1+2x^2\right)}. \tag{C.3.4}$$

For Walser theory, it is sufficient to make the above approximation of the hyperbolic cotangent in order to avoid numerical issues.

Bisection method

For the approximation of the self-consistent integral equations, they are brought to the form $x+f(x)=g(x)=0$, where $f(x)$ is the numerically evaluated integral (or its high-temperature approximation). Thus we have to find the root(s) of the above equation which is done using the slow but robust bisection method. Starting with an interval (x_0, x_1), where $g(x_0)$ and $g(x_1)$ must be of opposite sign, the method continuously splits the interval in two parts at the midpoint x^* and compares $g(x^*)$ to the values at the interval borders. That part of the split interval in which the sign change occurs is chosen as the interval for the next iteration step. This procedure is continued until the interval length is smaller than the desired accuracy (we choose 10^{-3}). Having opposite signs across the interval ensures that there is at least one root inside; it can get tricky to choose the right starting interval if there is more than one root (as for most of the mean-field theories). Since the interval gets halved at every iteration step, the method converges linearly to the solution.

C.4 Compressibility

The compressibility is defined as $\kappa = -\frac{1}{V}\frac{\partial V}{\partial p}\big|_{T,N}$. We can write

$$\left.\frac{\partial p}{\partial V}\right|_{T,N} = \left.\frac{\partial p}{\partial \mu}\right|_{T}\left.\frac{\partial \mu}{\partial V}\right|_{T,N}. \tag{C.4.1}$$

Using a Maxwell relation (derived from $\mathrm{d}F = -S\mathrm{d}T - p\mathrm{d}V + \mu\mathrm{d}N$) we have

$$\left.\frac{\partial \mu}{\partial V}\right|_{T,N} = \left.\frac{\partial^2 F}{\partial V \partial N}\right|_{T} = -\left.\frac{\partial p}{\partial N}\right|_{T,V} = -\left.\frac{\partial p}{\partial \mu}\right|_{T,V}\left.\frac{\partial \mu}{\partial N}\right|_{T,V} \tag{C.4.2}$$

and thus

$$\left.\frac{\partial p}{\partial V}\right|_{T,N} = -\left(\left.\frac{\partial p}{\partial \mu}\right|_{T}\right)^{2} \left.\frac{\partial \mu}{\partial N}\right|_{T,V}. \tag{C.4.3}$$

Using $\Omega = -\beta^{-1} \ln \mathcal{Z} = -pV$, equation (2.0.3) leads to

$$N = \frac{1}{\beta}\frac{\partial}{\partial \mu} \ln \mathcal{Z}\Big|_{T,V} = -\left.\frac{\partial \Omega}{\partial \mu}\right|_{T,V} = V \left.\frac{\partial p}{\partial \mu}\right|_{T}. \tag{C.4.4}$$

This yields eventually

$$\kappa = \frac{1}{V}\frac{V^2}{N^2}\left.\frac{\partial N}{\partial \mu}\right|_{T,V} = \frac{1}{n^2}\left.\frac{\partial n}{\partial \mu}\right|_{T,V}. \tag{C.4.5}$$

C.5 Cardan formulae and applications

The Cardan formulae, derived by Gerolamo Cardano in 1545, provide a solution of cubic equations of the form

$$z^3 + pz + q = 0. \tag{C.5.1}$$

Any cubic equation of the general shape $y^3 + ay^2 + by + c = 0$ can actually be brought to this form with the linear transformation $z = y + a/3$, where $p = b - \frac{a^2}{3}$ and $q = 2\left(\frac{a}{3}\right)^3 - \frac{ab}{3}$.

Now the substitution $z = u + v$ is made, and from (C.5.1) we get the relations

$$z^3 = u^3 + v^3 + 3uvz \;\Rightarrow\; p = -3uv,\; q = -(u^3 + v^3). \tag{C.5.2}$$

We deduce that

$$u^3 + v^3 = -q,\; u^3 \cdot v^3 = -\left(\frac{p}{3}\right)^3, \tag{C.5.3}$$

which means, remembering Vieta's formula, that u^3 and v^3 are solution of the quadratic equation $x^2 + qx - \left(\frac{p}{3}\right)^3 = 0$. Solving this equation, we get

$$x_{1,2} = -\frac{q}{2} \pm \sqrt{\left(\frac{q}{2}\right)^2 + \left(\frac{p}{3}\right)^3} \;\rightarrow\; u, v = \sqrt[3]{-\frac{q}{2} \pm \sqrt{\Delta}} \tag{C.5.4}$$

where we have introduced the discriminant $\Delta = \left(\frac{q}{2}\right)^2 + \left(\frac{p}{3}\right)^3$. Substituting back we get the solution

$$y = \sqrt[3]{-\frac{q}{2} + \sqrt{\Delta}} + \sqrt[3]{-\frac{q}{2} - \sqrt{\Delta}} - \frac{a}{3}. \tag{C.5.5}$$

This solution is only valid for $\Delta > 0$, giving the (in this case) only real solution of the equation.

Applying the formula to the high-temperature approximation of the thermal density from Hartree-Fock theory (dilute),

$$n' = \sqrt{\frac{1}{2(2n' - \mu)}} + \frac{\zeta(1/2)}{\sqrt{2\pi}}\sqrt{\beta_x} + \mathcal{O}(\beta_x), \tag{C.5.6}$$

which is transformed to

$$n'^3 - \left(\frac{\mu}{2} + 2\frac{\zeta(1/2)}{\sqrt{2\pi}}\sqrt{\beta_x}\right) n'^2 + \left(\frac{\zeta^2(1/2)}{2\pi}\beta_x + \frac{\zeta(1/2)}{\sqrt{2\pi}}\sqrt{\beta_x}\mu\right) n' - \left(\frac{\zeta^2(1/2)}{4\pi}\beta_x\mu + \frac{1}{4}\right) = 0, \tag{C.5.7}$$

we identify

$$\begin{aligned} q =& -\frac{2}{27}\left(\frac{\mu}{2} + 2\frac{\zeta(1/2)}{\sqrt{2\pi}}\sqrt{\beta_x}\right)^3 + \frac{1}{3}\left(\frac{\mu}{2} + 2\frac{\zeta(1/2)}{\sqrt{2\pi}}\sqrt{\beta_x}\right)\left(\frac{\zeta^2(1/2)}{2\pi}\beta_x + \frac{\zeta(1/2)}{\sqrt{2\pi}}\sqrt{\beta_x}\mu\right) \\ & - \frac{\zeta^2(1/2)}{4\pi}\beta_x\mu - \frac{1}{4} \end{aligned} \tag{C.5.8}$$

$$p = \frac{\zeta^2(1/2)}{2\pi}\beta_x + \frac{\zeta(1/2)}{\sqrt{2\pi}}\sqrt{\beta_x}\mu - \frac{1}{3}\left(\frac{\mu}{2} + 2\frac{\zeta(1/2)}{\sqrt{2\pi}}\sqrt{\beta_x}\right)^2. \tag{C.5.9}$$

Although this is of course not really handy, it gives correct values and we can use it to calculate the cross-over thermal density, i.e. the value at zero chemical potential. In this case we have,

$$q_0 = -\frac{1}{4} + \mathcal{O}(\beta_x^{3/2}) \tag{C.5.10}$$

$$p_0 = \mathcal{O}(\beta_x) \tag{C.5.11}$$

$$\Delta_0 = \frac{1}{64} + \mathcal{O}(\beta_x^3). \tag{C.5.12}$$

Plugging this into equation (C.5.5), we obtain

$$n_c' = 2^{-2/3} + \frac{2}{3}\frac{\zeta(1/2)}{\sqrt{2\pi}}\sqrt{\beta_x} + \mathcal{O}(\beta_x^{3/2}). \tag{C.5.13}$$

C.6 High-temperature expansions

Modified Popov theory

We want to find the small-β_x expansion of the integral (7.2.6), i.e.

$$I = \int_0^\infty \frac{\mathrm{d}k}{\pi}\left\{\frac{k^2/2}{E(k)}\left(\frac{1}{e^{\beta_x n_0 E(k)}-1}+\frac{1}{2}\right)-\frac{1}{2}+\frac{1}{k^2+2\mu/n_0}\right\} \tag{C.6.1}$$

with $E(k) = |k|\sqrt{k^2/4+1}$. The last term can be solved exactly:

$$I_3 = \int_0^\infty \frac{\mathrm{d}k}{\pi}\frac{1}{k^2+2\mu/n_0} = \sqrt{\frac{n_0}{2\mu}}\int_0^\infty \frac{\mathrm{d}x}{\pi}\frac{1}{1+x^2} = \sqrt{\frac{n_0}{2\mu}}\frac{1}{\pi}\arctan(x)\Big|_0^\infty = \frac{1}{2}\sqrt{\frac{n_0}{2\mu}}. \tag{C.6.2}$$

The vacuum level and the $-1/2$ together give also a convergent integral that can be solved exactly using the substitution $k = 2\sinh(x)$:

$$\begin{aligned} I_2 &= \int_0^\infty \frac{\mathrm{d}k}{\pi}\frac{k^2/2-E(k)}{2E(k)} = \int_0^\infty \frac{\mathrm{d}x}{\pi}\frac{2\cosh(x)\left(2\sinh(x)-2\left(1+\sinh^2(x)\right)^{1/2}\right)}{4\left(1+\sinh^2(x)\right)^{1/2}} \\ &= \int_0^\infty \frac{\mathrm{d}x}{\pi}\left\{\sinh(x)-\cosh(x)\right\} = -\int_0^\infty \frac{\mathrm{d}x}{\pi}e^{-x} = -\frac{1}{\pi} \end{aligned} \tag{C.6.3}$$

We add and subtract the large-k limit from the remaining integral,

$$I_1 = \int_0^\infty \frac{\mathrm{d}k}{\pi}\frac{k^2}{2E(k)}\left(\frac{1}{\beta_x n_0 E(k)}+\frac{1}{e^{\beta_x n_0 E(k)}-1}-\frac{1}{\beta_x n_0 E(k)}\right), \tag{C.6.4}$$

and solve the first term like (C.6.2), yielding:

$$I_{11} = \frac{1}{2\pi\beta_x n_0}\int_0^\infty \frac{\mathrm{d}k}{(k^2/4+1)} = \frac{1}{\pi\beta_x n_0}\int_0^\infty \frac{\mathrm{d}x}{x^2+1} = \frac{1}{2\beta_x n_0}. \tag{C.6.5}$$

For the rest of I_1 we add and subtract the large-k limit of the first factor,

$$I_{12} = \int_0^\infty \frac{\mathrm{d}k}{\pi} \left(1 + \frac{k^2}{2E(k)} - 1\right) \left(\frac{1}{e^{\beta_x n_0 E(k)} - 1} - \frac{1}{\beta_x n_0 E(k)}\right), \tag{C.6.6}$$

and evaluate the first part of it:

$$\begin{aligned} I_{121} &= \int_0^\infty \frac{\mathrm{d}k}{\pi} \left\{\frac{1}{e^{\beta_x n_0 E(k)} - 1} - \frac{1}{\beta_x n_0 E(k)}\right\} \\ &= \frac{1}{\sqrt{\beta_x n_0}} \int_0^\infty \frac{\mathrm{d}y}{\pi} \left\{\frac{1}{e^{y^2/2(1+4\beta_x n_0/y^2)^{1/2}} - 1} - \frac{1}{y^2/2\,(1+4\beta_x n_0/y^2)^{1/2}}\right\} \\ &\overset{\beta_x \ll 1}{=} \frac{1}{\sqrt{\beta_x n_0}} \int_0^\infty \frac{\mathrm{d}y}{\pi} \left\{\left(\frac{1}{e^{y^2/2+\beta_x n_0} - 1} - \frac{1}{y^2/2 + \beta_x n_0}\right) + \mathcal{O}(\beta_x^2)\right\}. \end{aligned} \tag{C.6.7}$$

We have used the substitution $y = \sqrt{\beta_x n_0} k$ and expanded for small $\beta_x \ll 1$. The first term is transformed into a Bose-Einstein integral with $x = y^2/2$ and then expanded using (A.1.5):

$$\begin{aligned} I_{1211} &= \frac{1}{\pi\sqrt{2\beta_x n_0}} \int_0^\infty \frac{\mathrm{d}x\, x^{-1/2}}{e^{\beta_x n_0} e^x - 1} + \mathcal{O}(\beta_x^{3/2}) = \frac{1}{\pi\sqrt{2\beta_x n_0}}\, \Gamma(1/2)\, g_{1/2}\left(e^{\beta_x n_0}\right) + \mathcal{O}(\beta_x^{3/2}) \\ &= \frac{1}{\sqrt{2}} \frac{1}{\beta_x n_0} + \frac{\zeta(1/2)}{\sqrt{2\pi}} \frac{1}{\sqrt{\beta_x n_0}} - \frac{\zeta(-1/2)}{\sqrt{2\pi}} \sqrt{\beta_x n_0} + \mathcal{O}(\beta_x^{3/2}) \end{aligned} \tag{C.6.8}$$

The term of order $\mathcal{O}(\beta_x^{-1})$ is cancelled by the second part of the integral I_{121} (C.6.7), which with $x^2 = y^2/(2\beta_x n_0)$ can be calculated easily like (C.6.2):

$$I_{1212} = -\frac{\sqrt{2}}{\pi \beta_x n_0} \int_0^\infty \frac{\mathrm{d}x}{x^2 + 1} + \mathcal{O}(\beta_x^{3/2}) = -\frac{1}{\sqrt{2}} \frac{1}{\beta_x n_0} + \mathcal{O}(\beta_x^{3/2}). \tag{C.6.9}$$

We have thus

$$I_{121} = \frac{\zeta(1/2)}{\sqrt{2\pi}} \frac{1}{\sqrt{\beta_x n_0}} - \frac{\zeta(-1/2)}{\sqrt{2\pi}} \sqrt{\beta_x n_0} + \mathcal{O}(\beta_x^{3/2}) \tag{C.6.10}$$

We are left with the rest of integral I_{12}. The expansion

$$\frac{1}{e^x - 1} - \frac{1}{x} = \frac{-\frac{1}{2} - \frac{x}{6}}{1 + \frac{x}{2}} + \mathcal{O}(x^2) = -\frac{1}{2} + \frac{x}{12} + \mathcal{O}(x^2) \tag{C.6.11}$$

for small $x \ll 1$ allows us to write

$$I_{122} = \int_0^\infty \frac{\mathrm{d}k}{\pi} \frac{k^2/2 - E(k)}{E(k)} \left(\frac{1}{e^{\beta_x n_0 E(k)} - 1} - \frac{1}{\beta_x n_0 E(k)} \right)$$
$$= \int_0^\infty \frac{\mathrm{d}k}{\pi} \frac{k^2/2 - E(k)}{E(k)} \left(-\frac{1}{2} + \frac{\beta_x n_0 E(k)}{12} \right) + \mathcal{O}(\beta_x^2) = \frac{1}{\pi} + \mathcal{O}(\beta_x), \tag{C.6.12}$$

which in leading order cancels I_2. To complete the expansion up to order $\mathcal{O}(\beta^{1/2})$, we need to determine the difference of the approximation and the original expression in (C.6.6) (ignoring thus terms of order $\mathcal{O}(\beta_x)$ and higher). For that we proceed exactly as we have done in (C.6.7) ($y = \sqrt{\beta_x n_0} k$), which leaves us after some algebra with the integral

$$I'_{122} = \int_0^\infty \frac{\mathrm{d}k}{\pi} \frac{k^2/2 - E(k)}{E(k)} \left(\frac{1}{e^{\beta_x n_0 E(k)} - 1} - \frac{1}{\beta_x n_0 E(k)} + \frac{1}{2} \right)$$
$$= \sqrt{\beta_x n_0} \int_0^\infty \frac{\mathrm{d}y}{\pi} \frac{(4 - y^2)^2 e^{y^2} - 8e^{y^2/2} + y^2 + 4}{y^4 \left(e^{y^2/2} - 1\right)^2} + \mathcal{O}(\beta_x^{3/2}). \tag{C.6.13}$$

We split the domain of integration into two parts and use the large-y approximation of the integrand, $-\frac{1}{y^2}$, for $y \geq 20$

$$-\int_{20}^\infty \frac{\mathrm{d}y}{\pi} \frac{1}{y^2} = -\frac{1}{20\pi}. \tag{C.6.14}$$

The rest of the integral is calculated numerically, using the IR-limit of the integrand, $-\frac{1}{12}$, for $y \leq 0.2$ and obtain $I'_{122} = a_3 \sqrt{\beta_x n_0}$ with $a_3 \approx -0.16591$. This adds to the term in (C.6.10), yielding the final expression

$$I = \frac{1}{2\beta_x n_0} + \frac{\zeta(1/2)}{\sqrt{2\pi}} \frac{1}{\sqrt{\beta_x n_0}} + \frac{1}{2} \sqrt{\frac{n_0}{2\mu}} + a_2 \sqrt{\beta_x n_0} + \mathcal{O}(\beta_x) \tag{C.6.15}$$

where $a_2 = a_3 - \frac{\zeta(-1/2)}{\sqrt{2\pi}} \approx -0.165912 + 0.082935 \approx -0.082977 \left(= \frac{\zeta(-1/2)}{\sqrt{2\pi}} + \mathcal{O}(10^{-5}) \right)$.

Mora-Castin theory

Fortunately, we can use the above results since the integral

$$I = \int_0^\infty \frac{\mathrm{d}k}{\pi} \left\{ \frac{k^2/2}{E(k)} \left(\frac{1}{e^{\beta_x \mu E(k)} - 1} + \frac{1}{2} \right) - \frac{1}{2} \right\} \tag{C.6.16}$$

is equivalent to $I_1 + I_2$ ((C.6.4),(C.6.3)) if n_0 is replaced by μ. We thus have

$$I = \frac{1}{2\beta_x \mu} + \frac{\zeta(1/2)}{\sqrt{2\pi}} \frac{1}{\sqrt{\beta_x \mu}} + a_2 \sqrt{\beta_x \mu} + \mathcal{O}(\beta_x). \tag{C.6.17}$$

In figure C.6.1 this high-temperature expansion is compared to the result obtained by numerically evaluating the integrals.

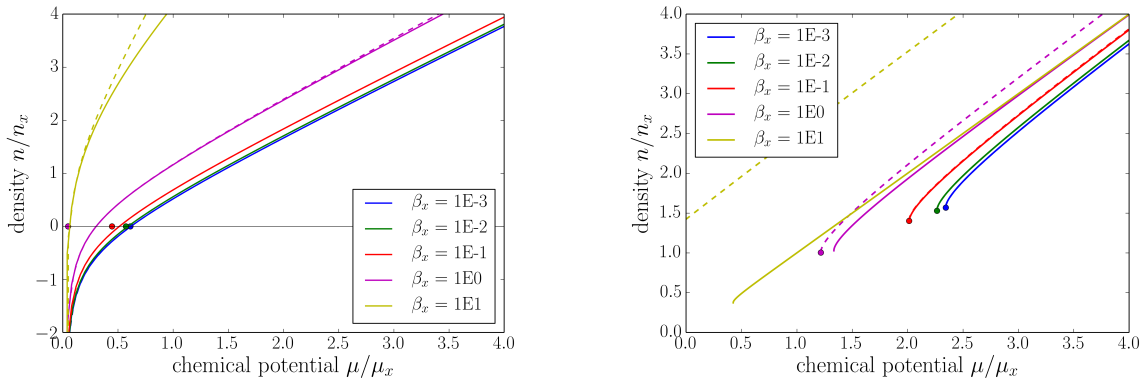

Figure C.6.1: Numerically calculated density of Mora-Castin theory (left) and Hartree-Fock theory (dense) (right) compared to their high-temperature approximations (dashed) with critical points (dots)

Walser theory

Thermal density

The integral that has to be approximated is

$$I = \int_0^\infty \frac{\mathrm{d}k}{\pi} \left\{ \frac{k^2/4 + \frac{1}{2}(1-\eta)}{E(k)} \left(\frac{1}{e^{2\beta_x n_0 E(k)} - 1} + \frac{1}{2} \right) - \frac{1}{2} \right\} \tag{C.6.18}$$

where $E(k) = \left[(k^2/4 + 1)\,(k^2/4 - \eta) \right]^{1/2}$ and $\eta = m'/n_0 < 0$.

This is split into

$$I_1 = \int_0^\infty \frac{\mathrm{d}k}{\pi} \frac{k^2/4 + \frac{1}{2}(1-\eta) - E(k)}{2E(k)} \tag{C.6.19}$$

and

$$I_2 = \int_0^\infty \frac{\mathrm{d}k}{\pi} \frac{k^2/4 + \frac{1}{2}(1-\eta)}{E(k)} \left(\frac{1}{2\beta_x n_0 E(k)} + \frac{1}{e^{2\beta_x n_0 E(k)} - 1} - \frac{1}{2\beta_x n_0 E(k)} \right) \tag{C.6.20}$$

where we have added and subtracted the large-k limit. The first part of I_2 can be written as

$$I_{21} = \frac{1}{2\beta_x n_0} \int_0^\infty \frac{\mathrm{d}k}{\pi} \frac{k^2/4 + \frac{1}{2}(1-\eta)}{(k^2/4+1)\,(k^2/4-\eta)} = \frac{1}{2\beta_x n_0} \int_0^\infty \frac{\mathrm{d}k}{\pi} \left\{ \frac{1}{(k^2/4+1)} + \frac{(1+\eta)}{2E^2(k)} \right\}, \quad \text{(C.6.21)}$$

whose first term yields as before (C.6.5) $I_{211} = \frac{1}{2\beta_x n_0}$. For the second integral we use the partial fraction decomposition

$$\frac{1}{(x^2+1)(x^2-\eta)} = -\frac{1}{1+\eta}\left(\frac{1}{x^2+1} - \frac{1}{x^2-\eta}\right) \quad \text{(C.6.22)}$$

and substitute $x \to x\sqrt{-\eta}$ ($\eta < 0$) in the second term to obtain

$$I_{212} = \frac{(1+\eta)}{2\pi\beta_x n_0} \int_0^\infty \frac{\mathrm{d}x}{(x^2+1)\,(x^2-\eta)} = \frac{\frac{1}{\sqrt{-\eta}} - 1}{2\pi\beta_x n_0} \int_0^\infty \frac{\mathrm{d}x}{(x^2+1)} = \frac{\frac{1}{\sqrt{-\eta}} - 1}{4\beta_x n_0}. \quad \text{(C.6.23)}$$

This combines to give

$$I_{21} = \frac{1}{4\beta_x n_0}\left(1 + \frac{1}{\sqrt{-\eta}}\right). \quad \text{(C.6.24)}$$

We continue with the second part of I_2

$$I_{22} = \int_0^\infty \frac{\mathrm{d}k}{\pi}\left(1 + \frac{k^2/4 + \frac{1}{2}(1-\eta)}{E(k)} - 1\right)\left(\frac{1}{e^{2\beta_x n_0 E(k)} - 1} - \frac{1}{2\beta_x n_0 E(k)}\right), \quad \text{(C.6.25)}$$

which is quite similar in structure to I_2 of Modified Popov theory. We therefore expand in the first part of the integral the dispersion relation for small β_x (after substitution $y = \sqrt{\beta_x n_0}k$) which becomes $2\beta_x n_0 E(k) \to y^2/2 + \beta_x n_0(1-\eta) + \mathcal{O}(\beta_x^2)$. Thus we can use the result of (C.6.10) promoting $n_0 \to n_0(1-\eta)$ and obtain

$$I_{221} = \int_0^\infty \frac{\mathrm{d}k}{\pi}\left(\frac{1}{e^{2\beta_x n_0 E(k)} - 1} - \frac{1}{2\beta_x n_0 E(k)}\right) = \frac{\zeta(1/2)}{\sqrt{2\pi}}\frac{1}{\sqrt{\beta_x n_0}} - \frac{\zeta(-1/2)}{\sqrt{2\pi}}(1-\eta)\sqrt{\beta_x n_0} + \mathcal{O}(\beta_x^{3/2}). \quad \text{(C.6.26)}$$

The second part of I_{22} can as well be treated as the corresponding integral of Modified Popov theory (C.6.12). Again it cancels I_1 (C.6.19) in leading order:

$$I_{222} = \int_0^\infty \frac{\mathrm{d}k}{\pi} \frac{k^2/4 + \frac{1}{2}(1-\eta) - E(k)}{E(k)} \left(\frac{1}{e^{2\beta_x n_0 E(k)} - 1} - \frac{1}{2\beta_x n_0 E(k)} \right)$$
$$= \int_0^\infty \frac{\mathrm{d}k}{\pi} \frac{k^2/2 - E(k)}{E(k)} \left(-\frac{1}{2} + \frac{\beta_x n_0 E(k)}{6} \right) + \mathcal{O}(\beta_x^2) = -I_1 + \mathcal{O}(\beta_x). \tag{C.6.27}$$

Differently from Popov theory, the correction that arises from this approximation is zero in order $\mathcal{O}(\beta_x^{1/2})$. We do not take it into account since in order $\mathcal{O}(\beta_x^{3/2})$ it is IR-divergent,

$$I'_{222} = \int_0^\infty \frac{\mathrm{d}k}{\pi} \frac{k^2/4 + \frac{1}{2}(1-\eta) - E(k)}{E(k)} \left(\frac{1}{e^{2\beta_x n_0 E(k)} - 1} - \frac{1}{2\beta_x n_0 E(k)} + \frac{1}{2} \right)$$
$$\simeq \eta (\beta_x n_0)^{3/2} \int_0^\infty \frac{\mathrm{d}k}{\pi} \frac{(8 - 2y^2)\, e^{y^2/2} - 2y^2 - 8}{y^6 \left(e^{y^2/2} - 1 \right)}. \tag{C.6.28}$$

We therefore have

$$I = \frac{1}{4} \left(1 + \sqrt{\frac{n_0}{-m'}} \right) \frac{1}{\beta_x n_0} + \frac{\zeta(1/2)}{\sqrt{2\pi}} \frac{1}{\sqrt{\beta_x n_0}} - \frac{\zeta(-1/2)}{\sqrt{2\pi}} \left(1 + \frac{m'}{n_0} \right) \sqrt{\beta_x n_0} + \mathcal{O}(\beta_x^{3/2}). \tag{C.6.29}$$

Anomalous average

We need to evaluate

$$I = \int_0^\infty \frac{\mathrm{d}k}{\pi} \frac{1}{E(k)} \left(\frac{1}{e^{2\beta_x n_0 E(k)} - 1} + \frac{1}{2} \right), \tag{C.6.30}$$

that is split into

$$I_1 = \int_0^\infty \frac{\mathrm{d}k}{\pi} \frac{1}{2E(k)}, \tag{C.6.31}$$

which is convergent due to the energy gap of the spectrum, and

$$I_2 = \int_0^\infty \frac{\mathrm{d}k}{\pi} \frac{1}{E(k)} \left(\frac{1}{2\beta_x n_0 E(k)} + \frac{1}{e^{2\beta_x n_0 E(k)} - 1} - \frac{1}{2\beta_x n_0 E(k)} \right). \tag{C.6.32}$$

The first part of the latter is similar to (C.6.23) and gives

$$I_{21} = \frac{1}{\beta_x n_0 \pi} \int_0^\infty \frac{\mathrm{d}x}{(x^2+1)(x^2-\eta)} = \frac{\frac{1}{\sqrt{-\eta}} - 1}{2(1+\eta)} \frac{1}{\beta_x n_0}. \tag{C.6.33}$$

The second part can be evaluated again like (C.6.12), cancelling I_1 in leading order:

$$I_{22} = \int_0^\infty \frac{\mathrm{d}k}{\pi} \frac{1}{E(k)} \left(\frac{1}{e^{2\beta_x n_0 E(k)} - 1} - \frac{1}{2\beta_x n_0 E(k)} \right) = -I_1 + \mathcal{O}(\beta_x). \tag{C.6.34}$$

Finally, we calculate the correction

$$I'_{22} = \int_0^\infty \frac{\mathrm{d}k}{\pi} \frac{1}{E(k)} \left(\frac{1}{e^{2\beta_x n_0 E(k)} - 1} - \frac{1}{2\beta_x n_0 E(k)} + \frac{1}{2} \right) = 4\sqrt{\beta_x n_0} \int_0^\infty \frac{\mathrm{d}x}{\pi} \left(\frac{\coth(x^2/4)}{x^2} - \frac{2}{x^4} \right) + \mathcal{O}(\beta_x^{3/2}) \tag{C.6.35}$$

numerically, using the IR-approximation $\frac{1}{24} - \frac{x^4}{5760}$ of the integrand for small $x \leq 0.1$. This yields the final result

$$I = \frac{\frac{1}{\sqrt{-\eta}} - 1}{2(1+\eta)} \frac{1}{\beta_x n_0} + a_4 \sqrt{\beta_x n_0} + \mathcal{O}(\beta_x^{3/2}), \tag{C.6.36}$$

where $a_4 = 0.331728 = -4\frac{\zeta(-1/2)}{\sqrt{2\pi}} + \mathcal{O}(10^{-5})$.

Ideal Bose gas

We apply the same techniques as for Hartree-Fock theory to the ideal Bose gas. Both high-temperature expansion and degenerate Bose gas approximate the numerically calculated curve the better the smaller β_x, the former being much more accurate of course (see figure C.6.2).

C.7 Critical points

At the critical point, the slope of $n = n(\mu)$ becomes infinitely large, or equivalently, the slope of $\mu = \mu(n)$ becomes zero. This will allow us to get some approximations of the corresponding values.

Hartee-Fock (dense)

From table 7.1 and $\mu = 2n' + n_0$ we deduce

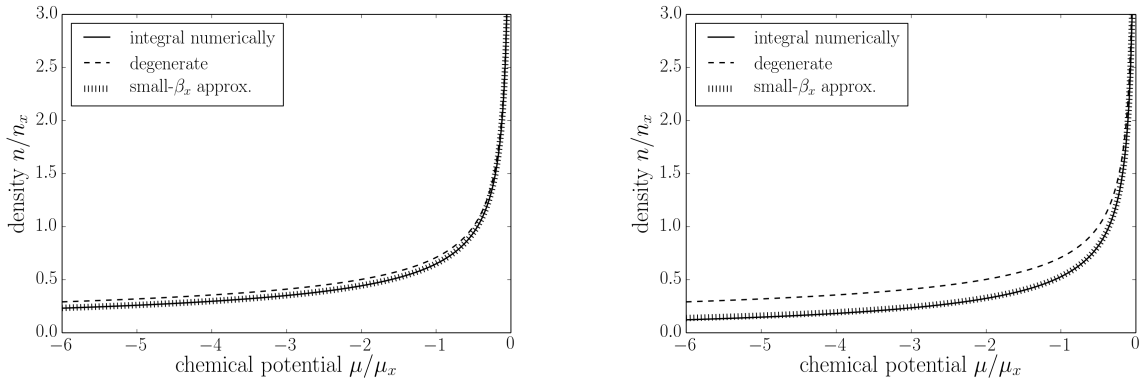

Figure C.6.2: Numerically calculated thermal density of the ideal Bose gas compared to its high-temperature approximations and the degenerate gas for $\beta_x = 10^{-2}$ (left) and $\beta_x = 10^{-1}$ (right)

$$\mu = n_0 + \sqrt{\frac{2}{n_0}} + 2a_1\beta_x^{1/2} + \mathcal{O}(\beta_x^{3/2}), \tag{C.7.1}$$

that permits to calculate the derivative

$$\frac{\partial\mu}{\partial n_0} = 1 - 2^{-1/2}n_0^{-3/2} + \mathcal{O}(\beta_x^{3/2}), \tag{C.7.2}$$

which set to zero yields

$$n_{0,c} = 2^{-1/3} + \mathcal{O}(\beta_x^{3/2}). \tag{C.7.3}$$

Plugging this back into (C.7.1) gives the critical value for the chemical potential, from where those of the density and the thermal density follow:

$$\mu_c = 3\cdot 2^{-1/3} + 2a_1\beta_x^{1/2} + \mathcal{O}(\beta_x^{3/2}), \qquad n_c' = 2^{-1/3} + a_1\beta_x^{1/2} + \mathcal{O}(\beta_x^{3/2}), \qquad n_c = 2^{2/3} + a_1\beta_x^{1/2} + \mathcal{O}(\beta_x^{3/2}). \tag{C.7.4}$$

Modified Popov theory

Differentiating

$$\mu = n_0 + \frac{1}{\sqrt{n_0}} + 2a_1\beta_x^{1/2} + \mathcal{O}(\beta_x) \tag{C.7.5}$$

yields here

$$n_{0,c} = 2^{-2/3} + \mathcal{O}(\beta_x). \tag{C.7.6}$$

This gives

$$\mu_c = 3\cdot 2^{-2/3}+2a_1\beta_x^{1/2}+\mathcal{O}(\beta_x), \qquad n_c' = 2^{-2/3}+a_1\beta_x^{1/2}+\mathcal{O}(\beta_x), \qquad n_c = 2^{1/3}+a_1\beta_x^{1/2}+\mathcal{O}(\beta_x). \tag{C.7.7}$$

Mora-Castin theory

For the first critical point near the cross-over we have $n_c \equiv 0 = n_{0,c} + n_c'$ and therefore with the high-temperature expansion of table 7.1

$$n_c' = \frac{1}{2\sqrt{n_c'}} + a_1\beta_x^{1/2}, \tag{C.7.8}$$

which solved iteratively yields

$$n_c' = -n_{0,c} = \mu_c = 2^{-2/3} + a_1\beta_x^{1/2}. \tag{C.7.9}$$

At the second critical point, the thermal density vanishes $n_{c2}' = 0$ and we have thus

$$\mu_{c2} = \frac{1}{4\left(a_1\beta_x^{1/2} + a_2\mu_{c2}\beta_x^{3/2} + \mathcal{O}(\beta_x^{5/2})\right)^2}, \tag{C.7.10}$$

yielding in a first iteration $\mu_{c2} = \frac{1}{4a_1^2\beta_x} + \mathcal{O}(1)$. Plugging this back into equation (C.7.10) gives

$$\mu_{c2} = n_{c2} = \frac{1}{4a_1^2\beta_x\left(1 + a2/(4a_1^2) + \mathcal{O}(\beta_x^2)\right)^2} = \frac{1}{4a_1^2\beta_x \underbrace{\left(1 + a2/(4a_1^2)\right)^2}_{\approx 1.126}} + \mathcal{O}(\beta_x) \tag{C.7.11}$$

Walser theory

We have

$$m' = \frac{1}{4\sqrt{n_0}} - \frac{1}{4\sqrt{-m'}} + \mathcal{O}(\beta_x^{3/2}) \;\Rightarrow\; n_0 = \left(4m' + \frac{1}{\sqrt{-m'}}\right)^{-2} + \mathcal{O}(\beta_x^{3/2}) \tag{C.7.12}$$

and

$$n' = m' + \frac{1}{2\sqrt{-m'}} + a_1\beta_x^{1/2} + \mathcal{O}(\beta_x^{3/2}), \tag{C.7.13}$$

thus we obtain

$$\mu = n_0 + 2n' + m' = \left(4m' + \frac{1}{\sqrt{-m'}}\right)^{-2} + 3m' + \frac{1}{\sqrt{-m'}} + 2a_1\beta_x^{1/2} + \mathcal{O}(\beta_x^{3/2}). \quad \text{(C.7.14)}$$

The equation resulting from the differentiation,

$$\frac{\partial\mu}{\partial m'} = 0 \;\Rightarrow\; 384\,m'^6 - 224(-m')^{9/2} - 40\,m'^3 + 8(-m')^{3/2} - 1 = 0, \quad \text{(C.7.15)}$$

has 5 solutions. We calculate the only real one numerically with the bisection method and obtain the approximate value

$$m'_c = -0.213528 + \mathcal{O}(\beta_x^{3/2}). \quad \text{(C.7.16)}$$

Equations (C.7.12), (C.7.13) and (C.7.14) evaluated at this point give respectively the critical quasi-condensate density, thermal density and chemical potential, yielding as well the critical density

$$n_c = \underbrace{\left(4m'_c + \frac{1}{\sqrt{-m'_c}}\right)^{-2} + m'_c + \frac{1}{\sqrt{-4m'_c}}}_{\approx 1.4512} + a_1\beta_x^{1/2} + \mathcal{O}(\beta_x^{3/2}) \quad \text{(C.7.17)}$$

$$\mu_c = \underbrace{\left(4m'_c + \frac{1}{\sqrt{-m'_c}}\right)^{-2} + 3m'_c + \frac{1}{\sqrt{-m'_c}}}_{\approx 2.1062} + 2a_1\beta_x^{1/2} + \mathcal{O}(\beta_x^{3/2}). \quad \text{(C.7.18)}$$

C.8 Density jumps

We calculate the density given by Hartree-Fock theory (dilute) at the critical chemical potential of the corresponding theory. This yields in a first approximation

$$n(\mu_c) = \frac{1}{2(2n(\mu_c) - \mu_c)} \;\rightarrow n^3 - \frac{1}{2}\mu_c n^2 - \frac{1}{4} = 0. \quad \text{(C.8.1)}$$

We calculate this using the Cardan formulae, yielding for example for the critical chemical potential of Hartree-Fock theory (dense) $\mu_c \approx 3 \cdot 2^{-1/3}$,

$$n(\mu_c) = \sqrt[3]{\frac{3+\sqrt{8}}{16}} + \sqrt[3]{\frac{3-\sqrt{8}}{16}} + 2^{-4/3} + a_1\beta_x^{1/2}. \quad \text{(C.8.2)}$$

and Modified Popov theory $\mu_c \approx 2^{1/3}$,

$$n(\mu_c) = \sqrt[3]{\frac{2.5+\sqrt{6}}{16}} + \sqrt[3]{\frac{2.5-\sqrt{6}}{16}} + 2^{-5/3} + a_1 \beta_x^{1/2}. \tag{C.8.3}$$

Subtracting these values from the critical density of the corresponding theory leads to the density jumps given in (7.4.8).

C.9 Second order correlation function

For Walser theory (as well as Mora-Castin theory), $g_2(z)$ does not reach its maximum at the origin and $g_2(0) < 1$ for chemical potentials $\mu \gtrsim 7.74\,\mu_x$ ("anti-bunching" effect):

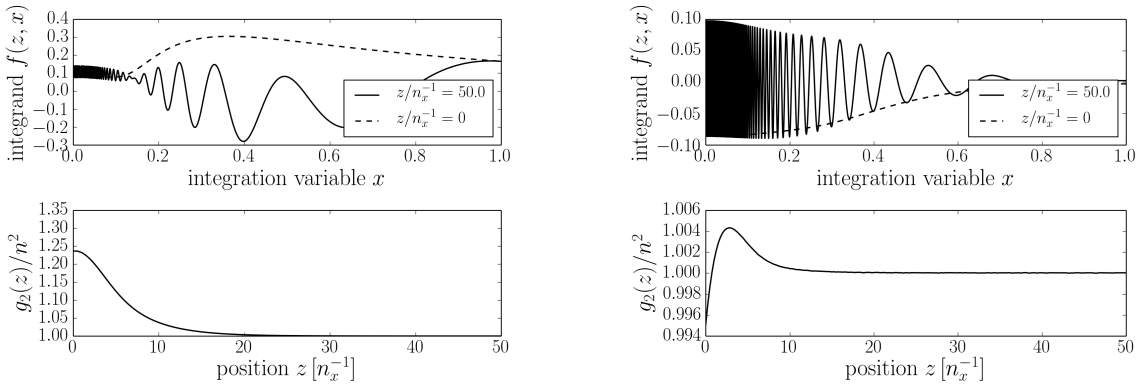

Figure C.9.1: Integrand of $n'(z) + m'(z)$ and second order correlation function for $\mu = 2.263\,\mu_x$ (left) and $\mu = 9.344\,\mu_x$ (right) for Walser theory

Appendix D

(S)GPE

D.1 Numerics

All numerical calculations concerning part III have been carried out in Fortran.

Crank-Nicholson scheme

For the numerical computation we write the spatial derivative in the standard form using finite differences, i.e. with $\phi_j^m \equiv \phi(z = j\Delta z, t = m\Delta t)$

$$\partial_z^2 \phi(z,t) = \underbrace{\frac{\phi_{j-1}^m - 2\phi_j^m + \phi_{j+1}^m}{\Delta z^2}}_{\delta_z^2} + \mathcal{O}(\Delta z^2). \tag{D.1.1}$$

Within the Crank-Nicholson method, the time derivative is evaluated using the trapezoidal rule, thus taking the time average of the rhs of our equation

$$\partial_t \phi(z,t) = -iK(z,t)\phi(z,t), \tag{D.1.2}$$

where $K = H - \mu = -\partial_z^2/2 + z^2/2 - \mu + g|\phi_j^m|^2$. In order to solve this system, we approximate $|\phi_j^m|^2\phi_j^m + |\phi_j^{m+1}|^2\phi_j^{m+1}$ by $1/2(|\phi_j^m|^2 + |\phi_j^{m+1}|^2)(\phi_j^m + \phi_j^{m+1})$ yielding

$$\frac{\phi_j^{m+1} - \phi_j^m}{\Delta t} = -\frac{i}{2}\left(-\frac{\delta_z^2}{2} + \frac{z^2}{2} - \mu + g|\phi_j^{m+1/2}|^2\right)\left(\phi_j^{m+1} + \phi_j^m\right) \tag{D.1.3}$$

or

$$\left[1+\frac{i\Delta t}{2}\left(\frac{\delta_z^2}{2}+V_j^m-\mu+g|\phi_j^{m+1/2}|^2\right)\right]\phi_j^{m+1}=\left[1-\frac{i\Delta t}{2}\left(\frac{\delta_z^2}{2}+V_j^m-\mu+g|\phi_j^{m+1/2}|^2\right)\right]\phi_j^m. \tag{D.1.4}$$

This scheme is energy and particle number conserving. In order to see this, we write the solution of the GPE (D.1.2) for infinitesimal small $\Delta t = t_{m+1} - t_m$ ($K(t+\Delta t) \approx K(t) \approx K(t+\Delta t/2)$) as

$$\phi_j^{m+1} = e^{-iK_j^{m+1/2}\Delta t}\phi_j^m. \tag{D.1.5}$$

The Crank-Nicholson method corresponds to approximating the exponential in the unitarity conserving form

$$e^{-iK_j^{m+1/2}\Delta t} = \underbrace{\frac{1-iK_j^{m+1/2}\Delta t/2}{1+iK_j^{m+1/2}\Delta t/2}}_{T} + \mathcal{O}(\Delta t^2), \qquad T^* = T^{-1}, \tag{D.1.6}$$

which also proves that it is accurate up to second order in time (and space, see (D.1.1)).

Periodic boundary conditions

For periodic boundary conditions we have to solve the matrix equation

$$\begin{pmatrix} b_1 & c_1 & & & a_1 \\ a_2 & b_2 & c_2 & & \\ & \ddots & \ddots & \ddots & \\ & & a_{N_x-1} & b_{N_x-1} & c_{N_x-1} \\ c_{N_x} & & & a_{N_x} & b_{N_x} \end{pmatrix} \begin{pmatrix} \phi_1 \\ \phi_2 \\ \vdots \\ \phi_{N_x-1} \\ \phi_{N_x} \end{pmatrix} = \begin{pmatrix} \Omega_1 \\ \Omega_2 \\ \vdots \\ \Omega_{N_x-1} \\ \Omega_{N_x} \end{pmatrix}. \tag{D.1.7}$$

where we have dropped the time indices of ϕ_j^{m+1} for matters of clarity. Eliminating the last column and the last line from the matrix M, we get the tridiagonal matrix M' which obeys the equation

$$\begin{pmatrix} b_1 & c_1 & & & \\ a_2 & b_2 & c_2 & & \\ & \ddots & \ddots & \ddots & \\ & & a_{N_x-2} & b_{N_x-2} & c_{N_x-2} \\ & & & a_{N_x-1} & b_{N_x-1} \end{pmatrix} \begin{pmatrix} \phi_1 \\ \phi_2 \\ \vdots \\ \phi_{N_x-2} \\ \phi_{N_x-1} \end{pmatrix} = \begin{pmatrix} \Omega_1 \\ \Omega_2 \\ \vdots \\ \Omega_{N_x-2} \\ \Omega_{N_x-1} \end{pmatrix} - \begin{pmatrix} a_1 \\ 0 \\ \vdots \\ 0 \\ c_{N_x-1} \end{pmatrix} \phi_{N_x}. \tag{D.1.8}$$

With $\boldsymbol{\phi} = (\boldsymbol{\phi}', \phi_N)^\mathsf{T}$ (vectors in bold), equation (D.1.8) can be solved with the ansatz $\boldsymbol{\phi}' = \boldsymbol{\chi}^{(1)} + \boldsymbol{\chi}^{(2)}\phi_{N_x}$ with

$$M'\boldsymbol{\chi}^{(1)} = \boldsymbol{\Omega}', \qquad M'\boldsymbol{\chi}^{(2)} = \begin{pmatrix} -a_1 \\ 0 \\ \vdots \\ 0 \\ -c_{N_x-1} \end{pmatrix}. \tag{D.1.9}$$

From equation (D.1.7) we have $c_{N_x}\phi_1 + a_{N_x}\phi_{N_x-1} + b_{N_x}\phi_{N_x} = \Omega_{N_x}$, which following equation (D.1.8) gives

$$c_{N_x}(\chi_1^{(1)} + \chi_1^{(2)}\phi_{N_x}) + b_{N_x}\phi_{N_x} + a_{N_x}(\chi_{N_x-1}^{(1)} + \chi_{N_x-1}^{(2)}\phi_{N_x}) = \Omega_{N_x} \tag{D.1.10}$$

and thus

$$\phi_{N_x} = \frac{\Omega_{N_x} - c_{N_x}\chi_1^{(1)} - a_{N_x}\chi_{N_x-1}^{(1)}}{b_{N_x} + c_{N_x}\chi_1^{(2)} + a_{N_x}\chi_{N_x-1}^{(2)}}. \tag{D.1.11}$$

The procedure amounts therefore to calculating to the two equations (D.1.9) with the tridiagonal matrix algorithm and ϕ_{N_x} from (D.1.11) to obtain the solution $\boldsymbol{\phi} = (\boldsymbol{\chi}^{(1)} + \boldsymbol{\chi}^{(2)}\phi_{N_x}, \phi_{N_x})^{\mathsf{T}}$.

SGPE

For the numerical integration of the SGPE the same scheme is applied. Additionally, the gamma term has to be calculated in order to incorporate the damping and the noise. This is done generally using the approximation (9.2.1) of the Keldysh self-energy. With that the damping, which is just a prefactor, and the strength of the noise are determined. How the latter may be included into the time stepping scheme can be deduced from the SGPE (9.1.7), that has the form of a general Langevin equation

$$\frac{\partial}{\partial t}\Phi(z,t) = -A(z,t)\Phi(z,t) + \Gamma(z,t), \tag{D.1.12}$$

where Γ is the noise term. This equation has for small Δt the formal solution (if A was not time dependent, it holds even for large Δt)

$$\begin{aligned} \Phi(z,t+\Delta t) &= \Phi(z,t)e^{-A\Delta t} + e^{-A(t+\Delta t)} \int_t^{t+\Delta t} \mathrm{d}t'\, \Gamma(z,t')e^{At'} \\ &= e^{-A\Delta t}\Big(\Phi(z,t) + \underbrace{e^{-At} \int_t^{t+\Delta t} \mathrm{d}t'\, \Gamma(z,t')e^{At'}}_{=:-i\xi(z,t+\Delta t)}\Big). \end{aligned} \tag{D.1.13}$$

For small $\Delta t \ll 1$, $\Gamma(z,t)$ can assumed to be almost constant and we can approximate ($\Gamma(z,t) = -i\eta(z,t)$)

$$\xi(z,t) \approx \xi(z,t+\Delta t) = \eta(z,t)\Delta t + \mathcal{O}(\Delta t^2). \tag{D.1.14}$$

Since equation (D.1.13) is of the same form as equation (D.1.5), it can be evaluated analogously, i.e. with $A = i(1-\gamma(z,t))H_{GP}$ in harmonic oscillator units

$$\begin{aligned}\left[1 + \frac{i\Delta t(1-\gamma(z,t))}{2}\left(\frac{\delta_z^2}{2} + V_j^m - \mu + g|\phi_j^{m+1/2}|^2\right)\right]\Phi_j^{m+1} = \\ \left[1 - \frac{i\Delta t(1-\gamma(z,t))}{2}\left(\frac{\delta_z^2}{2} + V_j^m - \mu + g|\phi_j^{m+1/2}|^2\right)\right]\left(\Phi_j^m - i\xi_j^m\right).\end{aligned} \tag{D.1.15}$$

On a discrete grid, the delta functions have to be replaced by Kronecker deltas as usual ($\delta(z-z') \to \frac{2\pi}{\Delta z}\delta_{zz'}$) and we have therefore

$$\langle \xi_j^m \xi_{j'}^{m'} \rangle = \langle \eta_j^m \eta_{j'}^{m'} \rangle \, \Delta t^2 = \frac{2\gamma(\mathbf{r},t)}{\beta}\frac{\Delta t}{\Delta z}\,\delta_{jj'}\,\delta_{mm'}. \tag{D.1.16}$$

We know for a Gaussian distribution that

$$\sigma^2 \equiv \langle \xi_j^m \xi_j^m \rangle = \frac{2\gamma(\mathbf{r},t)}{\beta}\frac{\Delta t}{\Delta z}. \tag{D.1.17}$$

In order to produce Gaussian white noise on a grid obeying (D.1.16), we therefore have to generate for every timestep and every node independently a (pseudo-) random number from a Gaussian distribution with a variance (D.1.17). This is done with the Box-Muller transformation [130], which consists in generating two uniformly distributed (pseudo-) random numbers q and $w \in (0,1)$ and calculating

$$r = \sigma\sqrt{-2\ln(1-q)}, \qquad \phi = 2\pi w \tag{D.1.18}$$

to obtain two independent, Gaussian distributed (pseudo-) random numbers with vanishing mean from

$$x = r\cos\phi, \qquad y = r\sin\phi. \tag{D.1.19}$$

D.2 Wigner function and quantum Boltzmann equation

The Wigner function f is the quantum generalisation of the classical phase space density ϱ and was introduced by Wigner in 1932 [131]. It can formally be defined as the Weyl-transform [132] (denoted with a tilde) of the density matrix ρ via

$$f(x,p) = \frac{\tilde{\rho}}{\hbar} = \frac{1}{\hbar}\int \mathrm{d}y\, \langle x + y/2|\rho|x - y/2\rangle e^{ipy/\hbar}. \tag{D.2.1}$$

Due to the quantum nature, f is not limited to positive values (in fact, $f < 0$ signalises non-classical states) and is therefore only a quasi-probability distribution. It is still normalised to unity and can be used to calculate expectation values of an operator A,

$$\langle A\rangle = \mathrm{tr}(\tilde{\rho}\tilde{A}) = \int \mathrm{d}x\mathrm{d}p\, f(x,p)\tilde{A}, \tag{D.2.2}$$

where the Weyl-transform $\tilde{A}$ of the operator A is obtained in same way as $\tilde{\rho}$. On the other hand, we know that in thermodynamic equilibrium the phase space density behaves like an incompressible fluid and obeys the Louiville equation

$$\frac{\partial\rho}{\partial t} + \dot{x}\,\nabla\varrho + \dot{p}\nabla_p\varrho = 0. \tag{D.2.3}$$

Collisions between particles can be incorporated via a collision integral, leading to the Boltzmann equation. The Wigner function can consequently be described by a quantum Boltzmann equation of the form (9.1.1).

D.3 Thermal field theory

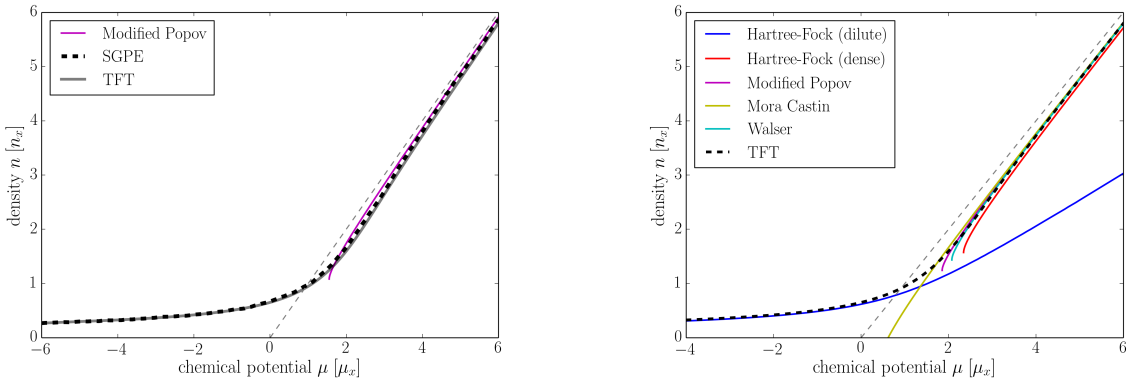

Figure D.3.1: Equation of state of the Thermal field theory (data from [127], see as well for more details) compared to SGPE results at $\beta_x = 10^{-1}$ (left) and mean-field theory results at $\beta_x = 10^{-3}$ (right)

Bibliography

[1] London, F. The phenomenon of liquid helium and the Bose-Einstein degeneracy. *Nature* **141**, 643–644 (1938).

[2] Uhlenbeck, G. E. Over statistische methoden in de theorie der quanta (1927). Nijhoff's-Gravenhage.

[3] London, F. On the Bose-Einstein condensation. *Phys. Rev.* **54**, 947 (1938).

[4] Allen, J. & Jones, H. New phenomena connected with heat flow in helium II. *Nature* **141**, 243–244 (1938).

[5] Kapitza, P. Viscosity of liquid helium below the l-point. *Nature* **141**, 74 (1938).

[6] Tisza, L. Transport phenomena in helium II. *Nature* **141**, 913 (1938).

[7] Penrose, O. & Onsager, L. Bose-Einstein condensation and liquid helium. *Phys. Rev.* **104**, 576 (1956).

[8] Fierz, M. & Pauli, W. On relativistic wave equations for particles of arbitrary spin in an electromagnetic field. *Proc. Roy. Soc. London Ser. A* 211–232 (1939).

[9] Pauli, W. The connection between spin and statistics. *Phys. Rev.* **58**, 716 (1940).

[10] Bose, S. N. Plancks Gesetz und Lichtquantenhypothese. *Z. phys* **26**, 178 (1924).

[11] Einstein, A. Quantentheorie des einatomigen idealen gases (1924). Akademie der Wissenschaften, in Kommission bei W. de Gruyter.

[12] Yang, C. N. Concept of off-diagonal long-range order and the quantum phases of liquid He and of superconductors. *Rev. Mod. Phys.* **34**, 694 (1962).

[13] Anderson, M. H., Ensher, J. R., Matthews, M. R., Wieman, C. E. & Cornell, E. A. Observation of Bose-Einstein condensation in a dilute atomic vapor. *Science* **269**, 198–201 (1995).

[14] Davis, K. B. *et al.* Bose-Einstein condensation in a gas of sodium atoms. *Phys. Rev. Lett.* **75**, 3969 (1995).

[15] Bradley, C. C., Sackett, C., Tollett, J. & Hulet, R. G. Evidence of Bose-Einstein condensation in an atomic gas with attractive interactions. *Phys. Rev. Lett.* **75**, 1687 (1995).

[16] Bradley, C. C., Sackett, C. A., Tollett, J. J. & Hulet, R. G. Evidence of Bose-Einstein condensation in an atomic gas with attractive interactions [Phys. Rev. Lett. 75, 1687 (1995)]. *Phys. Rev. Lett.* **79**, 1170–1170 (1997).

[17] Mermin, N. D. & Wagner, H. Absence of ferromagnetism or antiferromagnetism in one- or two-dimensional isotropic Heisenberg models. *Phys. Rev. Lett.* **17**, 1133 (1966).

[18] Hohenberg, P. Existence of long-range order in one and two dimensions. *Phys. Rev.* **158**, 383 (1967).

[19] Popov, V. Long-wave asymptotic form of the many-body green's functions of a one-dimensional Bose gas. *JETP Lett.* **31**, 35 (1980).

[20] Safonov, A., Vasilyev, S., Yasnikov, I., Lukashevich, I. & Jaakkola, S. Observation of quasicondensate in two-dimensional atomic hydrogen. *Phys. Rev. Lett.* **81**, 4545 (1998).

[21] Feshbach, H. Unified theory of nuclear reactions. *Ann. Phys.* **5**, 357–390 (1958).

[22] Kevrekidis, P. G., Frantzeskakis, D. J. & Carretero-González, R. *Emergent nonlinear phenomena in Bose-Einstein condensates: Theory and experiment*, vol. 45, Springer Science & Business Media (2007).

[23] Fischer, U. R. & Schützhold, R. Quantum simulation of cosmic inflation in two-component bose-einstein condensates. *Physical Review A* **70**, 063615 (2004).

[24] Bogoliubov, N. N. On the theory of superfluidity. *J. Phys.* **11**, 23–32 (1947).

[25] Stoof, H. & Bijlsma, M. Dynamics of fluctuating Bose-Einstein condensates. *J. Low Temp. Phys.* **124**, 431–442 (2001).

[26] Stoof, H. & Bijlsma, M. Kosterlitz-Thouless transition in a dilute Bose gas. *Phys. Rev. E* **47**, 939 (1993).

[27] Mora, C. & Castin, Y. Extension of Bogoliubov theory to quasicondensates. *Phys. Rev. A* **67**, 053615 (2003).

[28] Walser, R., Cooper, J. & Holland, M. Reversible and irreversible evolution of a condensed bosonic gas. *Phys. Rev. A* **63**, 013607 (2000).

[29] Hohenberg, P. & Martin, P. Microscopic theory of superfluid helium. *Ann. Phys.* **34**, 291–359 (1965).

[30] Griffin, A. Conserving and gapless approximations for an inhomogeneous Bose gas at finite temperatures. *Phys. Rev. B* **53**, 9341 (1996).

[31] Cockburn, S., Negretti, A., Proukakis, N. & Henkel, C. Comparison between microscopic methods for finite-temperature Bose gases. *Phys. Rev. A* **83**, 043619 (2011).

[32] Schwabl, F. Statistical mechanics (2006). Springer-Verlag.

[33] Pitaevskii, L. & Stringari, S. Bose-Einstein condensation (2003). Oxford University Press.

[34] Wang, F. Y.-H. Specific heat of an ideal Bose gas above the Bose condensation temperature. *Am. J. Phys.* **72**, 1193–1194 (2004).

[35] Robinson, J. E. Note on the Bose-Einstein integral functions. *Phys. Rev.* **83**, 678 (1951).

[36] Lipa, J., Nissen, J., Stricker, D., Swanson, D. & Chui, T. Specific heat of liquid helium in zero gravity very near the lambda point. *Phys. Rev. B* **68**, 174518 (2003).

[37] Buckingham, M. & Fairbank, W. Progress in low temperature physics (1961). North-Holland, Amsterdam.

[38] Osheroff, D., Richardson, R. & Lee, D. Evidence for a new phase of solid He 3. *Phys. Rev. Lett.* **28**, 885 (1972).

[39] Keesom, W. & Clusius, K. On the anomaly in the specific heat of liquid helium. *Leiden Comm.* **219**, 307 (1932).

[40] Pethick, C. J. & Smith, H. Bose-Einstein condensation in dilute gases (2002). Cambridge university press.

[41] De Groot, S., Hooyman, G. & Ten Seldam, C. On the Bose-Einstein condensation. *Proc. Roy. Soc. London Ser. A* **203**, 266–286 (1950).

[42] Ensher, J., Jin, D., Matthews, M., Wieman, C. & Cornell, E. Bose-Einstein condensation in a dilute gas: Measurement of energy and ground-state occupation. *Phys. Rev. Lett.* **77**, 4984 (1996).

[43] Feynman, R. Atomic theory of the λ transition in helium. *Phys. Rev.* **91**, 1291 (1953).

[44] Chester, G. λ transition in liquid helium. *Phys. Rev.* **100**, 455 (1955).

[45] Castin, Y. Simple theoretical tools for low dimension Bose gases. In *Journal de Physique IV (Proceedings)*, vol. 116, EDP sciences, 89–132 (2004).

[46] Phillips, W. D. Nobel lecture: Laser cooling and trapping of neutral atoms. *Rev. Mod. Phys.* **70**, 721 (1998).

[47] Hess, H. F. Evaporative cooling of magnetically trapped and compressed spin-polarized hydrogen. *Phys. Rev. B* **34**, 3476 (1986).

[48] Raab, E., Prentiss, M., Cable, A., Chu, S. & Pritchard, D. E. Trapping of neutral sodium atoms with radiation pressure. *Phys. Rev. Lett.* **59**, 2631 (1987).

[49] Castin, Y. Bose-Einstein condensates in atomic gases: simple theoretical results. In *Coherent atomic matter waves*, Springer, 1–136 (2001).

[50] Roberts, J. *et al.* Resonant magnetic field control of elastic scattering in cold Rb 85. *Phys. Rev. Lett.* **81**, 5109 (1998).

[51] Olshanii, M. Atomic scattering in the presence of an external confinement and a gas of impenetrable bosons. *Phys. Rev. Lett.* **81**, 938 (1998).

[52] Reichel, J. & Vuletic, V. Atom chips (2011). John Wiley & Sons.

[53] Hänsel, W., Hommelhoff, P., Hänsch, T. & Reichel, J. Bose-Einstein condensation on a microelectronic chip. *Nature* **413**, 498–501 (2001).

[54] Ott, H., Fortagh, J., Schlotterbeck, G., Grossmann, A. & Zimmermann, C. Bose-Einstein condensation in a surface microtrap. *Phys. Rev. Lett.* **87**, 230401 (2001).

[55] Van Amerongen, A., Van Es, J., Wicke, P., Kheruntsyan, K. & Van Druten, N. Yang-Yang thermodynamics on an atom chip. *Phys. Rev. Lett.* **100**, 090402 (2008).

[56] Dirac, P. A. The quantum theory of the emission and absorption of radiation. In *Proc. Roy. Soc. London Ser. A*, vol. 114, 243–265 (The Royal Society, 1927).

[57] Fock, V. Konfigurationsraum und zweite Quantelung. *Z. Phys.* **75**, 622–647 (1932).

[58] Schwartz, M. Off-diagonal long-range behavior of interacting Bose systems. *Phys. Rev. B* **15**, 1399–1403 (1977).

[59] Haldane, F. Effective harmonic-fluid approach to low-energy properties of one-dimensional quantum fluids. *Phys. Rev. Lett.* **47**, 1840 (1981).

[60] Ginzburg, V. & Landau, L. On the theory of superconductivity. *JETP* **20** (1950).

[61] Landau, L. & Lifshitz, E. Course of theoretical physics: Statistical physics, part 2 (1980). Pergamon International.

[62] Penrose, O. On the quantum mechanics of helium II. *Lond. Edinb. Dubl. Phil. Mag.* **42**, 1373–1377 (1951).

[63] Popov, V. N. Functional integrals in quantum field theory and statistical physics (1983). D. Reidel Publishing Company.

[64] Petrov, D., Shlyapnikov, G. & Walraven, J. Regimes of quantum degeneracy in trapped 1d gases. *Phys. Rev. Lett.* **85**, 3745 (2000).

[65] Kheruntsyan, K., Gangardt, D., Drummond, P. & Shlyapnikov, G. Pair correlations in a finite-temperature 1D Bose gas. *Phys. Rev. Lett.* **91**, 040403 (2003).

[66] Lieb, E. H. & Liniger, W. Exact analysis of an interacting Bose gas. I. the general solution and the ground state. *Phys. Rev.* **130**, 1605 (1963).

[67] Lieb, E. H. Exact analysis of an interacting Bose gas. II. the excitation spectrum. *Phys. Rev.* **130**, 1616 (1963).

[68] Bethe, H. Zur Theorie der Metalle. *Z. Phys.* **71**, 205–226 (1931).

[69] Tonks, L. The complete equation of state of one, two and three-dimensional gases of hard elastic spheres. *Phys. Rev.* **50**, 955 (1936).

[70] Girardeau, M. Relationship between systems of impenetrable bosons and fermions in one dimension. *J. Math. Phys* **1**, 516–523 (1960).

[71] Yang, C.-N. & Yang, C. Thermodynamics of a one-dimensional system of bosons with repulsive delta-function interaction. *J. Math. Phys* **10**, 1115–1122 (1969).

[72] Bouchoule, I., Van Druten, N. & Westbrook, C. I. Atom chips and one-dimensional Bose gases. *arXiv preprint 0901.3303* (2009). Reichel, J. & Vuletic, V. *Atom chips*, John Wiley & Sons (2011).

[73] Ketterle, W. & Van Druten, N. Bose-Einstein condensation of a finite number of particles trapped in one or three dimensions. *Phys. Rev. A* **54**, 656 (1996).

[74] Bogoliubov, N. N. A new method in the theory of superconductivity. *Soviet. Phys. JETP* **34**, 41–46 (1958).

[75] Lee, T. D., Huang, K. & Yang, C. N. Eigenvalues and eigenfunctions of a Bose system of hard spheres and its low-temperature properties. *Phys. Rev.* **106**, 1135 (1957).

[76] Goldman, V. V., Silvera, I. F. & Leggett, A. J. Atomic hydrogen in an inhomogeneous magnetic field: Density profile and Bose-Einstein condensation. *Phys. Rev. B* **24**, 2870 (1981).

[77] Wick, G.-C. The evaluation of the collision matrix. *Phys. Rev.* **80**, 268 (1950).

[78] Andersen, J., Al Khawaja, U. & Stoof, H. Phase fluctuations in atomic Bose gases. *Phys. Rev. Lett.* **88**, 070407 (2002).

[79] Khawaja, U. A., Andersen, J., Proukakis, N. & Stoof, H. Low-dimensional Bose gases. *Phys. Rev. A* **66**, 013615 (2002).

[80] Castin, Y. & Dum, R. Bose-Einstein condensates in time dependent traps. *Phys. Rev. Lett.* **77**, 5315 (1996).

[81] Walser, R. Ground state correlations in a trapped quasi one-dimensional Bose gas. *Opt. Commun.* **243**, 107–129 (2004).

[82] Proukakis, N. P. Self-consistent quantum kinetics of condensate and non-condensate via a coupled equation of motion formalism. *J. Phys. B: At. Mol. Phys.* **34**, 4737 (2001).

[83] Proukakis, N., Morgan, S., Choi, S. & Burnett, K. Comparison of gapless mean-field theories for trapped Bose-Einstein condensates. *Phys. Rev. A* **58**, 2435 (1998).

[84] Yukalov, V. & Kleinert, H. Gapless Hartree-Fock-Bogoliubov approximation for Bose gases. *Phys. Rev. A* **73**, 063612 (2006).

[85] Higgs, P. Broken symmetries and the masses of gauge bosons. *Phys. Rev. Lett.* **13**, 508 (1964).

[86] Higgs, P. Broken symmetries, massless particles and gauge fields. *Phys. Lett.* **12**, 132 (1964).

[87] Gardiner, C. W. Particle-number-conserving Bogoliubov method which demonstrates the validity of the time-dependent Gross-Pitaevskii equation for a highly condensed Bose gas. *Phys. Rev. A* **56**, 1414 (1997).

[88] Goldstone, J. Field theories with «superconductor» solutions. *Il Nuovo Cimento* **19**, 154–164 (1961).

[89] Goldstone, J., Salam, A. & Weinberg, S. Broken symmetries. *Phys. Rev.* **127**, 965 (1962).

[90] Nambu, Y. Quasi-particles and gauge invariance in the theory of superconductivity. *Phys. Rev.* **117**, 648 (1960).

[91] Lange, R. V. Nonrelativistic theorem analogous to the Goldstone theorem. *Phys. Rev.* **146**, 301 (1966).

[92] Hugenholtz, N. & Pines, D. Ground-state energy and excitation spectrum of a system of interacting bosons. *Phys. Rev.* **116**, 489 (1959).

[93] Beliaev, S. Application of the methods of quantum field theory to a system of bosons. *Sov. Phys. JETP* **7**, 289–299 (1958).

[94] Beliaev, S. Energy-spectrum of a non-ideal Bose gas. *Sov. Phys. JETP* **7**, 299–307 (1958).

[95] Griffin, A. Excitations in a Bose-condensed liquid (1993). Cambridge University Press.

[96] Stein, E. M. & Weiss, G. L. Introduction to fourier analysis on euclidean spaces (1971). Princeton University Press.

[97] Mandel, L. Sub-poissonian photon statistics in resonance fluorescence. *Opt. Lett.* **4**, 205–207 (1979).

[98] Cockburn, S. P. *Bose gases in and out of equilibrium within the Stochastic Gross-Pitaevskii equation*. Ph.D. thesis, University of Newcastle upon Tyne (2010).

[99] Gross, E. P. Structure of a quantized vortex in boson systems. *Il Nuovo Cimento Series 10* **20**, 454–477 (1961).

[100] Pitaevskii, L. Vortex lines in an imperfect Bose gas. *Sov. Phys. JETP* **13**, 451–454 (1961).

[101] Burger, S. *et al.* Dark solitons in Bose-Einstein condensates. *Phys. Rev. Lett.* **83**, 5198 (1999).

[102] Denschlag, J. *et al.* Generating solitons by phase engineering of a Bose-Einstein condensate. *Science* **287**, 97–101 (2000).

[103] Shabat, A. & Zakharov, V. Exact theory of two-dimensional self-focusing and one-dimensional self-modulation of waves in nonlinear media. *Sov. Phys. JETP* **34**, 62 (1972).

[104] Chiao, R. Y., Garmire, E. & Townes, C. Self-trapping of optical beams. *Phys. Rev. Lett.* **13**, 479 (1964).

[105] Parker, N. *Numerical studies of vortices and dark solitons in atomic Bose-Einstein condensates*. Ph.D. thesis, University of Durham (2004).

[106] Crank, J. & Nicolson, P. A practical method for numerical evaluation of solutions of partial differential equations of the heat-conduction type. In *Math. Proc. Cambridge*, vol. 43, Cambridge Univ. Press, 50–67 (1947).

[107] Charney, J. G., Fjörtoft, R. & Von Neumann, J. Numerical integration of the barotropic vorticity equation. *Tellus A* **2** (1950).

[108] Cockburn, S. & Proukakis, N. The Stochastic Gross-Pitaevskii equation and some applications. *Laser Phys.* **19**, 558–570 (2009).

[109] Proukakis, N. P. & Jackson, B. Finite-temperature models of Bose-Einstein condensation. *J. Phys. B: At. Mol. Phys.* **41**, 203002 (2008).

[110] Zaremba, E., Nikuni, T. & Griffin, A. Dynamics of trapped Bose gases at finite temperatures. *J. Low Temp. Phys.* **116**, 277–345 (1999).

[111] Kirkpatrick, T. & Dorfman, J. Transport in a dilute but condensed nonideal Bose gas: Kinetic equations. *J. Low Temp. Phys.* **58**, 301–331 (1985).

[112] Steel, M. *et al.* Dynamical quantum noise in trapped Bose-Einstein condensates. *Phys. Rev. A* **58**, 4824 (1998).

[113] Sinatra, A., Lobo, C. & Castin, Y. The truncated Wigner method for Bose-condensed gases: limits of validity and applications. *J. Phys. B: At. Mol. Phys.* **35**, 3599 (2002).

[114] Stoof, H. Coherent versus incoherent dynamics during Bose-Einstein condensation in atomic gases. *J. Low Temp. Phys.* **114**, 11–108 (1999).

[115] Stoof, H. Initial stages of Bose-Einstein condensation. *Phys. Rev. Lett.* **78**, 768 (1997).

[116] Davis, M. J., Gardiner, C. W. & Ballagh, R. J. Quantum kinetic theory. VII. the influence of vapor dynamics on condensate growth. *Phys. Rev. A* **62**, 063608 (2000).

[117] Gardiner, C. W., Anglin, J. R. & Fudge, T. I. A. The stochastic Gross-Pitaevskii equation. *J. Phys. B: At. Mol. Phys.* **35**, 1555 (2002).

[118] Cockburn, S., Gallucci, D. & Proukakis, N. Quantitative study of quasi-one-dimensional Bose gas experiments via the Stochastic Gross-Pitaevskii equation. *Phys. Rev. A* **84**, 023613 (2011).

[119] Gallucci, D. *Ab initio modelling of quasi-one-dimensional Bose gas experiments via the Stochastic Gross-Pitaevskii equation.* Ph.D. thesis, University of Newcastle upon Tyne (2013).

[120] Duine, R. & Stoof, H. Stochastic dynamics of a trapped Bose-Einstein condensate. *Phys. Rev. A* **65**, 013603 (2001).

[121] Keldysh, L. Diagram technique for nonequilibrium processes. *Sov. Phys. JETP* **20**, 1018–1026 (1965).

[122] Penckwitt, A. A., Ballagh, R. J. & Gardiner, C. W. Nucleation, growth, and stabilization of Bose-Einstein condensate vortex lattices. *Phys. Rev. Lett.* **89**, 260402 (2002).

[123] Prokof'ev, N., Ruebenacker, O. & Svistunov, B. Critical point of a weakly interacting two-dimensional Bose gas. *Phys. Rev. Lett.* **87**, 270402 (2001).

[124] Prokof'ev, N. & Svistunov, B. Two-dimensional weakly interacting Bose gas in the fluctuation region. *Phys. Rev. A* **66**, 043608 (2002).

[125] Proukakis, N. Spatial correlation functions of one-dimensional Bose gases at equilibrium. *Phys. Rev. A* **74**, 053617 (2006).

[126] Stamper-Kurn, D. *et al.* Reversible formation of a Bose-Einstein condensate. *Phys. Rev. Lett.* **81**, 2194 (1998).

[127] Polster, H. *Das eindimensionale Bose-Einstein-Quasi-Kondensat.* Diploma thesis, University of Potsdam (2015).

[128] Carusotto, I. & Castin, Y. Superfluidity of the 1D bose gas. *Comptes Rendus Physique* **5**, 107–127 (2004).

[129] Abramowitz, M. & Stegun, I. A. Handbook of mathematical functions: with formulas, graphs, and mathematical tables (1964). Courier Corporation.

[130] Box, G. E. & Muller, M. E. A note on the generation of random normal deviates. *Ann. Math. Stat.* **31**, 610–611 (1958).

[131] Wigner, E. On the quantum correction for thermodynamic equilibrium. *Phys. Rev.* **40**, 749 (1932).

[132] Weyl, H. Quantenmechanik und Gruppentheorie. *Z. Phys.* **46**, 1–46 (1927).